12-18-2014

Maintenance of Neuron Activity by Homeostatic Alterations in Receptors and Ion Channels in a Rett Syndrome Mouse Model

Max Oginsky

MAINTENANCE OF NEURON ACTIVITY BY HOMEOSTATIC ALTERATIONS IN RECEPTORS AND ION CHANNELS IN A RETT SYNDROME MOUSE MODEL

by

MAX F. OGINSKY

Under the Direction of Chun Jiang, PhD

ABSTRACT

Rett Syndrome (RTT) is a developmental disorder that affects numerous neuronal systems that underlie problems with breathing, movement, cognition and sleep. RTT is caused by mutations in the methyl-CpG-binding protein 2 (*Mecp2)* gene. MeCP2 is a ubiquitous protein that is found in all mature neurons and binds to methylated DNA to repress transcription; thus regulating protein expression levels in neurons. The mutations in *Mecp2* affect a large number of proteins that are crucial for regulating neuronal activity. Despite the abnormal expression of many of these proteins, mice with a total loss of MeCP2 can live to adulthood and some people with RTT can live to a very late age as well. It is possible that mutations in the *Mecp2* gene not only cause widespread defects, but also elicit neuroadaptive

processes that may limit the impact of the MeCP2 dysfunction. To test this hypothesis we performed these studies in which we focused on how synaptic and membrane currents were altered to maintain normal neuronal activity in *Mecp2*-null mice. We show two examples from different neurons where neuroadaptations of ion channel expression allowed the neuron to remain viable. First, the properties of the nicotinic acetylcholine receptor (nAChR) current were altered in LC neurons in *Mecp2*-null mice. This was caused by changes in the nicotinic receptor subunit expression. Despite the changes in the nAChR current, the cholinergic modulation of LC neuron activity in WT and *Mecp2*-null mice were similar. Secondly, we show that the fast Na^+ voltage-gated and the hyperpolarization-activated currents were altered in mesencephalic trigeminal V (Me5) propriosensory neurons. The changes in the hyperpolarization-activated current caused a smaller sag and post-inhibitory rebound. Opposite to what we expected, these cells were hyperexcitable. The hyperexcitability was due to changes in the fast Na^+ voltage-gated current causing a decreased action potential threshold. Alterations in the ionic currents in Me5 neurons seem to be due to changes in subunit expression patterns. These results indicate that despite the complications caused by defects in the *Mecp2* gene, neurons respond by rearranging receptor / ion channel expression. This reorganization allows neurons to remain viable despite the MeCP2 deficiency.

INDEX WORDS: Rett syndrome, Homeostasis, Nicotinic receptor, Hyperpolarization-activated current, Voltage-gated sodium current, *Mecp2*

MAINTENANCE OF NEURON ACTIVITY BY HOMEOSTATIC ALTERATIONS IN RECEPTORS AND ION CHANNELS IN A RETT SYNDROME MOUSE MODEL

by

Max F. Oginsky

A Dissertation Submitted in Partial Fulfillment of the Requirements for the Degree of

Doctor of Philosophy

in the College of Arts and Sciences

Georgia State University

2014

MAINTENANCE OF NEURON ACTIVITY BY HOMEOSTATIC ALTERATIONS IN RECEPTORS AND ION CHANNELS IN A RETT SYNDROME MOUSE MODEL

by

Max F. Oginsky

Committee Chair: Chun Jiang

Committee: William Walthall

Vincent Rehder

Electronic Version Approved:

Office of Graduate Studies

College of Arts and Sciences

Georgia State University

December 2014

DEDICATION

To my Wife Dana and my Daughter Amelia.
Both of who I am eternally blessed and forever grateful to have in my life.

To my Mother Patricia
A lovely, lovely woman who has always been there for me and showed me how to persevere through all of life's trials, a significant key to my success.

To my Father Robert and step-Mother Rosanne
A couple who has instilled a hard work ethic and love of music in me, both of which have been crucial to my well-being

To my Brother Robert
A wonderful source of inspiration at a critical time in my life

To my Brother Daniel
My Rock of Gibraltar

To my in-laws Russell and Eileen
Both have been a wonderful addition to my life and have been very supportive in my educational pursuits

ACKNOWLEDGEMENTS

I will do my best to mention everyone that has helped me and guided me through this entire process of earning my PhD. Please forgive me if I forget to acknowledge someone. There are so many people at GSU that have provided either words of wisdom, helped me with a problem or pushed me to excel. For that, I am forever grateful.

First and foremost, I would like to express my appreciation for my Ph.D. advisor, Chun Jiang. He has been a constant source of guidance and motivation throughout my time in his lab. Each day he pushed me to become a better scientist. Without his support and mentorship, I would not be where I am today.

Secondly, I would like to thank my committee members, Dr. William Walthall and Dr. Vincent Rehder. Dr. Walthall was the first person I met here at GSU when I started as a Master's student. He has always been supportive and gone above and beyond with helping me during my time here at GSU. Dr. Rehder is wonderful person who has offered me sage advice and helpful comments during my dissertation experience.

I would also like to thank other faculty members at GSU. Thanks to Dr. Deborah Baro for giving me a start in the GSU PhD program. I am not sure I would be having the career I am having without her help and for that I am very grateful. Thanks to Dr. Yuan Liu for her guidance when I first came to GSU as a Master's student and during my qualification exam. Thanks to Dr. Gennady Cymbalyuk for taking a lot of time out of his schedule to teach me computational neuroscience skills. I am confident this will very useful in my future. Thank you to Dr. Julia Hilliard for being very helpful when it was extremely needed. Thank you to Dr. Timothy Bartness for helping me with me to secure

a postdoc position. Dr. Robert Simmons for his help with my microscopy experiments and good conversations. Dr. Blaustein and Nancy Russell for providing a wonderful student teaching experience.

I would also like to thank the staff at GSU. LaTesha Warren has always been there to provide professional assistance and helpful guidance. Barry Grant for his help with some maintenance repairs. Elizabeth Weaver for her help with all Brains and Behavior events and issues. Debby Walthall, Sonja Young and Ping Jiang have been very helpful throughout the years.

Thank you to the many friends and colleagues I have made during my time at GSU. From the early days, Dr. Wulf Krenz, Dr. Edmund Rodgers, Dr. Hongmei Zhang, Amarallys Citron, Kimi Kent, Anna Huff and Jingjing Fu. Members of the Jiang lab, Dr. Ningren Cui, Dr. Xin Jin, Dr. Yang Yang, Dr. Xiaotao Jin, Dr. Shanshan Li, Christopher M. Johnson, Shuang Zhang, Vivian Zhong, Dawn Wu, Casey Trower. Also, Johnny Garretson for all his help with problems, difficulties, issues, complications, crises and conundrums, Dr. Lei Zhong, Stephen Estes, Dr. Liana Artinian, William Barnett, Hasti Ghabel, Jill Weathington, Devaleena Pradham, Lori Eidson, Dr. Tim Balmer, Katherine Sturman and Anna Dunigan.

TABLE OF CONTENTS

LIST OF TABLES

LIST OF FIGURES

1 SPECIFIC AIMS OF THE DISSERTATION

The loss of proper Methyl-CpG-binding protein 2 (MeCP2) function is the molecular basis of Rett syndrome (RTT). RTT is characterized by abnormalities in breathing, motor function, cognition and sleep, in addition to other autistic features. These problems have largely been linked to dysfunction in signaling between neurons as well as neuronal intrinsic membrane properties. The decrease in GABA and norepinephrine (NE) signaling has been shown to be associated with breathing disorders, characteristics of RTT that underlie the high (26%) sudden and unexpected death rates (Abdala et al. 2010; Viemari et al. 2005). This may be partially due to the decrease in the expression of the NE -synthesizing enzymes, tyrosine hydroxylase and dopamine-β- hydroxylase in locus coeruleus (LC) neurons, and the GABA-synthesizing enzyme glutamic acid decarboxylase in GABAergic neurons (Chao et al. 2010; Zhang et al. 2010b). Abnormalities in LC neuronal intrinsic membrane properties also contribute to the defects in breathing (Zhang et al. 2010a; Zhang et al. 2011). The coexistence of the defects in NE and GABA systems suggest that brainstem neuronal networks are affected by the *Mecp2* disruption, which may involve other neurotransmitter systems such as serotonin and acetylcholine (ACh) as well. ACh regulates the expression of enzymes for NE and GABA biosynthesis and may be involved in the problems associated with the NE and GABAergic systems (Gueorguiev et al. 2000; Maloku et al. 2011). Indeed, ACh signaling has been shown to be defective in RTT (Nag and Berger-Sweeney 2007; Weng et al. 2011; Wenk and Hauss-Wegrzyniak 1999; Wenk and Mobley 1996). The NE, GABA and cholinergic systems regulate certain behaviors

including arousal state and sleep/wake cycles. Experimental evidence suggests that the modulation of the NE system by GABA is deficient and contributes to neuronal hyperexcitability. A similar defect may occur in the cholinergic system, a hypothesis that we have proposed experiments to test.

The involvement of multiple neurotransmitter systems in the development of RTT-like disorders in *Mecp2*-null mice suggests that an appropriate regulation of these neurotransmitter systems is necessary to maintain them in a homeostatic state. Homeostasis of neurotransmitter systems will not only allow a better control of neurotransmission, but also enable potential compensatory neuroadaptations to the defects in receptors and ion channels. The latter may be in action in RTT mouse models to limit the impact of the loss of MeCP2 function, a novel hypothesis that we have proposed in these studies.

The homeostatic adaptive mechanism is known to occur in response to genetic perturbation. In animals with a specific ion channel gene knocked out, neurons alter the expression of other ion channels to maintain normal function. (Bonin et al. 2013; Kim and Hoffman 2012; Ortinski et al. 2006). There is evidence for neuroadaptations in Parkinson's disease animal models as well (Golden et al. 2013; Lloyd 1977; McCallum et al. 2006). Therefore, it is possible that similar types of alterations in channel expression may be occurring in RTT mouse models to maintain normal function. Despite the belief of its existence, it was unclear how the homeostatic compensatory mechanism would work. Since RTT affects signaling between neurons, we investigated the mechanisms for neuronal activity and communication, in which receptors and ionic channels are known to play an important role.

To validate the homeostatic neuroadaptation hypothesis, we investigated receptors and ion channels in two different neuron types, i.e., cholinergic synaptic currents in LC neurons and membrane ionic currents in mesencephalic trigeminal V (Me5) neurons. The LC is the center for NE production in the CNS, whereas the Me5 neurons are propriosensory cells that are crucial for coordinated movement. They function in autonomic regulation and motor behaviors, respectively. These two systems show the most severe defects in RTT. Therefore, we have proposed studies to address two specific aims:

Specific Aim 1 (tested in Chapter 5): <u>How does ACh modulate LC neurons through presynaptic and postsynaptic mechanisms in WT and Mecp2$^{-/Y}$ mice?</u>

NE is deficient in humans with RTT and mouse models (Panayotis et al. 2011; Zoghbi et al. 1989). This seems to be due to inherent defects and abnormal synaptic inputs in LC neurons (Jin et al. 2013a; Zhang et al. 2010a; Zhang et al. 2011). ACh has several functional overlaps with the NE system. ACh is a classical neurotransmitter involved with many functions in the CNS and peripheral nervous system. It plays a role in CNS function by regulating attention, memory function, arousal, transitions in sleep cycles and mood. These behaviors are dysregulated in RTT (Carotenuto et al. 2013; Maloku et al. 2011; Schaevitz et al. 2012). The loss of MeCP2 function on cholinergic signaling is unclear. Few have focused on the dysfunction of the cholinergic system caused by the knockout of the *Mecp2* gene. However, it is clear that NE and ACh regulate similar behaviors. In one example, LC neurons and ACh neurons regulate each other resulting in alternations between non-REM and REM sleep states. It is unclear,

however, whether the modulation of LC neurons by ACh is altered in *Mecp2*$^{-/Y}$ mice. Therefore, in this study we investigated the cholinergic modulation of LC neurons in these mice. These experiments may provide insight into how the knockout of the *Mecp2* gene alters the expression of nicotinic acetylcholine receptors (nAChR) in LC neurons, and whether neurons can alter the expression of synaptic receptors to maintain normal modulation.

Specific Aim 2 (tested in Chapter 6): How does the loss of MeCP2 affect ionic currents and firing activity in mesencephalic trigeminal V propriosensory neurons?

Motor dysfunction is a characteristic of RTT, which may result from motor, extrapyramidal and propriosensory neuron dysfunction. Propriosensory neurons are important for relaying information to the brain about the position of the limb in space. This is critically important for coordinated and directed movement such as locomotion and mastication. Girls with RTT have problems chewing and swallowing which leads to malnutrition and poor health (Motil et al. 2012). Whereas most work has been focused on motor neurons to determine the underlying causes of movement problems, little is known about how the loss of MeCP2 impairs propriosensory function. In these experiments we took advantage of the presence of Me5 neurons in the brainstem to test the homeostatic neuroadaptation hypothesis by focusing on ion channels and intrinsic member properties. The experiments herein test the hypothesis that the Me5 neurons from *Mecp2*$^{-/Y}$ mice are dysfunctional due the knockout of the gene. This study provides

insight into the membrane ionic currents that affect the intrinsic membrane properties of Me5 neurons in *Mecp2*$^{-/Y}$ mice.

Taken together, this dissertation addresses the effects of the *Mecp2* knockout on synaptic and membrane ionic currents. It addresses two important questions: 1) how does the disruption of *Mecp2* impair ion channels and receptors? 2) Do neurons respond to these defects by rearranging other ion channels and receptors to minimize and compensate for the defects? The NE-ergic system and the Me5 propriosensory system were chosen as they represent major defective functions in RTT. Ion channels and receptors were studied in these neurons as they underlie the intrinsic membrane properties of neurons as well as neuronal communication, both of which are known to be defective in RTT. Therefore, this dissertation provides evidence that the loss of proper MeCP2 function affects neuronal communication by changing synaptic transmission and by altering membrane ionic currents. It is possible that these types of neuroadaptations may exist in other diseases with a basis in genetic defects.

2 INTRODUCTION

2.1 Definition of key concepts

There is growing evidence suggesting the reason that some diseases progress through different stages, instead of the victims dying quickly, is because neurons are able to compensate for the problems caused by the disease. Compensation can be described as a neuroadaptive mechanism by which one attribute is altered to limit the problems created by a deficiency in another attribute. For example, in Parkinson's disease, the decrease in dopamine in the striatum is caused the death of substantia

nigra pars compacta neurons. The remaining dopaminergic neurons compensate by increasing their production of dopamine. This is done by increasing expression of tyrosine hydroxylase, the rate-limiting enzyme for dopamine synthesis (Zigmond et al. 1984). Here, we provide evidence of compensation done by homeostatic reorganization of receptors and ion channels. The reorganization refers to the increase in one subunit of the receptor/ion channel family while another is decreased, or vice versa. These changes in expression seem to be a homeostatic mechanism because it provides a way for the neuron to remain viable. These concepts provide a basis for understanding how neurons adapt to perturbation caused by a disease.

2.2 Signaling in the CNS is governed by synaptic transmission and neuron activity

There are two major components that regulate how a neuron communicates to other neurons. First, the release of neurotransmitters from a presynaptic neuron and the subsequent binding of the transmitter to its receptor on the postsynaptic neuron has been widely studied. Secondly, the intrinsic membrane properties of the neuron governs how it fires action potentials and how the neuron responds to input from presynaptic neurons. While not a focus of the thesis, electrical synapses are found in a small number of neurons. These synapses are formed by gap junctions and allow neurons to communicate by directly passing electrical current from one cell to another. Because there is no chemical intermediary, the communication is very fast and usually involved in simple behaviors such as the escape reflex in lobsters and crayfish. Understanding how these processes underlie normal communication is essential for understanding neuron signaling problems found in disease.

2.2.1 Overview of chemical synaptic transmission in the mammalian CNS

The synapse is the basic structure of chemical neurotransmission in the CNS. The synapse consists of a presynaptic neuron that releases transmitters and a postsynaptic neuron that has ligand-gated receptors that convert the chemical message into an electrical signal. Depending on whether the electrical signal is made up of cations or anions, the neuron becomes excited or inhibited.

The synaptic communication between two neurons is modified by modulatory inputs. These inputs can change the amount of neurotransmitter released at the presynaptic terminal (Garcia-Ramirez et al. 2014). The modulatory inputs can influence the movement of receptors in and out of the synapse in the postsynaptic neuron (Gao et al. 2006; Zou et al. 2005). These mechanisms are involved with increasing or decreasing the synaptic strength and ultimately are thought to underlie compensatory neuroadaptations such as long term potentiation (LTP) and long term depression (LTD) (Bassani et al. 2013; Castillo 2012) .

It is unclear how certain genetic diseases that affect signaling between neurons affect these normal neuromodulatory processes. Experimental evidence from transgenic animals indicate that the defect in a given gene produces a phenotype that lacks function (Drago et al. 2003). Whereas in other animals, molecular and systemic compensation occurs by activating other gene(s) that have similar functions, reducing and in some cases even masking the defect (Bonin et al. 2013). Evolutionarily, it is reasonable to believe that compensatory neuroadaptations are necessary for survival or preservation of a biological system when a crucial gene is mutated.

The transcription repressor protein, methyl-CpG-binding protein 2 (*Mecp2*) plays a role in the expression of enzymes crucial for the synthesis of neurotransmitters (Maloku et al. 2011). As a result, its defect can affect a large number of downstream genes including several neurotransmitter systems (Chao et al. 2010; Zhang et al. 2010b). In this thesis we elucidate some of the effects that the loss of functioning MeCP2 has on neuronal activity.

2.2.2 Presynaptic mechanisms of neurotransmitter release

The release of neurotransmitters from a nerve terminal occurs through action potential dependent and action potential independent mechanisms. The action potential induced release of neurotransmitters from a presynaptic terminal involves many events to occur in a choreographed manner. The invasion of the action potential into the presynaptic terminal causes local depolarization and opening of voltage-gated Ca^{2+} channels. The influx of Ca^{2+} into the cell is critical for neurotransmitter release and blocking of these channels or reducing extracellular Ca^{2+} prevents the release of the transmitters. Further, even when the action potential is blocked with tetrodotoxin, neurotransmitter release at the presynaptic terminal can occur. Depolarization of the membrane potential at the presynaptic terminal, without the influence from an action potential, can activate Ca^{2+} channels (Nakamura and Jang 2010; Yang et al. 2011). Therefore, action potential independent mechanisms are in place to regulate the release of neurotransmitters.

Ca^{2+} binds to molecular targets in the terminal causing the release of neurotransmitters into the synapse. The vesicles that store the neurotransmitter at the terminal present at the active zone or site of release. Ca^{2+} entry causes these vesicles

to fuse to the membrane and release the neurotransmitters into the synapse (Sudhof 2012). However, since some neurons can respond to stimuli by firing at > 200Hz, it is important to know how this is possible. Vesicles are tethered and stored in compartments that are distant from the active zone. Ca^{2+} binds to synapsin, a protein that tethers the vesicles, and initiates the vesicle movement to the active zone (Kile et al. 2010).

Neurotransmitters are released as discrete units called quanta. Each quantum results in a fixed postsynaptic potential. A single quantum has been linked to the release of neurotransmitters in a single vesicle. After the action potential invades the terminal, many quanta are released at once and can affect the membrane potential of the postsynaptic neuron. However, the release of neurotransmitters independent of an action potential can be modulated by other inputs at the presynaptic terminal. Acetylcholine alters the amount of GABA and glutamate released at terminals by depolarizing the membrane potential. This causes an increase in the frequency of quanta release. Therefore, increasing the quanta release enhances the effect the presynaptic neuron has on the postsynaptic neuron.

2.2.3 Postsynaptic mechanisms mediating the chemical message

The ligand-gated ionotropic receptors found in the postsynaptic membrane are the most common mode of converting the chemical signal from the presynaptic neuron to an electrical signal in the postsynaptic neuron. In the mammalian CNS, glutamate mediates the excitatory signal by binding to NMDA and AMPA receptors in the postsynaptic membrane. Opening of these receptors allows Na^{+} and Ca^{2+} to enter and depolarize the cell. GABA mediates the inhibitory signal by binding to $GABA_A$ receptors

causing Cl^- to pass into the cell. Also, GABA may bind to $GABA_B$ receptors and initiate a second messenger cascade resulting in activation of K^+ currents. In both instances, GABA can hyperpolarize the cell. Another class of signaling molecule is acetylcholine (ACh), which is most commonly associated with signaling between motoneurons and muscles in the peripheral nervous system. In the CNS, ACh acts through the ionotropic nicotinic acetylcholine receptors (nAChRs) and muscarinic acetylcholine receptors and is involved with diverse behaviors such as attention, cognition, sleep as well as others (Romanelli et al. 2007).

Glutamate, GABA and ACh elicit postsynaptic currents that affect the firing activity of the postsynaptic neuron. Since NMDA, AMPA and nicotinic acetylcholine receptors allow Na^+ and Ca^{2+} into the cell, the cell depolarizes increasing the likelihood of an action potential and increasing the firing frequency. GABA- elicited inhibition through $GABA_A$ receptors is caused by Cl^- moving into the cell causing the membrane potential to become hyperpolarized. Hyperpolarization of the membrane potential increases the likelihood of the cell to be silent or at least reduce the firing frequency. The activation of these receptors will affect the firing activity of neurons by directly altering the membrane potential

Long-term potentiation (LTP) Long-term Depression (LTD) are the major mechanisms of changing the synaptic strength in the CNS. Most often these mechanisms are associated with excitatory synapses but have been found at inhibitory synapses as well (Arendt et al. 2013; Cohen et al. 1999; Nugent and Kauer 2008). Pre- and postsynaptic mechanisms have been described. In brief, the presynaptic mechanisms involve the increase of neurotransmitter release in LTP and a decrease in

LTD. Postsynaptically, the ligand-gated receptors move into the synapse during LTP and are removed during LTD. Many methods have been used to stimulate LTP and LTD, whether its high/low frequency stimulation of the presynaptic neuron (Martin et al. 2013; Mizuno et al. 2001) or coincidental firing of an action potential between the pre and postsynaptic neurons (Banerjee et al. 2014; Kodangattil et al. 2013). LTP and LTD are important for normal cognitive function the brain and disruption of these mechanisms because of disease leads to improper communication between neurons (Han et al. 2014; Liu et al. 2008; Mori et al. 2014). This suggests people with diseases that have altered signaling processes in neurons have impaired learning and memory.

2.2.4 Intrinsic membrane ionic currents affect neuronal activity

Besides synaptic transmission, the intrinsic membrane properties of neurons governs their firing properties. These intrinsic membrane properties have been extensively studied and can be generally attributed to specific ionic membrane currents. Here, we will introduce specific firing properties in the neurons studied and how these properties affect signaling and function.

The relationship between the injected current and the voltage response of the neuron is very important for understanding the input resistance of the neuron. The input resistance is a good measure of the number of channels that are either open or closed in the membrane of the neuron (John and Manchanda 2011). More specifically, it is a valuable tool in determining how a drug may affect the membrane ion channels thus altering the activity of the neuron (Podda et al. 2010). Consequently, the opening and closing of ion channels alters the excitability of neurons. According to Ohm’s law, the input resistance has a large effect on membrane potential. If the input resistance is

large, a current injection is going to change the membrane potential more than if the input resistance is small. Therefore, membrane ion channels alter the response of the postsynaptic neuron to presynaptic currents by changing the input resistance of the neuron.

The delayed excitation found in many neurons affects the interspike interval. The time it takes from the end of one action potential to the start of the next is regulated by subthreshold currents. A major contributor to the interspike interval is the fast-transient K^+ current (I_A) (McDermott and Schrader 2011). This current is mediated by Kv(4.1-4.3) channels in mammals and is inactivated during an action potential. Kv4 channels become deinactivated at subthreshold potentials and activate during the interspike interval allowing K^+ to flow out of the cell. The movement of K^+ out of the cell causes the depolarization of the cell toward threshold to take longer than it would if I_A was not present. Therefore, this particular K^+ current regulates the interspike interval and allows cells to spontaneously fire action potentials at low frequencies.

The post-inhibitory rebound (PIR) is very important to how neurons respond to the release from inhibition. The phenomenon is very important in half-center oscillators found in central pattern generators and in reciprocal inhibition found in locomotion. In both cases, the firing of one neuron causes a second neuron to be inhibited from firing (Harris-Warrick et al. 1995). When the first neuron stops firing action potentials, the second neuron rebounds from silence and fires action potentials. Without the PIR, the neuron would just return to its resting membrane potential without firing an action potential. Therefore, the PIR depolarizes the neuron past its resting membrane potential to threshold.

The underlying mechanism for the PIR has been attributed to the hyperpolarization- activated current (I_H) (Ascoli et al. 2010). I_H is a nonspecific cation current that depolarizes the cell after it has been inhibited. The removal of the inhibition happens much faster than the deactivation of the HCN channels. This allows cations to keep moving into the cell driving the voltage past the resting membrane potential to threshold (Dean et al. 1989).

The spike frequency adaptation (SFA) is a phenomenon that describes how neurons respond to a sustained depolarizing pulse. When a neuron is subjected to a depolarizing pulse, a train of action potentials will be elicited. If the SFA is present, then the frequency of action potentials will decrease during the time of depolarizing pulse (Chen et al. 2014). This is found in both sensory and motor neurons and has been related to different mechanisms. The most prominent is the action potential-dependent SFA. In this case, Ca^{2+} is brought into the cell during the action potential and Ca^{2+}-dependent K^+ currents (I_{KCa}) are activated. The activation of these currents increases the afterhyperpolarization (AHP). The larger AHP slows the depolarization of the membrane potential. With each successive action potential, the net concentration of Ca^{2+} in the cell grows, thus activating more and more K_{Ca} channels (Vandael et al. 2012). Therefore, the interspike interval becomes longer during the depolarizing pulse. This is how the neuron is able to accommodate to the depolarization and slow the action potential frequency.

2.2.5 Overview of K^+ currents role in neuronal activity

Two of the most important functions performed by K^+ currents in neurons is the setting of the resting membrane potential, the repolarization of the action potential and

the interspike interval. The resting membrane potential is mainly set by K^+ leak currents mediated by TWIK-related acid sensitive K^+ (TASK) and K_{ir} channels (Butt and Kalsi 2006). These channels are not voltage or ligand-gated. The conductance of K^+ obeys Ohm's law. Consequently, the driving force created by the concentration gradient of K^+ and the membrane potential of the neuron causes K^+ to move out of the neuron. For most cells, the resting membrane potential is very near the equilibrium potential of the K^+ leak current. When the cell is hyperpolarized below the K^+ equilibrium potential the polyamine block is removed and the channels conduct K^+ into the cell. Usually if I_{Kir} plays a large role in setting the resting membrane potential, the potential is usually near the K^+ reversal potential.

The delayed rectifier K^+ current (I_K) repolarizes neurons during the action potential. I_K activates slowly so that it only influences the membrane potential after the voltage-gated Na^+ current (I_{Na}) is inactivated. With no inactivation gate, once the membrane potential becomes hyperpolarized, the driving force for K^+ movement is lost and thus stops conducting K^+. As mentioned before, I_{KCa} regulates spike frequency adaptation. This is accomplished by its regulation of the AHP of the action potential. With the exception of the I_{KCa} mediated by SK channels, I_{KCa} is voltage-activated and modulated by Ca^{2+}. Just as increasing the voltage increases the K^+ conductance, so does increasing the Ca^{2+}. There are three main channel types, BK, IK and SK that possess different conductance values and Ca^{2+} dependences (Vergara et al. 1998). Whereas the BK channel has a voltage dependence independent of Ca^{2+}, the IK and SK channels have a relatively low voltage-dependence and rely on Ca^{2+} to be activated.

Therefore, these channels have a different effect on the afterhyperpolarization and consequently different SFA characteristics.

I_A is a subthreshold K^+ current that opposes the depolarization of the membrane potential thus affecting a neuron's response to presynaptic signaling. This current is interesting because a hyperpolarized membrane potential deinactivates the channel. Then when the membrane potential is quickly depolarized, the activation gate opens allowing K^+ to flow out of the cell. The current ceases when the inactivation gate closes which happens quickly giving the current its transient characteristic. These channels are located in the somatodendritic compartment of neurons and their intrinsic gating mechanisms make them suitable to regulate signaling between the dendrites and the soma (Johnston et al. 2000). For many cells, I_A acts as a shunting mechanism to limit the propagation of postsynaptic potentials to the soma. Therefore, it regulates how much presynaptic neurons affect the firing of the postsynaptic neuron. Another way that the expression of these channels affects neuronal communication is in coincidence detection. The back-propagation of action potentials in the postsynaptic neuron is necessary for spike timing-dependent LTP. Since I_A acts as a shunt, it can limit the back-propagation of action potentials (Harnett et al. 2013) thus limiting the coincidence detection that occurs to induce LTP (Ramakers and Storm 2002).

In sum, K^+ currents are vital to normal neuronal activity. Not only do they affect the intrinsic membrane properties during and in between action potentials, but also signaling between neurons as well. Therefore, the expression levels of the K^+ channels in neurons has an immense impact on firing activity.

2.2.6 Role of I_H in neuron firing properties

As mentioned before, I_H is responsible for the PIR found in many neurons. I_H is a nonselective cation current that conducts mostly Na^+, but also some K^+, when it is activated by hyperpolarization. This results in the depolarization of the membrane potential back towards the threshold. Not only is this property of the channel critical in half-center oscillators and locomotion, but also in pacemaking of neuronal activity, setting the resting membrane potential and integration of excitatory postsynaptic currents (Altomare et al. 2003; He et al. 2014).

I_H has been well-studied in heart myocytes and contributes to the pacemaking of the cells (Baruscotti et al. 2005). Just as I_A opposed the depolarization of the membrane potential in between action potentials to make the interspike interval longer, I_H enhances the depolarization of the membrane potential to decrease the interspike interval. I_H plays a large role in setting the interval and it is because of this it is considered a pacemaker current (Deng et al. 2014). When I_A and I_H are both present, both contribute to the interspike interval and can coregulate the interval.

I_H is mediated by hyperpolarization and cyclic nucleotide-activated (HCN) channels. Depending on which HCN channels are expressed, the half-activation may be anywhere from -70mV to -110mV. Therefore, they do contribute to the setting of the resting membrane potential. Further, when I_H is blocked by its specific blocker, ZD7288, the resting membrane potential becomes hyperpolarized.

Similar to I_A, I_H has the ability to affect the propagation of EPSPs from the dendrites to the soma. Since HCN channels are partially activated at the resting membrane potential, they decrease the input resistance of the cell. Therefore, the signal

is much larger in the distal dendrites and much smaller in the proximal dendrites. Depending on how the HCN channels are expressed in the dendrites they affect how postsynaptic potentials propagate to the soma (Rusznak et al. 2013).

2.2.7 Voltage-gated Na^+ channels are crucial for action potential generation

The voltage-gated Na^+ current (I_{Na}) is required for the fast depolarization phase of the action potential. I_{Na} is a transient current that depolarizes the cell toward the Na^+ equilibrium potential. Functional Na^+ channels contain one α pore-forming subunit and two β auxiliary subunits. The α subunit consists of SCN(1-9)A and the β consists of SCN(1-4)B gene transcripts (Aman et al. 2009). The threshold of the action potential is, at least partially, regulated by subunits expressed in the neuron. Regulation of the threshold ultimately affects the excitability of the neuron. With a lower threshold, less contribution of depolarizing subthreshold currents is required to fire an action potential.

The Na^+ channels that mediate I_{Na} are mainly expressed in the axonal compartment. Therefore, when the action potential is initiated in the axon hillock, the signal can be propagated down the axon to the terminal, thus initiating the release of neurotransmitters. The propagation of the action potential is a series of electrical self-stimulation. The movement of Na^+ into the cell depolarizes the local area of the membrane. This depolarization of the membrane causes the Na^+ channels to open next to it and the process repeats itself allowing the movement of the signal down the axon to the terminal.

2.2.8 Membrane ionic current regulation of mesencephalic trigeminal V neuron activity

Mesencephalic trigeminal V (Me5) neurons are propriosensory neurons that monitor the stretch and tension of jaw masseter muscles thus sending critical information to the motor neurons needed for coordinated movement. These neurons are the only propriosensory neurons that are located in the CNS. Most propriosensory neurons are located in the dorsal root ganglia. Me5 neurons receive signals from the muscle spindles and relay the information of the limb placement to the motor neurons (Hidaka et al. 1999; Luo et al. 2001). This controls movement of the limb by communicating with the inhibitory neurons innervating the muscles that control the antagonizing muscle.

The membrane currents found in the Me5 neurons are important for their response to stimuli from the jaw and synaptic inputs from cortical areas. The voltage-gated K^+ currents that are sensitive to tetraethylammonium (TEA) and 4-aminopyridine (4-AP) play a role in how the neuron responds to stimuli. Depending on the resting membrane potential at the time of depolarization, these neurons respond with either single action potentials or multiple action potentials (Del Negro and Chandler 1997). Blocking the current with 4-AP, caused the cells to respond to depolarization with only multiple action potentials. Therefore, the K^+ currents do play a role in Me5 neuron excitability.

A clear response of the Me5 neurons to a hyperpolarizing current injection is a strong sag and PIR. The sag is a depolarization of the membrane potential despite a sustained hyperpolarizing pulse. As stated before, the major contributor responsible for

the sag is I_H. The deactivation of I_H after the hyperpolarizing current injection is responsible for the PIR. Also, the presence of HCN channels provides a basis for dendritic integration and postsynaptic potential propagation to the soma. Since Me5 neurons receive input from muscle spindle fibers and synaptic inputs, I_H may play a large role with how Me5 neurons respond to stimuli.

There are several types of Na^+ currents in the Me5 neurons. Besides I_{Na} that controls the action potential initiation and propagation, there are the persistent Na^+ current (I_{NaP}) and the resurgent current (I_{NaR}) (Enomoto et al. 2007). Unlike, I_{Na} that inactivates very quickly, I_{NaP} does not inactivate. I_{NaP} induces bursting in these neurons and regulates resonance properties (Enomoto et al. 2006). I_{NaR} is much less studied than I_{Na} and I_{NaP}. I_{NaR} is a subthreshold current that is activated during repolarization but still is quickly inactivated. Studies indicate that I_{NaR} plays a role in spontaneous firing in neurons and multipeaked action potentials (Raman and Bean 1997).

2.3 Brainstem circuitry underlying autonomic behaviors

2.3.1 LC-ACh-GABA brainstem circuit

Within the dorsal pons of the brainstem near the lateral edge of the 4th ventricle is the locus coeruleus (LC). These neurons produce about 95% of the entire norepinephrine (NE) in the mammalian brain. NE has been shown to be involved with learning and memory, proper sleep, pain analgesia, breathing and attention (Brightwell and Taylor 2009; Doi and Ramirez 2008; O'Donnell et al. 2012). Therefore, the proper activity of LC neurons is very important to the maintenance of NE in the brain, thus keeping function and behavior normal.

The relationship between LC neurons and ACh neurons in the brainstem is very important for the transitions between rapid eye movement (REM) sleep and non-REM sleep. During REM sleep cholinergic neurons are very active. ACh is able to suppress the firing of LC neurons. Eventually, cholinergic neuron activity is decreased and LC neurons are able to start firing more causing the transition to a non-REM state during sleep.

GABAergic neurons are the main inhibitory neurons in the mammalian CNS. These neurons regulate neuronal excitability through synaptic transmission and through tonic release of GABA. During the transition from non-REM to REM sleep, cholinergic neurons excite GABAergic neurons which in turn silence the LC neurons through $GABA_A$ receptor- mediated synaptic transmission. $GABA_A$ receptors also mediate the tonic inhibition in the LC (Kawahara et al. 1999) which has been shown to be mediated by the Δ (Ye et al. 2013), α5 (Groen et al. 2014) and Θ subunits in other brain regions. Throughout the brain, GABAergic neurons play many roles by regulating neuronal activity. Within the brainstem, there are areas that regulate the neurons that are involved with breathing, pain analgesia, cranial motoneuron activity and heart rate. Besides these behaviors, GABAergic neurons from the forebrain send projections to the LC nucleus. This is important because NE plays a role in all of these behaviors. GABAergic neurons projecting from the central amygdala and the posterior lateral hypothalamic area seem to synapse on LC neurons at the dendrites (i.e., in the peri-LC region) (Dimitrov et al. 2013). Much less enter into the LC proper. Lastly, there is a local group of GABAergic neurons near the LC. These neurons are located in the peri-LC

region with many in the dendritic field (Aston-Jones et al. 2004). These neurons may be important for integrating information from afferents.

2.3.2 Neuronal activity during autonomic behavior

The autonomic system is involved in regulating involuntary behaviors such as breathing, body temperature and heart rate. NE, ACh and GABA have all shown to play a role in breathing. These neurotransmitters modulate the activity of pre-Bötzinger complex (PBC) neurons in the medulla oblongata (Doi and Ramirez 2008). PBC neurons are considered the center for breathing rhythmogenesis because the bursting of these neurons consistently corresponds to extracellular recordings of activity from the phrenic, vagus and hypoglossal nerves. All of which are involved in breathing but not rhythmogenesis.

NE, ACh and GABA affect the activity of PBC neurons. LC neurons fire tonically and the interspike interval seems to be related to the breathing rate (Zhang et al. 2011). Indeed, disruption in LC activity alters breathing. NE alters the activity of PBC neurons through two different mechanisms. First, the activation of α2 noradrenergic receptors is required for cadmium-insensitive bursting PBC neurons (Viemari et al. 2011). Second the activation of β-noradrenergic receptors increases the frequency of sighs during breathing. Further, NE modulation through β-noradrenergic receptors increases the frequency in PBC neurons by modulating I_{NaP} (Viemari et al. 2013). GABAergic neurons play a vital role in breathing as well. Blocking $GABA_A$ receptors increases the frequency and amplitude of the activity recorded from phrenic and hypoglossal nerves (Bongianni et al. 2010; Shao and Feldman 1997). This suggests that there is a baseline inhibitory input to the PBC which can be altered to regulate their firing properties. ACh is another

neurotransmitter that affects PBC activity and breathing. Activation of muscarinic receptors in the PBC leads to an increase in breathing frequency (Muere et al. 2013). It also decreases the normal PBC activity and increases the amount of sigh-causing bursts (Tryba et al. 2008).

It is clear that NE plays a large role in modulating breathing. Since about 95% of NE is produce in LC neurons, the modulation of LC activity by GABA and ACh is important. The majority of the GABA input to the LC is mediated by $GABA_A$ receptors. Indeed, $GABA_A$ agonists reduce the firing frequency, decrease input resistance and hyperpolarize the membrane potential in LC neurons (Jin et al. 2013a). Cholinergic modulation of LC activity has been shown to be mediated by nicotinic acetylcholine receptors (nAChR) (Cucchiaro et al. 2006; Ganesh et al. 2008). However, the activation of muscarinic receptors increases LC activity as well (Ennis and Shipley 1992; Yang et al. 2000). Our preliminary experiments showed that most of the cholinergic modulation of the increase in LC firing frequency was mediated by the nAChRs. Therefore, we studied how ACh modulates LC activity both through nAChRs postsynaptically and presynaptically at GABAergic neurons.

2.3.3 Expression of nAChRs in LC neurons

nAChRs are ligand-gated ion channels that are ionotropic receptors. In mammals, the nAChRs are found in the peripheral nervous system as well as the CNS. Each receptor is made up of five subunits with each subunit having four transmembrane domains. In the CNS of mammalian systems, two types of subunits (α and β) are expressed: α2-α7, α9-α10 and β2-β4 (Gotti et al. 2005). These eleven subunits can form a functional receptor with many different combinations of subunits. Further, many

subunits come together to form heteromeric receptors with the most prevalent consisting of α4β2 and α6β4 in the mammalian brain or they can be homomeric with most abundant channel being the α7 (Alkondon et al. 1997; Garduno et al. 2012; Yang et al. 2011). However, it is possible for the α9 receptor to form homomeric channels, but much of the time it is expressed with the α10 subunit (Boffi et al. 2013). The nAChR channel opens when two (in heteromers) or five molecules (in homomers) of acetylcholine (ACh) binds to the receptors allowing Na^+ to flow into the cell. In some cases, certain receptors may be more permeable to Ca^{2+}. The major effect of the nAChR activation on the cell is the depolarization of the membrane by the movement of cations into the cell. However, the Ca^{2+}-permeable receptors such as the α7, may also induce second messenger systems that affect various cellular processes (Gueorguiev et al. 2000; Nordman et al. 2014).

The LC has been shown to have many types of nAChR subunits expressed. Using immunohistochemistry (IHC), the α3, α4, α7 and β3 subunits were found throughout the LC nucleus suggesting these receptors play a strong role in cholinergic modulation of LC activity (Vincler and Eisenach 2003). To a much lesser extent, the α5, β2 and β4 were expressed as well but mostly in the dorsal portion of the LC. Also, it has been shown that the expression of nAChRs in the LC may be based on different cells within the nucleus (Lena et al. 1999). In rats, larger LC cells (capacitance > 65pF) had a larger response to cytisine, a nAChR agonist, than smaller LC cells (capacitance <45pF) suggesting differential expression of nAChRs. Indeed, single cell PCR showed that the larger cells showed a preference for expressing α6 and β3 whereas the smaller cells expressed α3 and β4 (Lena et al. 1999). It should be noted that both cell types

expressed other receptors but without the consistency of the ones mentioned. There is a wide diversity of nAChRs expressed in the LC. Based on IHC and electrophysiological data, LC activity should be significantly modulated by nAChRs.

2.4 Rett Syndrome

2.4.1 History

Rett Syndrome (RTT) was first described by Dr. Andreas Rett in 1966 and later by Dr. Bengt Hagberg (Hagberg et al. 1983). Hagberg was unaware of Rett's findings because they were published in German. Nonetheless, from the early findings of Rett to the later evidence provided by Hagberg, RTT was recognized as a major neurodevelopmental disorder. Until the 1983 publication by Hagberg, many physicians in the United States were unaware of the disease. As interest grew in determining the underlying causes of the disease, the Baylor Rett Syndrome clinic was established. The Zogbhi lab at Baylor determined that mutations in the *MECP2* gene underlies the problems found in RTT (Amir et al. 1999). Since this discovery, mouse models have been developed to study the consequences of the loss of proper MeCP2 function in an attempt to find a cure for the disease.

2.4.2 Progression and symptoms of RTT

RTT is neurodevelopmental disorder meaning it occurs through a progression of stages that can be clearly delineated by physicians during clinical exams. Normal development occurs for the first 6 months of life. In stage I, from 6 months to 1.5 years, the onset begins characterized by a stagnation of development in language and behavior skills. Stage II is usually defined by a regression of development and starts

between 1 and 4 years of age. The loss of communication skills and symptoms of mental retardation are evident as well. Many times during stage III, which can last up to many years, there is a period of the reacquiring of communication skills. By the onset of stage IV, patients lose the ability to walk and usually need wheelchairs for mobility. This last stage can last up to decades. In some of the less severe cases, women can live up to fifty years of age.

2.4.3 Mutations in the MECP2 gene underlies RTT

As mentioned above, mutations in the *MECP2* gene underlies RTT. There have been about 600 mutations detected in the *MECP2* gene. Most of these result in missense and nonsense mutants. Also, variations in the 5' UTR and 3' UTR, intron variations, insertions and deletions have been found. However, most of the mutations are found among exons 3 and 4. Further, most of the well-known mutations found in RTT are found in the methyl-CpG- binding domain and the transcriptional repression domain.

Random X-inactivation is a process that silences one of the 2 chromosomes found in females to avoid having twice the amount of proteins created than are found in males which only have one X chromosome. The designation of which X chromosome will be inactivated is random in mammals resulting in not only being inactive for the entirety of the cell's life but also to all its descendants as well. The inactivation is accomplished by condensing the X chromosome into heterochromatin that has structure in such a way that it is unable to be transcribed. Since most of the girls with RTT are heterozygous for the mutations in the Mecp2 gene, the random X-inactivation plays a large role in the phenotype of the disease. Therefore, in RTT depending on which X

chromosome is inactivated and in which cell type, the inactivation has a large effect on the severity and variety of symptoms.

2.4.4 NE deficiencies contribute to RTT symptoms

The reduction in NE is a hallmark of RTT. NE metabolites were diminished in cerebrospinal fluid in RTT victims (Zoghbi et al. 1989; Zoghbi et al. 1985). In *Mecp2*$^{-/Y}$ mouse models, NE reductions were seen at 14 days and 1 month after birth (Ide et al. 2005; Viemari et al. 2005). These reductions have been associated with breathing problems. The use of desipramine, a NE reuptake blocker, has been used to reduce breathing problems in *Mecp2*$^{-/Y}$ mice (Roux et al. 2007; Zanella et al. 2008; Zhang et al. 2011) . These data indicate that NE signaling is important for proper breathing.

The locus coeruleus (LC) provides about 95% of the norepinephrine to the brain. Therefore, disruption in the normal function of neurons from this nucleus can have adverse effects throughout the brain. We have shown in the Jiang lab that LC neurons from *Mecp2*$^{-/Y}$ mice are hyperexcitable, smaller in size than WT, have a lower action potential threshold and increased input resistance (Zhang et al. 2010a). The norepinephrine synthesizing enzymes tyrosine hydroxylase (TH) and dopamine-β-hydroxylase (DBH) are expressed much less in *Mecp2*$^{-/Y}$ mice (Zhang et al. 2010b). This indicates that the activity of LC neurons and subsequent release of NE are deficient in *Mecp2*$^{-/Y}$ mice. LC neurons are chemosensory neurons. This is thought to occur primarily by the sensing of pH by K_{ir} channels. The ability of LC neurons to sense changes in pH is defective in *Mecp2*$^{-/Y}$ mice. This has been attributed to alterations in the expression of K_{ir} channels (Zhang et al. 2011). Therefore, the chemosensory input

from the LC may be defective and likely due to insufficient NE release in the pre-Bötzinger complex, neurons thought to initiate breathing.

The GABA system is defective in RTT. Low GABA has been shown in cerebrospinal fluid of RTT patients (Perry et al. 1988). Also, there is an increase in GABA receptor expression in the basal ganglia of RTT victims (Blue et al. 1999). In *Mecp2*$^{-/Y}$ mice, GABA signaling is reduced in these mice and has been attributed to low glutamic acid decarboxylase (GAD) expression (Medrihan et al. 2008). The GABA modulation of LC neurons in *Mecp2*$^{-/Y}$ mice is defective as well. The $GABA_B$ receptor-mediated reduction in the K_{ir} current in *Mecp2*$^{-/Y}$ mice is defective and the mIPSC frequency and amplitude are reduced (Jin et al. 2013a). These defects seem to account for the decreased inhibition of LC firing activity in *Mecp2*$^{-/Y}$ mice. Further, the allopregnanolone modulation of $GABA_A$ receptor currents is defective which contribute to the hyperexcitability of LC neurons in *Mecp2*$^{-/Y}$ mice.

2.4.5 Motor system deficiencies underlie RTT symptoms

The most common feature of RTT investigated has been defects in breathing. However, the motor problems in RTT have received much less attention. These girls with RTT develop normally but the earliest symptoms involve the loss of muscle tone. Eventually, these girls have difficulties with coordinated and purposeful hand movements including a stereotypical hand-wringing movement or they place their hands in their mouths. As these girls become older, their posture is compromised and walking becomes almost impossible. Many times, these women become wheel chair bound.

Coordinated movement is not only controlled by motor neurons. The requirement for coordinated movement is proper function in the pyramidal, extrapyramidal and

propriosensory neuron systems. The pyramidal neurons control the contraction of muscles. The extrapyramidal system provides information to the motor neurons that help control muscle tone, joint angle and posture. Lastly, the propriosensory neurons provide feedback to the other systems about the place of the limb in space, the muscle force, and joint angles. Whereas motor neurons have been studied in RTT, extrapyramidal and propriosensory neurons have not.

It has been shown that the movement of limbs is deficient in RTT patients. These girls also have problems chewing and swallowing (Motil et al. 2012) and the difficulty in eating causes malnutrition. Therefore, the understanding of the complications caused by *MECP2* mutations in the motor system is important to developing therapies to help RTT patients. Propriosensory neurons of the mesencephalic trigeminal V (Me5) neurons are crucial for the coordinated movement required during mastication. Thus, we investigated the dysfunction of these neurons in RTT and provide evidence that Me5 neurons in *Mecp2*$^{-/Y}$ mice have altered membrane currents which seem to lead to hyperexcitability.

2.5 Mecp2$^{-/Y}$ mice as a model system

In order to study the ramifications of the various mutations in exons 3 and 4, many mouse model systems have been created. Some have been created that have specific mutations. The *Mecp2*^{tm1Vnar} or *Mecp2*^{*a140v} consists of a missense mutation that results in abnormal cellular morphologies in brain regions but no behavioral phenotypes in males. However, phenotypes in females are arbitrary because of random X-chromosome activation. A nonsense point mutation in *Mecp2*^{R168X} mice results in a truncated protein that seems to impair function tremendously. These animals present

many of the behavioral phenotypes found in other strains that have been widely used. Also, when exons 3 and 4 were knocked out of GABAergic neurons only in Viaat-*Mecp2* mice, the behavioral phenotypes found in these mice were similar to other mouse models (Chao et al. 2010). It is worth noting that not only do mice with limited MeCP2 expression, but the overexpression of MeCP2 has proven to be detrimental to animals as well. The overexpression of MeCP2 in mice causes abnormal nervous system phenotypes, cognitive behaviors and seizures (Na et al. 2012; Taylor and Doshi 2012) .

The model system chosen for this study is commonly referred to as the “bird model” named after the lab that originally created the strain. The *Mecp2*$^{tm1.1Bird}$ strain created with a deletion of exons 3 and 4 (Guy et al. 2001). The deletion of both exons in this model recapitulates all of the classical symptoms of RTT. The purpose of our studies was to study the general impact of the *Mecp2* gene mutations in neurons. Therefore, we used a common mouse model where exons 3 and 4 have been removed from the gene.

2.5.1 Benefits and drawbacks of the system

Every animal used in science as a model system has its positives and negatives. These mice have been created by removing exons 3 and 4. We know from human studies that over 600 known mutations have been discovered in girls suffering from RTT (Weng et al. 2011). Each mutation will have its own, varying effect on the system.

We use male animals to study a disease that affects females primarily. Human males still suffer from the disease, but they usually die at a very young age. That is the reason for us to think of it as a female disease. We study males because the abnormal movement, coordination and poor breathing are most prevalent in these animals. The

decrease in the severity of the female symptoms is presumably due to the random X-inactivation described above. Conducting experiments on female *Mecp2*$^{-/Y}$ mice may lead to confounding results. For example, it is very difficult to know if the cell that one is patch clamping expresses the normal Mecp2 gene or the knockout in female mice. Behavioral studies in female mice have seemed to be less conclusive as well. Therefore, male mice may not be a perfect model for the disease, but it is appropriate for studies that are not sex-related.

3 SIGNIFICANCE

RTT is a devastating disease with a high prevalence among females (Kerr et al. 1997). Not only do mutations in the *MECP2* gene cause autism-like features in RTT, it is also the origin of the breathing irregularities and motor dysfunction that underlie long-term disability and sudden death. Therefore, developing strategies to limit the impact of *MECP2* mutations on respiratory and movement centers in the CNS is necessary.

A cure for RTT has not been found. Many of the treatments are symptom-specific. NE and GABA reuptake blockers improve breathing in mouse models (Abdala et al. 2010; Roux et al. 2007; Zanella et al. 2008). Each of these drugs only improves a certain symptom, suggesting that multiple systems are affected. Indeed, recent studies suggest serotonergic agonists seem helpful for breathing in humans with RTT (Andaku et al. 2005; Gokben et al. 2012). Another important neurotransmitter system in the brainstem is the cholinergic system. Increasing cholinergic signaling improves movement problems (Nag and Berger-Sweeney 2007; Schaevitz et al. 2012). The cholinergic system interacts with the NE and GABA systems regulating arousal state

and other autonomic functions that are known to be defective in RTT. Therefore, information on how the cholinergic system is affected by the *Mecp2* disruption and how it interacts with NE and GABA systems is highly significant, and should impact the finding of novel therapeutic modalities for RTT.

The involvement of multiple neurotransmitter systems in RTT raises a new question as to how these neurotransmitter systems are regulated so that each is coordinated in the network and functions precisely in neuronal activity. The elaborate control of neurotransmitter release or homeostatic regulation may allow central neurons to respond to the deficiency in neurotransmitters and their receptors by upregulating another neurotransmitter system or other members within the defective neurotransmitter system. Such cell mechanisms are known as compensatory neuroadaptation that is widely seen in experimental gene knockout as well as naturally occurring genetic variations. Therefore, it is possible that the compensatory neuroadaptation takes place in receptors and ion channels caused by *Mecp2* disruption. We believe that demonstration of the compensatory neuroadaptation in *Mecp2*–null mice is significant, as this cellular mechanism may encourage further studies of the endogenously upregulated proteins that can be targeted by therapeutic agents. The information may also motivate people with RTT and their caretakers to actively boost or amplify the existing endogenous mechanisms in the body by changing their lifestyle and using more appropriate medication.

It is likely that the body can adapt to the *MECP2* defects to avoid a complete collapse of the system (death). The adaptations are not perfect since these women still struggle with normal tasks. If we can intervene with therapeutics and reinforce what the

body is doing already, it may reduce many of the complications associated with RTT. Therefore, the identification of mechanisms that are in place in neurons to maintain normal activity in *Mecp2*-null mice appears to be a significant first step towards finding the cure for the disease.

4 METHODS

4.1 Animals

All experimental procedures in the animal were conducted in accordance with the National Institutes of Health (NIH) *Guide for the Care and Use of Laboratory Animals* and were approved by the Georgia State University Institutional Animal Care and Use Committee. Female heterozygous *Mecp2*$^{tm1.\ 1Bird\ mice}$ with the genotype *Mecp2*$^{+/-}$ were purchased from the Jackson Laboratory (Bar Harbor, ME). *Mecp2*$^{+/-}$ females were crossed with WT C57BL/6 males to produce the *Mecp2*$^{-/Y}$ male mice. The Jackson Laboratory PCR protocol was used to confirm the *Mecp2*$^{-/Y}$ phenotype. The F1-generation of 3 week-old, *Mecp2*$^{-/Y}$ males were used and their age-matched littermates served as WT controls because overt symptoms do not show until 3 weeks.

4.2 Brain Slice Preparation

Brain slices were prepared as described previously (Cui et al. 2011; Zhang et al. 2010a). In brief, mice were decapitated after deep anesthesia with inhalation of saturated isoflurane. The brain stem was obtained rapidly and placed in an ice-cold, sucrose-rich artificial cerebrospinal fluid (sucrose aCSF) containing (in mM) 200 sucrose, 3 KCl, 2 $CaCl_2$, 2 $MgCl_2$, 26 $NaHCO_3$, 1.25 NaH_2PO_4 and 10 D-glucose. The solution was bubbled with 95% O_2 and 5% CO_2 (pH 7. 40). , Transverse pontine sections (250-300 µM) containing the LC area were obtained using a vibratome

sectioning system. The slices were transferred to normal aCSF in which the sucrose was substituted with 124 mM NaCl, allowed to recover at 33°C for 1 h, and then kept in room temperature before being used for recording. One of the slices was transferred to a recording chamber that was perfused with oxygenated aCSF at a rate of 2 ml/min and maintained at 34°C.

4.3 Identification of LC neurons

The LC neurons were identified by 1) their location between the pons and midbrain below the lateral end of the 4th ventricle, 2) their morphological characteristics, as seen under the CCD camera, and 3) their electrophysiological properties. Only neurons with stable resting membrane potentials (V_m) more negative than -40 mV and action potentials with amplitudes of >75 mV were used in the studies.

4.4 Identification of Me5 neurons

The Me5 neurons were identified by 1) their location between the pons and midbrain below the lateral end of the 4th ventricle and lateral to the locus coeruleus area 2) their morphological characteristics, as seen under the CCD camera, and 3) their electrophysiological properties. Only neurons with stable resting V_m more negative than -50 mV and action potentials with amplitudes of ≥60 mV were used in the studies.

4.5 Electrophysiology in LC neurons

Whole-cell voltage clamp and current clamp studies were performed on cells visualized using a near-infrared charge-coupled device (CCD) camera. Patch pipettes were pulled with a Sutter pipette puller (Model P-97, Novato, CA) with a resistance of 4–6 MΩ. The internal (pipette) solution for current clamp and whole cell nAChR current

voltage clamp recordings contained (in mM) 130 K gluconate, 10 KCl, 10 HEPES, 2 Mg-ATP, 0. 3 Na-GTP and 0. 4 EGTA (pH 7.30). The aCSF solution was applied to the bath, containing (in mM) 124 NaCl, 3 KCl, 1. 3 NaH_2PO_4, 2 $MgCl_2$, 10 D-glucose, 26 $NaHCO_3$, 2 $CaCl_2$ (pH 7.40 bubbled with 95% O_2 and 5% CO_2).The slices were perfused with the external solution continuously with superfusion of 95% O_2 and 5% CO_2 at 34°C. Whole-cell voltage clamp experiments were performed at a holding potential of –70mV. For whole-cell nAChR current experiments, the synaptic currents were blocked with the *N*-methyl-D-aspartate (NMDA) receptor antagonist, DL-2-Amino-5-phosphonopentanoic acid (DL-APV, 10μM), the α-amino-3-hydroxy-5-methyl-4-isoxazolepropionic acid (AMPA) receptor antagonist 6-cyano-7-nitroquinoxaline-2, 3-dione (CNQX, 5 μM), the glycine receptor antagonist strychnine (1 μM), the $GABA_A$ receptor antagonist, bicuculline (20μM) and the voltage-gated sodium channel blocker, tetrodotoxin (TTX, 0.5 μM). When acetylcholine (ACh) was applied, the muscarinic receptor antagonist, atropine (10μM) was used. The local perfusion pipette had a resistance of 0.5-1 MΩ and just prior to either 100μM ACh or 100 μM nicotine in 1s and 44nl with the Nanoject II (Drummond Scientific, Broomall, PA), the perfusion pipette was moved to within 20 to 30μm of the cell. Studies were conducted with food coloring to make sure the pipettes did not leak the drug and to make sure the drug diffused quickly in the bath. Immediately after drug application the perfusion pipette was removed from the bath. A minimum of 45 min was allowed between each drug treatment to eliminate any desensitization and no slice was exposed to the drug more than four times. After the current was elicited by the drug, the cell contents were harvested into the patch pipette with negative pressure and dropped into an Eppendorf tube containing 10XRT

buffer, RNase-free water and RNase out (4.5:4.5:1), and then quickly placed in liquid nitrogen until further processing. The cell capacitance was measured at the beginning of the recording and any recordings where the series resistance changed during the course of the experiment were rejected from further analysis. The internal pipette solution for spontaneous $GABA_A$ receptor-mediated inhibitory postsynaptic currents (sIPSCs) recordings contained (in mM): 50KCl, 2 $MgCl_2$, 85 CsCl, 2 Mg-ATP, 1 Na-GTP, 10 HEPES (pH 7.30). The external solution consisted of (in mM): 130 NaCl, 3. 5 KCl, 1. 25 NaH_2PO_4, 1. 5 $MgSO_4$, 10 D-glucose, 24 $NaHCO_3$, 2 $CaCl_2$ (pH 7.40 with 95% O_2 and 5% CO_2). The sIPSCs were pharmacologically isolated by using 5 µM CNQX, 10 µM DL-APV, and 1µM strychnine. The internal pipette solution for glutamatergic spontaneous excitatory post-synaptic currents (sEPSCs) contained (in mM): 135 Cs-methanesulfonate, 10 KCl, 1 $MgCl_2$, 10 HEPES, 4 MgATP, 0.3 NaGTP and 0.2 NaEGTA. The sEPSCs were isolated using 20µM bicuculline and 1µM strychnine. Recorded signals were amplified with an Axopatch 200B amplifier (Molecular Devices, Union City, CA), digitized at 10 kHz, filtered at 2 kHz, and collected with the Clampex 9.2 data acquisition software (Molecular Devices).

4.6 Electrophysiology in Me5 neurons

All experiments were performed on brains slices. Cells from at least 3 animals were used for data analysis. Patch pipettes were fabricated from borosilicate glass with a resistance of 4-6MΩ. For current clamp and I_H experiments, pipettes were filled with (in mM): K-gluconate 130, KCl 10, Mg-ATP 2, Na-GTP 0.3, HEPES 10, EGTA 0.4 with pH 7.35, and osmolarity 285 mmol/kg. NaCl (5mM) was included in the pipette solution when recording Na^+ currents. The bath solution for all recordings was regular aCSF.

The post-inhibitory rebound (PIR) was elicited by giving a series of hyperpolarizing current injections to the neuron. After the termination of the current injection, the cell responded with a rebound that was more depolarizing than the resting membrane potential. With step hyperpolarizations, the rebound became larger and larger until it reached threshold and fired an action potential. The PIR was defined as the difference between the peak depolarization (taken from the trace immediately before the action potential was elicited) and the resting membrane potential. Using the same recording as from the PIR, the sag was defined as the difference between the peak voltage during the current injection and the steady-state voltage. The sag activation time constant was determined using a single exponential Boltzmann equation. The I_H was elicited by using a step protocol from -140mV to +80mV. The half activation was determined by fitting the data from the tail current to a curve created by using a single exponential Boltzmann equation. The I_H activation time constant was calculated using a single exponential Boltzmann equation. The 4-Ethylphenylamino-1,2-dimethyl-6-methylaminopyrimidinium chloride (ZD7288, Tocris Bioscience) and cesium chloride (Sigma Aldrich) were used to block I_H. The Na^+ concentration was reduced from 140mM to 56mM when recording the Na^+ currents to reduce space clamp issues. For the Na^+ current experiments, the cell was held at -80mV. The Na^+ currents were elicited using a step protocol from -70mV to 100mV. A second step protocol was performed that had a preceding step to +20mV that lasted for 3.5ms to inactivate some K^+ currents. We digitally subtracted the 2nd trace from the 1st trace to minimize the K^+ currents in the analysis, To measure the inactivation of the Na^+ currents we performed a step protocol from -120 to +30mV that at the end had a depolarizing step held at +30mV for +80ms. The inactivation curve was

fit to data from this protocol using a Boltzmann equation. The threshold was determined using the maximum second derivative method (Sekerli et al. 2004). The Axopatch 200B (Molecular Devices) were used for current clamp and voltage-clamp experiments. Data were acquired using pCLAMP 9.0 sampled at 20kHz and filtered at 2kHz. Data were analyzed using Clampfit and AXUM.

4.7 Reverse Transcription

Reverse transcription was performed on tissue obtained from brain slice micropunches from either the LC or the Me5 area. The first strand cDNA synthesis was performed using the high capacity cDNA reverse transcription kit (Life Technologies, Grand Island, NY) per the manufacturer's instructions. The reverse transcription product was kept at -20°C until either single-cell PCR or qPCR was performed.

4.8 Single-cell PCR

PCR primers for the target genes were designed with the computer software program primer express (Applied Biosystems). PCR product lengths were ~200bp so as to not confuse them with primer dimers. 3µl of reverse transcription product was loaded into an Eppendorf tube with PCR solution containing 10µl of 5X green GoTaq flexi buffer, 2µl $MgCl_2$, 1µl of 10mM dNTP mix, 1µl of 10mM forward and reverse primers, 0.25µl of GoTaq polymerase and diluted to 50µl with nuclease –free water. The thermal cycling program was set to the initial denaturation for 5min at 95˚C for 1 cycle. The denaturation, annealing, extension cycles were done at 95˚C for 45s, 58˚C for 45s and 72˚C for 1min, respectively for 35 cycles. A final extension cycle was done at 72˚C for 10min. 3µl of the PCR reaction placed into a 2^{nd} PCR tube with the same solution as before. The same cycling protocol was performed as before. 20µl from the 2^{nd} PCR

reaction was run on a 2% agarose gel containing ethidium bromide. Gels were imaged using Alpha Innotech Imaging System (Alpha Innotech Corp., Santa Clara, CA). Images were taken normally and a second with a high background. Presence of receptor subunits in the LC cell was defined by having a band at the correct size regardless of strength. Cells that had lanes with smearing or possible degradation were eliminated from the experiment. Cells were tested for the glial fibrillary acidic protein (GFAP) transcript for possible glia contamination. Any cells with positive results for GFAP were eliminated from decay time analysis.

4.9 Quantitative PCR

qPCR primers for the target genes were designed with the computer software program primer express (Applied Biosystems). qPCR product lengths were ~200bp so as to not confuse them with primer dimers. For the qPCR, we used the SYBR select master mix (Applied Biosystems). 2µl of reverse transcription product was added to the master mix with 100nM of each primer. The directions for the PCR protocol were followed per the manufacturer's instructions. The qPCR was performed using the 7500 Real-Time PCR System (Applied Biosystems).

4.10 Data Analysis

The electrophysiological data were analyzed with Clampfit 10.3 software (Molecular Devices) and Mini Analysis Program 6.0.7 software (Synaptosoft Inc. New Jersey, USA). Decay time constants were determined using a single exponential equation in Clampfit. Data are presented as means ± SE. Statistical analysis of other parameters were performed using the ANOVA and/or the two-tailed Student's *t*-test. Difference was considered significant when $P \leq 0.05$.

5 ALTERATIONS IN THE CHOLINERGIC SYSTEM OF BRAINSTEM NEURONS IN A MOUSE MODEL OF RETT SYNDROME

Published as Oginsky MF, Cui N, Zhong W, Johnson CM and Jiang C. (2014) Alterations in the cholinergic system of brain stem neurons in a mouse model of Rett syndrome. Am J Physiol Cell Physiol. 2014 Sep 15;307(6):C508-20.

5.1 Acknowledgements

This work was supported by National Institute of Neurological Disorders and stroke Grant NS-073875 to Chun Jiang. Also, this work was supported by the Brains and Behavior fellowship to Max F. Oginsky.

5.2 Abstract

Rett syndrome (RTT) is an autism-spectrum disorder resulting from mutations to the X-linked gene, methyl-CpG binding protein 2 (MeCP2), which causes abnormalities in many systems. It is possible that the body may develop certain compensatory mechanisms to alleviate the abnormalities. The norepinephrine (NE) system originating mainly in the locus coeruleus (LC) is defective in RTT and *Mecp2*-null mice. LC neurons are subject to modulation by GABA, glutamate and acetylcholine (ACh), providing an ideal system to test the compensatory hypothesis. Here we show evidence for potential compensatory modulation of LC neurons by post- and presynaptic ACh inputs. We found that the post-synaptic currents of nicotinic acetylcholine receptors (nAChR) were smaller in amplitude and longer in decay time in the *Mecp2*-null mice than in the WT. Single cell PCR analysis showed a decrease in the expression of α3, α4, α7 and β3 subunits and an increase in the α5 and α6 subunits in the mutant mice. The α5 subunit

was present in many of the LC neurons with slow decay nAChR currents. The nicotinic modulation of spontaneous $GABA_A$–ergic IPSCs in LC neurons was enhanced in *Mecp2*-null mice. In contrast, the nAChR manipulation of glutamatergic input to LC neurons was unaffected in both groups of mice. Our current clamp studies showed that the modulation of LC neurons by ACh input was reduced moderately in *Mecp2*-null mice despite the major decrease in nAChR currents suggesting possible compensatory processes may take place, thus reducing the defects to a lesser extent in LC neurons.

5.3 Introduction

Rett syndrome (RTT) is an autism-spectrum disorder caused by mutations to the X-linked gene, methyl-CpG binding protein 2 (MeCP2)(Weng et al. 2011). The MeCP2 protein regulates transcription by binding to methylated DNA(Guy et al. 2011). Knockout of this gene in mouse models leads to neurodevelopmental abnormalities such as improper dendritic formation (Belichenko et al. 2009; Chapleau et al. 2009; Nguyen et al. 2012), impaired synaptic transmission (Belichenko et al. 2009; Chao et al. 2007; Shepherd and Katz 2011) and defective neurotransmitter-synthesizing enzyme expression (Chao et al. 2010; Zhang et al. 2010b), all of which resemble symptoms of RTT and may underlie the dysfunctional signaling between neurons.

People with RTT have defects in autonomic functions and brainstem neuromodulatory systems. Norepinephrine (NE) is a major neuromodulator in the central nervous system (CNS), that acts on breathing(Viemari et al. 2004; Viemari et al. 2011; Viemari and Ramirez 2006), cognition(Arnsten et al. 1988; Franowicz and Arnsten 1999; Murchison et al. 2011; Veyrac et al. 2007), motor movement, pain(Baba et al. 2000a; Baba et al. 2000b; Brightwell and Taylor 2009; Yoshizumi et al. 2012) and

paradoxical sleep(Carter et al. 2010; Dugger et al. 2012; Pal and Mallick 2007; Takahashi et al. 2010). The NE concentration is low in RTT patients and mouse models of RTT (Panayotis et al. 2011; Santos et al. 2010; Zoghbi et al. 1989; Zoghbi et al. 1985). Application of desipramine, a NE-reuptake blocker, ameliorates the breathing problems (Zanella et al. 2008; Zhang et al. 2011), further suggesting that the NE-ergic system plays a role in the *Mecp2*-null phenotype. NE-synthesizing neurons are found mainly in the locus coeruleus (LC) and project throughout the CNS. The NE deficiency appears to result from inadequate expression of tyrosine hydroxylase (TH) and dopamine-β-hydroxylase (DBH) in LC neurons of *Mecp2*$^{-/Y}$ mice (Zhang et al. 2010b). Other problems that may contribute to low NE include smaller cell size, defects in intrinsic membrane properties, and a decrease in CO_2 chemosensitivity (Taneja et al. 2009; Zhang et al. 2011). Recent studies have shown that defects in presynaptic modulation may affect normal LC neuronal activity as well. The GABA input to the LC is decreased with reduced IPSC frequency and amplitude (Jin et al. 2013a). Also, as opposed to 1-2 week old *Mecp2*$^{-/Y}$ mice, the allopregnanolone modulation of $GABA_A$ receptors in 3 week old *Mecp2*$^{-/Y}$ mice is reduced, which is consistent with the onset time of RTT-like symptoms in these mice (Jin et al. 2013b). Other studies indicate that glutamic acid decarboxylase (GAD), the enzyme responsible for GABA production, is down-regulated leading to less quantal release of GABA (Chao et al. 2010). Also, blocking of the GABA transporter results in higher synaptic GABA levels and RTT breathing symptoms are alleviated(Abdala et al. 2010). Lastly, when the *Mecp2* gene is knocked out of the GABA-ergic neurons only, RTT-like symptoms are apparent (Chao et

al. 2010). Therefore, defects in NE-ergic and GABA-ergic signaling systems contribute to the development of RTT symptoms.

A common link between the NE-ergic and GABA-ergic systems is the cholinergic system. Through nicotinic acetylcholine receptors (nAChR), TH and GAD expressions levels are regulated by the cholinergic system. The GAD expression levels are increased by the activation of α4β2 receptors causing phosphorylation of MeCP2 and release from DNA in cortical GABA-ergic neurons (Maloku et al. 2011). Less is known about the mechanism, but the TH expression levels are increased by activation of nAChRs in the LC (Osterhout et al. 2005) and the activation of α7 receptors in heterologous expression systems up-regulates TH and dopamine-β-hydroxylase (DBH) expression (Gueorguiev et al. 2000). The loss of cholinergic neurons (Wenk and Hauss-Wegrzyniak 1999) and a decline in activity of choline acetyltransferase, an enzyme for acetylcholine (ACh) biosynthesis (Wenk and Mobley 1996), impairs cholinergic signaling. The dysregulation of the cholinergic system is believed to underlie the down-regulation of the enzymes for GABA and NE biosynthesis.

These three systems are intimately linked in transitions between sleep states. During rapid eye movement (REM) sleep, cholinergic neuron activity is increased (for a full review (Pal and Mallick 2007)). In brief, acetylcholine silences LC neurons through GABA-ergic input during REM sleep. LC neurons eventually escape this GABA-mediated suppression and in turn cease cholinergic neuron firing during non-REM sleep. Children with RTT have sleep abnormalities (Carotenuto et al. 2013) which have been implicated in affecting cognition and memory (McCoy and Strecker 2011).

Therefore, determining the modulation of LC neurons by ACh and GABA inputs in the *Mecp2*$^{-/Y}$ mice may provide a basis for treatment in children with RTT.

Previous studies (Lena et al. 1999; Mitchell 1993; Vincler and Eisenach 2003) and our own preliminary experiments indicated that the major cholinergic modulation of presynaptic GABAergic and LC neurons occurs through nAChRs. The nAChRs are pentameric cation-selective ligand-gated channels, which are found throughout the CNS (Hogg et al. 2003; Romanelli et al. 2007). The nAChRs are abundant in LC neurons, and activation of these receptors leads to an increase in neurotransmitter release in several brain regions as well as the spinal cord (Hogg et al. 2003; Lena et al. 1999). The subunit composition of nAChRs in the CNS is highly diversified with major receptors consisting of homomeric α7, heteromeric α4β2, α6β4 and α9α10, although other combinations have the potential to form functional channels.

There is a wealth of information on how the cholinergic, NE-ergic and GABA-ergic systems work to affect various behaviors. However, it is not known how the signaling between these systems is compromised by neurodevelopmental diseases when all three are affected. Lately, disease models have been emphasized for study of RTT in an attempt to find possible pharmacological therapeutic approaches. However, it is unclear how the widespread defects caused by the *Mecp2* disruption affect multiple modulatory systems. We hypothesize that the presynaptic and postsynaptic cholinergic modulation of LC activity is compromised. Using patch clamp electrophysiology we studied presynaptic and postsynaptic cholinergic modulation of LC neurons in WT and *Mecp2*$^{-/Y}$ mice. This and single cell PCR allowed us to determine how changes in nAChR expression altered nicotinic current kinetics in *Mecp2*$^{-/Y}$ mice. Our results

suggest that the nicotinic receptor expression in LC and GABAergic neurons is altered to maintain the cholinergic modulation of LC neurons in *Mecp2*$^{-/Y}$ mice.

5.4 Results

5.4.1 The whole-cell nAChR currents were altered in Mecp2$^{-/Y}$ *mice*

LC neurons were studied in brain slices obtained from WT and *Mecp2*$^{-/Y}$ mice. We verified that the neuron was from the LC both visually and electrophysiologically as we did previously (Zhang et al. 2010a). nAChR currents were recorded from the LC neurons after the synaptic input was blocked with AP-5 (10μM), DNQX (5μM), bicuculline (20μM), strychnine (1μM), TTX (1μM) and the muscarinic receptor antagonist atropine (10μM). With the membrane potential held at -70mV in the voltage clamp mode, a local application of 100μM acetylcholine (ACh, 44nl, in 1s) to the LC area evoked large inward currents. The currents in the WT animal rose quickly, reached the peak and decayed rapidly (Fig. 5.1A). However, a long lasting current was observed in *Mecp2*$^{-/Y}$ cells (Fig. 5.1B). In comparison, the current amplitude was much larger in WT neurons than in *Mecp2*$^{-/Y}$ cells (-109.7 ± 12.2pA, n= 31 and -46.8 ± 12.7 pA, n=11, respectively; P<0.001, Mann-Whitney test; Fig. 5.1C), while the decay time was longer in *Mecp2*$^{-/Y}$ neurons. The time constant obtained by fitting the decay time of the nAChR currents with a single exponential equation was 2.4 ± 0.0.3 s (n=31) for the WT neurons and 6.1 ± 2.3 s (n=10) for the *Mecp2*$^{-/Y}$ (P<0.01; Mann-Whitney test; Fig. 1E). The longer decay time in *Mecp2*$^{-/Y}$ neurons was not due to the cell size, as LC neurons are smaller in *Mecp2*$^{-/Y}$ mice than in the WT(Zhang et al. 2010a). With the cell size taken into consideration, we compared the current density between the WT and *Mecp2*$^{-/Y}$ mice, which was -7.2 ± 1.0 pA/pF (n=31) and -4.4 ± 1.4 pA/pF (n=11), respectively

(P<0.05; Mann Whitney test; Fig. 5.1D). When we measured the area under the curve, we found that there was no difference between the WT and *Mecp2*$^{-/Y}$ mice (-202.0 ± 32.4nA•ms WT vs. -170.3 ± 101.8nA•ms; n=31 and n=11, respectively; student's *t*-test; P>0.05; Fig. 5.1F). These results suggest that the *Mecp2* knockout leads to nAChR currents that are smaller in amplitude but last longer as shown in the decay time.

Previous studies indicated that atropine, a muscarinic receptor antagonist, may interfere with nAChR activation (Zwart and Vijverberg 1997). Therefore, we verified the ACh results by applying nicotine, a specific nAChR agonist, without any atropine to the LC neuron during patch clamp recordings. A local application of 100μM nicotine (44nl, in 1s) resulted in larger currents in WT than in *Mecp2*$^{-/Y}$ mice (-122.7 ± 18.7 pA, n=10 in WT vs. -41.1 ± 3.1 pA, n=12 in *Mecp2*$^{-/Y}$; P<0.001; Mann-Whitney test*;* Fig. 5.2A-C). Nicotine elicited similar whole cell current characteristics as ACh. The nicotine current density differed significantly between WT and *Mecp2*$^{-/Y}$ (-7.7 ± 1.1 pA/pF WT vs. -2.8 ± 0.2 pA/pF *Mecp2*$^{-/Y}$*;* P<0.001; Mann-Whitney test; Fig. 5.2D), and the decay time constant was longer in *Mecp2*$^{-/Y}$ mice than in WT mice (2.7 ± 1.1s, n=10 in WT vs. 8.1 ± 0.7s, n=12 in *Mecp2*$^{-/Y}$; P<0.001; Mann-Whitney test; Fig. 5.2E). The area was not different either (-150.9 ± 34.6nA•ms vs. -107.09 ± 34.7nA•ms; n=10 and n=17, respectively; student's *t*-test; P>0.05; Fig. 5.2F).

5.4.2 The increase in decay time was attributable to alterations in nAChR subunit expression

The changes in the amplitude and kinetics of nAChR currents may be due to the alterations of the receptor species. Therefore, we analyzed the expression of nAChR

subunits (α2-7, α9, α10 and β2-4) in each LC neuron with distinct nAChR currents using the single-cell PCR assay. WT neurons expressed various combinations of α3, α4, α5, α6, α7, α9, β2 and β3 transcripts although they were not expressed in every neuron tested. Figure 3A shows the expression of α3, α4, α6, α7, α9 and β2, β3 in one LC neuron, whereas another cell expressed α3, α7, α9, and β3 (Fig. 5.3B). Of the 19 WT cells tested, the α7 and α9 transcripts were expressed in 14 and 18 cells, respectively (Fig. 5.3D). The α5 and α6 subunits were expressed in 3 and 1 cells, respectively. The α3 transcript was found in 9 cells, and the α4 subunit was found in 6 cells. The β3 subunit was seen in 16 neurons and the β2 subunit was only expressed in 2 cells and the β4 subunit was not expressed in any cell tested (Table 2).

LC neurons from *Mecp2*$^{-/Y}$ mice expressed only α3, α5, α6, α9 and β3 subunits. The α4 and α7, seen in most WT neurons, were not found in any of the 18 cells tested. Although the β3 subunit was found in *Mecp2*$^{-/Y}$ neurons (Fig. 5.3C), there was a major reduction in its expression which was seen in 8 of 18 cells in *Mecp2*$^{-/Y}$ mice instead of 16 of 19 in the WT. The only transcript that did not alter expression (in 17 out of 18 cells) was the α9 subunit. The α5 and α6 subunits were increased in the *Mecp2*$^{-/Y}$ mice with the α5 subunit expression increased from 3 WT cells to 8 *Mecp2*$^{-/Y}$ cells and the α6 subunit increased from 1 WT cell to 3 *Mecp2*$^{-/Y}$ cells.

In order to determine whether the increase in decay time in *Mecp2*$^{-/Y}$ neurons is attributable to alterations in the composition of nAChRs, we analyzed the decay times and subunit expression. Owing to the sampling sizes, we combined the data with the ACh and nicotine application. The WT decay time was shorter than the *Mecp2*$^{-/Y}$ mice (3.3 ± 0.7s WT vs. 6.7 ± 1.2s *Mecp2*$^{-/Y}$; n=19 WT and n=18 *Mecp2*$^{-/Y}$; $P<0.05$; Mann-

Whitney; Fig. 5.4A). Based on the single-cell PCR data and the fact that others have noticed the interchangeability of these subunits (Dash et al. 2011; Gotti et al. 2005), suggesting they may serve similar functions, the α5 and β3 subunits were likely candidates for the decay time changes. We compared decay times of cells that expressed either the α5 or β3 subunits, but not both. To do this, we omitted 4 cells from the group that contained α9 only and 2 cells that expressed both α5 and β3. When the α5 subunit was expressed, the decay time was 10.7 ± 2.5s (n = 6; Fig. 5.4B). When the β3 subunit was present in WT and *Mecp2*$^{-/Y}$ mice without α5, the time constants were similar (2.8 ± 0.5s WT vs. 4.23 ± 1.1s *Mecp2*$^{-/Y}$; n=14 WT and n=6 *Mecp2*$^{-/Y}$; student's *t*-test; P>0.3). When all 3 groups were compared to each other using a one-way ANOVA, significant differences were found between the *Mecp2*$^{-/Y}$ group expressing the α5 subunit and both β3- expressing groups (P<0.01). It is important to note that we also compared the current amplitudes in the *Mecp2*$^{-/Y}$ mice for when α5 and β3 were present or not, and found that there was no significant difference (data not shown).

The *Mecp2*$^{-/Y}$ mice had populations of cells that only contained combinations of either α9β3 or α9α5. By removing one cell that expressed the α9, α3 and β3 and another cell that expressed the α5, α6 and α9, we were able to take advantage of the expression patterns in these neurons to determine whether α5 and β3 play a role in decay time kinetics. We compared the decay time constants of these populations and found that the α9β3-expressing neurons had a shorter decay time constant than the α9α5-containing neurons (3.9 ± 1.2s α9β3 vs. 12.2 ± 2.5s α9α5; P<0.05; n=5 and n=5, respectively; Fig. 5.4C).

We also compared the contributions of the other subunits that were downregulated in the *Mecp2*$^{-/Y}$ mice. The α3, α4 and α7 were downregulated in the *Mecp2* knockout, which may contribute to the decrease in current amplitude and the increase in the decay time. Since these subunits were largely not present in the *Mecp2*$^{-/Y}$ mice, we compared the current amplitudes and decay times when the subunit was present or not in WT mice only. The presence of the α3 and α4 subunits did not have any significant effect on the amplitude or decay time of the current (data not shown). However, alteration in the nAChR current amplitude was seen depending on the presence of the α7 subunit (-134.6 ± 19.0pA α7 vs. -67.9 ± 9.9pA no α7; n=14 and n=5, respectively; student's *t*-test; $P<0.01$; Fig. 5.5A). The decay was longer when α7 was not present (2.8 ± 0.6s α7 vs. 5.7 ± 1.6s no α7; n=14 and n=5, respectively; student's *t*-test; $P<0.05$; Fig. 5.5B). By teasing apart the data to determine the contribution of the receptor subunits to the current amplitude and decay time, our data suggest that the lack of α7 contributes mostly to the decrease in the current amplitude in *Mecp2*$^{-/Y}$ mice and has some effect on the longer decay time, while the β3 subunit contributes to the shorter decay time constant and the α5 confers a longer decay time constant to the nAChR current. Therefore, the change of the subunit expression in the *Mecp2*$^{-/Y}$ mice appears to cause alterations in the nAChR currents. The increase in the proportion of cells with the α5 in *Mecp2*$^{-/Y}$ mice compared to WT and the decrease in the β3 subunit proportion allows for the decay time to be increased in the knockout mice.

5.4.3 GABA-ergic input but not glutamatergic input was augmented by nicotinic presynaptic modulation in Mecp2$^{-/Y}$ mice

The nAChRs modulate GABA and glutamate release in several brain areas. We chose to study sPSCs of $GABA_A$ and glutamate receptors, as they are the prominent synaptic currents in the CNS and are known to be dysregulated in RTT. To understand the presynaptic modulation of LC neurons by acetylcholine in *Mecp2*$^{-/Y}$ mice, we performed whole-cell patch clamp in the LC neurons and bath-applied the nAChR agonist DMPP (10μM). The $GABA_A$ sIPSC frequency was augmented by the DMPP application in LC neurons of WT and *Mecp2*$^{-/Y}$ mice, which was more obvious in the *Mecp2*$^{-/Y}$ mice by 189.0 ± 10.1% (n=8) than in the WT by 147.1 ± 7.0% (n=8) ($P<0.01$, Mann-Whitney test; Fig. 5.6A and B). The sIPSC amplitude was augmented in WT and *Mecp2*$^{-/Y}$ mice, to a lesser degree though (110.5 ± 7.6% WT vs. 105.4 ± 6.7% *Mecp2*$^{-/Y}$; Mann-Whitney; $P>0.05$; n=8 for both; Fig. 5.6A and C). These led to a shift of the inter-event interval cumulative probability to the higher frequency, which was greater in the *Mecp2*$^{-/Y}$ mice without evident shift in the amplitude cumulative probability (Fig. 5.6E & F). Consistently, the application of the nAChR antagonist mecamylamine (30μM) caused a reduction in $GABA_A$–mediated sIPSC frequency in WT mice to 78.2 ± 4.8% (n=11, Fig. 5.7A & C). There was little change in the amplitude (96.4 ± 3.5%; n=11in WT; Fig. 5.7D). The effect of mecamylamine on nicotinic modulation of GABA-ergic sIPSC frequency was lowered to 62.6 ± 4.5% (n=11) in *Mecp2*$^{-/Y}$ neurons (Fig. 5.7B & C), and the amplitude was unchanged 102.3 ± 4.0% (n=17; Fig. 5.7D). The shift to the lower frequency of inter-event interval cumulative probability was larger in the *Mecp2*$^{-/Y}$ mice than in WT (Fig. 5.7E). There was no shift in the amplitude cumulative probability

(Fig. 5.7F). The inhibition of sIPSC frequency by mecamylamine was significantly greater in *Mecp2*$^{-/Y}$ mice than that in the WT (P<0.01; Mann-Whitney), whereas the amplitude difference was not (P>0.05; Mann-Whitney).

A decrease in MeCP2 expression levels dysregulates the excitatory synaptic strength by reducing the number of glutamatergic synapses and by interrupting synaptic scaling mechanisms (Blackman et al. 2012; Lozada et al. 2012a). Also, α7 and β2 subunits are instrumental in synapse and spine formation (Lozada et al. 2012a; b). Because of this we tested whether the glutamatergic input to the LC is altered in *Mecp2*$^{-/Y}$ mice and whether the cholinergic modulation was dysfunctional as well. We recorded sEPSCs while applying DMPP (10μM). The baseline frequency was not different between WT and *Mecp2*$^{-/Y}$ (2.1 ± 0.5 Hz WT vs. 2.2 ± 0.6 Hz *Mecp2*$^{-/Y}$; n=11 and n=5, respectively). We found that there was an increase in frequency and amplitude after the DMPP application. This increase in frequency was seen in both groups of mice and showed no significant difference, though slightly smaller in the *Mecp2*$^{-/Y}$ mice (159.1 ± 12.8% WT vs. 145.0± 6.9% *Mecp2*$^{-/Y}$, n= 11 and n=5, respectively; P>0.05).

5.4.4 Cholinergic modulation of LC neuronal activity was sustained in Mecp2$^{-/Y}$ *mice despite a large decrease in nAChR currents*

In order to determine the consequences of the cholinergic modulatory dysfunction on the LC neuron firing activity we performed current clamp in WT and *Mecp2*$^{-/Y}$ mice. Bath-application of DMPP (10μM) increased the activity of LC neurons in WT mice from 4.5 ± 0.4 Hz to 6.7 ± 0.6 Hz (n=11; P<0.001; student's *t*-test. Fig. 5.8A and C), a 48% increase (Fig. 5.8E). The Input resistance was decreased from 424.8 ± 34.1 MΩ to 336.0 ± 27.5 MΩ (n=11; P<0.001; student's *t*-test; Fig. 8A), a 20% decrease

(Fig. 5.8F), and the neurons were depolarized from -45.9 ± 1.1 mV to -44.6 ± 1.2 mV (n=11; P>0.05; student's *t*-test; Fig. 5.8G). We also performed the same experiment by applying 50μM ACh (data not shown). There was very little difference between the ACh and DMPP treatments (~6%). This suggests very little muscarinic receptor influence on LC neuron postsynaptic properties. The DMPP treatment raised the LC neuronal firing activity in *Mecp2*$^{-/Y}$ mice from 3.8 ± 0.5 Hz to 5.2 ± 0.7 Hz (n=11; P<0.001; student's *t*-test; 5.8B and D), a 37% increase (Fig. 5.8E), and reduced the input resistance from 547.5 ± 67.7 MΩ to 454.4 ± 54.8 MΩ (n=11; P<0.001; student's t-test; 5.8B), a 17% decrease (Fig. 5.8F). The neuron was depolarized from -48.5 ± 2.2 mV to -46.3 ± 2.5 mV (n=11; P>0.05; student's *t*-test; Fig 5.8G). When the changes in firing frequency, input resistance and membrane potential were compared using the Mann-Whitney test, there were no differences between the WT and *Mecp2*$^{-/Y}$ mice (Fig 5.8E-G).

5.5 Discussion

In the present study we found that the postsynaptic nAChR currents in LC neurons of *Mecp2*$^{-/Y}$ mice is altered. This alteration in the current amplitude and decay time constant is likely due to changes in expression of specific nAChR subunits, namely the α5, β3 and α7. We also found that the nAChR modulation of GABA input to the LC is enhanced in *Mecp2*$^{-/Y}$ mice whereas the cholinergic modulation of glutamatergic input is unchanged.

5.5.1 Changes in nAChR subunit expression may be responsible for altered current

Previous studies have shown that nAChR mediated current characteristics can be attributed to the expression of the subunits by a particular cell. Many have used

pharmacological agents and molecular techniques to block different subunits and thus alter the amplitude and decay time constant of the current (Albuquerque et al. 1997; Alkondon and Albuquerque 1993; Alkondon et al. 1999; Rothlin et al. 2000) . This line of research leads one to some generalizations of the subunit contribution to the nAChR current. The α7 subunit is usually associated with a large transient peak whereas the α3 and α4 subunits are associated with smaller amplitude currents with a longer decay time (Flood et al. 1997; Liu and Berg 1999; Zhao et al. 2003). In single channel recordings, the α5 subunit increases the mean open time (Ciuraszkiewicz et al. 2013) and the insertion of β3 can shorten the decay time (Boorman et al. 2003). WT LC neurons display a variety of nAChR subunits that contribute to different kinetics of an elicited current (Lena et al. 1999). Consistent with these findings we found that these current changes are attributable to changes in subunit expression. The loss of α7 expression in the *Mecp2*$^{-/Y}$ group seems to underlie the decrease in the current amplitude. When we compared the current amplitudes for when α7 was present or not in WT mice, the absence of the α7 subunit caused a reduction in amplitude that was similar to the *Mecp2*$^{-/Y}$ amplitude. When we compared the decay times to the presence of certain receptor subunits, we found that the α5 and β3 seemed to make a large impact on it. The α5 seemed to confer a long decay time whereas the β3 subunit caused a short decay time. These data seem to suggest that since the α3, α4 and α7 are severely down-regulated in the *Mecp2*$^{-/Y}$ mice, there may be direct regulation of their expression by MeCP2 as opposed to the other subunits. The β3 is down-regulated by half which implies that it may be indirectly regulated by MeCP2 or not at all. Consequently, it may be altered by the overall changes in other receptors. Since MeCP2 is a transcription

repressor, the loss of function may result in a larger expression of the α5 subunit. However, it is still unclear which upstream proteins affect expression of the β3 or α5 subunits.

5.5.2 Adaptations in LC neurons of Mecp2$^{-/Y}$ mice

Maintaining homeostasis is essential for living and adapting to new environments, stimulations or perturbations. Much work has been done to study homeostatic mechanisms in the nervous systems of normal animals, while much less is known about how the body adapts to disease. The understanding of disease progression requires knowledge of how the system (body) acts to prevent the onset of symptoms or diminish them. However, compensation mechanisms for neuronal dysfunction in disease models have received relatively little attention. It is understandable when functional assay results do not show any difference between WT and the knockout, one would assume there is no change in the system. In the case here, we found that the nAChR whole-cell currents and receptor expression changed in the *Mecp2*$^{-/Y}$ mice without any cholinergic modulatory deficits to the LC neurons. Our data support the possibility that compensatory mechanisms may be in place to alleviate deficits in neurotransmission found in RTT.

Whether compensatory mechanisms exist in RTT is still elusive. We have found that the *Mecp2* knockout leads to a reduction in the nAChR current amplitude while the decay time of the currents is much longer. The decrease in amplitude is likely mediated by deficient expression of α7 subunits. However, it seems that the LC neurons are capable of limiting the effect of the reduction in amplitude by up-regulating α5 in the *Mecp2*$^{-/Y}$ mice. These changes lead to prolonged nAChR currents that appear to

maintain postsynaptic modulation of LC neurons. Concerning a difference in the cholinergic facilitation, the firing activity of *Mecp2*$^{-/Y}$ neurons was only 11% smaller (Fig. 8) than that of the WT in contrast to ~64% deficiency in the postsynaptic nAChR current amplitude (Fig. 2). Thus, these results are consistent with certain endogenous compensatory processes that may exist, allowing LC neurons to significantly diminish the consequences of *Mecp2* knockout defects**.** The question arises, can a current amplitude reduction of ~64% result in more than an 11% decrease in LC activity? We feel that it is highly likely. Based on the literature, nAChR activation has several effects on neurons that are consistent with this line of thought. Activation of nAChRs increases can induce cell firing from silence. When the α7 receptor is blocked, the action potential induction is blocked as well (Ji and Dani 2000). The firing frequency in area prostrema neurons are increased more with 30μM nicotine than with 10μM. nAChR activation also increases the excitability of these neurons thus causing an increased response to a depolarizing current (Funahashi et al. 2004). Further, Neurons can be depolarized and the input resistance decreases in a dose-dependent manner (Zhong et al. 2013). Lastly, we measured the area of the nAChR current by multiplying the current amplitude by the total time. When we compared the WT and *Mecp2*$^{-/Y}$ mice areas, they were not different (Fig. 1F & 2F). If the current amplitude was reduced without a change in the decay time constant, then the area would be much smaller. Since the total cation charge crossing the membrane would be much less, the changes in membrane potential, input resistance and firing frequency of LC neurons would be less. Here we do not see that. Therefore, it does seem that the changes in expression of subunits does have some positive effect on the cholinergic modulation of LC neurons. The decrease in α7 and β3

may indirectly contribute to the increase in the decay time as well. When we compared decay times based on the presence of α7 in WT mice, we found that when no α7 was present, the decay time was longer. Since no *Mecp2*$^{-/Y}$ mice expressed the α7 subunit, it is reasonable to assume the loss of α7 had some impact on the decay time constant. The impact of the loss of β3 may be substantial as well. In the 2 *Mecp2*$^{-/Y}$ cells that contained both α5 and β3, the cells had a short decay time. With this data and the fact that most WT cells with short decay times expressed β3, we can assume the β3 plays a large role in shaping the nAChR current decay. We studied mice at the age where the neurodevelopmental symptoms of RTT occur. At this age, if the cell is adapting to the loss of the α7 subunit by reducing β3 expression and increasing α5, then there may be a larger variability in the subunit expression here than one would see at older ages. Therefore, other studies should be done to thoroughly examine how the receptor subunit expression changes in LC neurons at different ages in WT and *Mecp2*$^{-/Y}$ mice.

The nAChR modulation of GABA-ergic inputs to the LC is enhanced in the *Mecp2*$^{-/Y}$ mice. This enhancement is likely caused by an increased sensitivity of the nAChR to DMPP. It is not clear if the increased sensitivity is due to an up-regulation of the same receptor subtype or an alteration in the composition of the nAChR. The α4β2, α7 and α6-containing nAChRs increase release of GABA through different mechanisms in different brain regions (Aracri et al. 2010; Nakamura and Jang 2010; Yang et al. 2011; Zappettini et al. 2011). One of these receptor types could mediate the increase in nAChR modulation of GABA release. Our data suggests that alterations in nAChR composition seem to occur in GABA-ergic neurons. However, an alternative hypothesis is that the α4β2 nAChR, a known regulator of GAD expression, is up-regulated to

compensate for the low GAD expression in GABA neurons. In this case, the increase in GABA release may be an unintended consequence to the up-regulation of the α4β2. In this second scenario, the disruption of normal MeCP2 function would have to be occurring through a different mechanism than in the LC or at different ages than we were testing.

The adaptations seen here at the neuronal level help to maintain proper modulation of LC neurons. One may make some predictions if these adaptations did not exist or were not compensatory. Due to the reduction in ACh release and subunit expression in animal models for RTT, If there were no compensatory mechanisms in place, the cholinergic modulation of LC neurons and GABA neurons would be much less. Here, we do not see this. We see that the LC modulation is relatively maintained and cholinergic modulation of GABAergic neurons is enhanced. If the adaptations were independent or linked with no compensatory benefit, then one would predict these values would be similar to a neuron with a nAChR current with a small amplitude and small decay. Thus, the cholinergic modulation of LC neurons would be greatly diminished.

In conclusion, our studies demonstrate several potential endogenous mechanisms underlying the avoidance of a total collapse of the LC system due to the *Mecp2* knockout. The up-regulation of the α5 subunit seems to increase the decay time of the whole cell nAChR current in *Mecp2*$^{-/Y}$ mice thereby reducing the impact of the major decrease in current amplitude by the down-regulation of the α7 subunit. This compensation seems to maintain some level of cholinergic modulation to the LC neurons. We have also shown that the nAChR modulation of GABA input to the LC is

enhanced in *Mecp2*$^{-/Y}$ mice, which appears to compensate for the defects in GABA-ergic input to LC neurons found previously. We believe that these findings are encouraging, as the information may help the design of a new generation of therapies by targeting possible endogenous compensatory mechanisms.

5.6 Figures

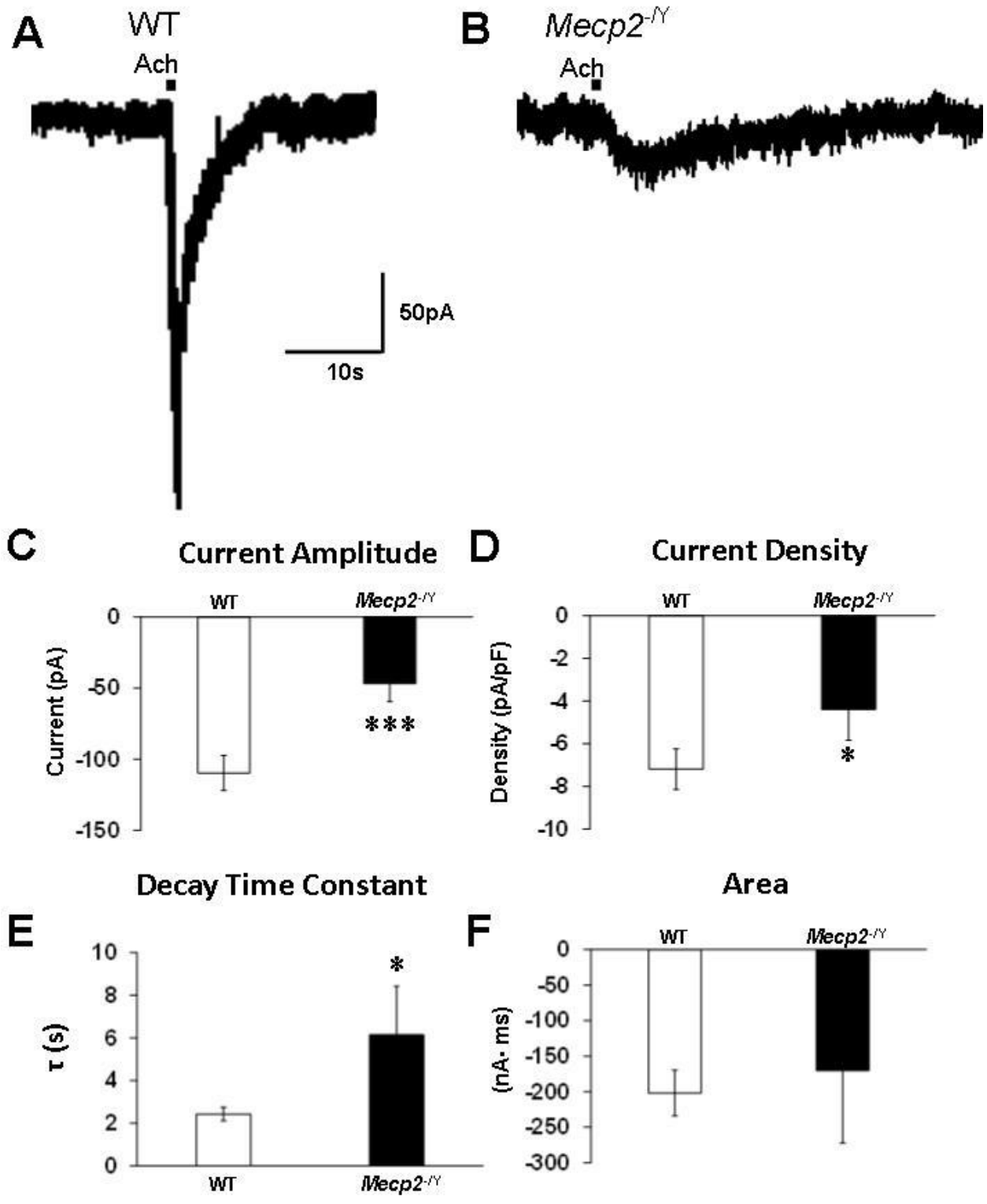

Figure 5.1 The nAChR currents were altered in LC neurons from *Mecp2*$^{-/Y}$ mice.

A: A 100µM ACh pulse (1s, 44nl) elicited a large transient current with a short decay time in LC neurons from WT mice *B:* A 100µM ACh pulse (1s, 44nl) elicited currents with a small amplitude and a long decay time in LC neurons *Mecp2*$^{-/Y}$ mice. *C:* The current amplitude was smaller in *Mecp2*$^{-/Y}$ mice than WT mice. *D:* The current density was smaller in *Mecp2*$^{-/Y}$ mice than WT mice. *E:* The decay time was longer in *Mecp2*$^{-/Y}$ mice than in WT mice. The decay time was determined using a single exponential equation. F. The area under the current curve measured by multiplying the amplitude by the time was similar between both groups. Bar graphs are means ± SE; n = 31 WT and n = 11 *Mecp2*$^{-/Y}$ (Mann-Whitney; $P < 0.05$ *, $P < 0.001$ ***)

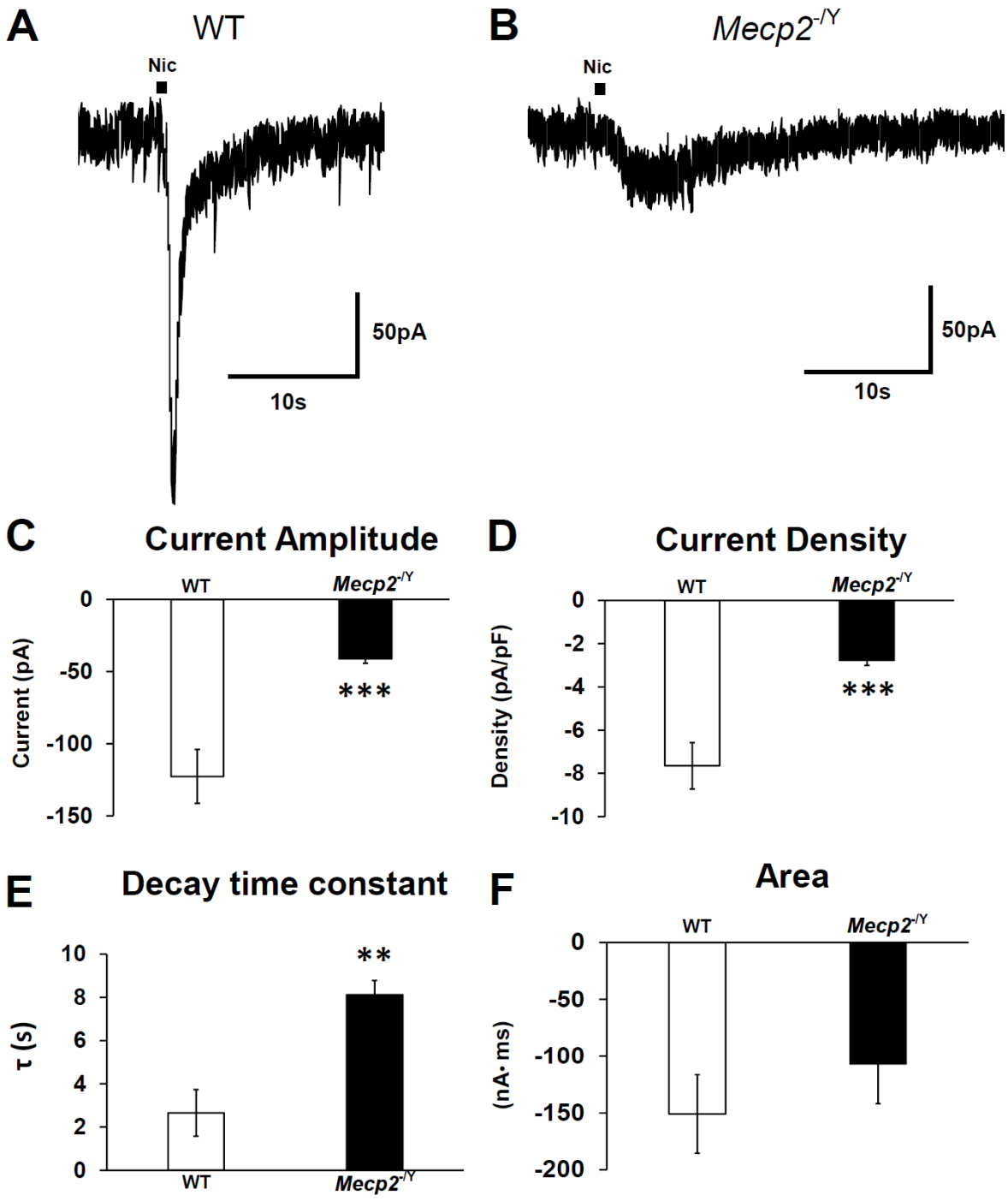

Figure 5.2 Nicotine elicited a similar current to ACh in WT and *Mecp2*$^{-/Y}$ mice.

A: 100µM nicotine pulse (1s, 44nl) elicited a large transient current with a short decay time in LC neurons from WT mice. *B:* A 100µM nicotine pulse (1s, 44nl) elicited a small amplitude current with a long decay time in LC neurons *Mecp2*$^{-/Y}$ mice. *C:* The current amplitude was smaller in *Mecp2*$^{-/Y}$ mice than WT mice. *D:* The current density was smaller in *Mecp2*$^{-/Y}$ mice than WT mice. *E:* The decay time is longer in *Mecp2*$^{-/Y}$ mice than in WT mice. The decay time was determined using a single exponential equation. F. The area under the current curve measured by multiplying the amplitude by the time was not significantly different between both groups. n = 10 WT and n = 12 *Mecp2*$^{-/Y}$; Mann-Whitney; $P < 0.01$ **, $P < 0.001$ ***.

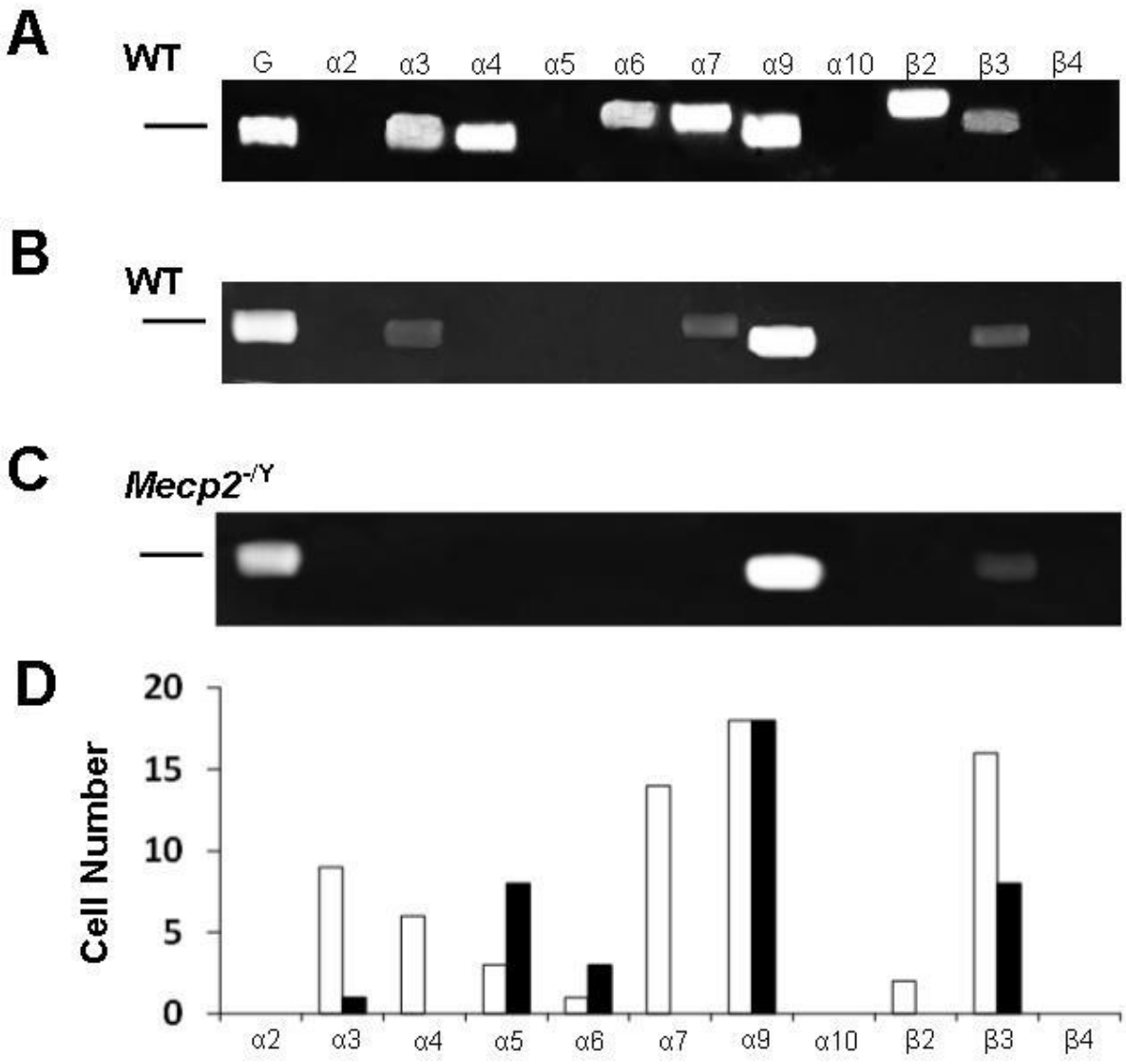

Figure 5.3 Receptor subunit expression in identified LC neurons.

Cytoplasm was extracted from LC neurons after local perfusion with either ACh or nicotine. *A:* nAChR expression from one WT LC neuron *B:* A second LC neuron showing a different expression pattern than in (A). *C:* nAChR expression in LC neuron from *Mecp2*$^{-/Y}$ mice *D:* Number of cells that contained each nAChR subunit. (n =19 cells WT and n =18 cells *Mecp2*$^{-/Y}$). Black bar is equal to 200 base-pairs.

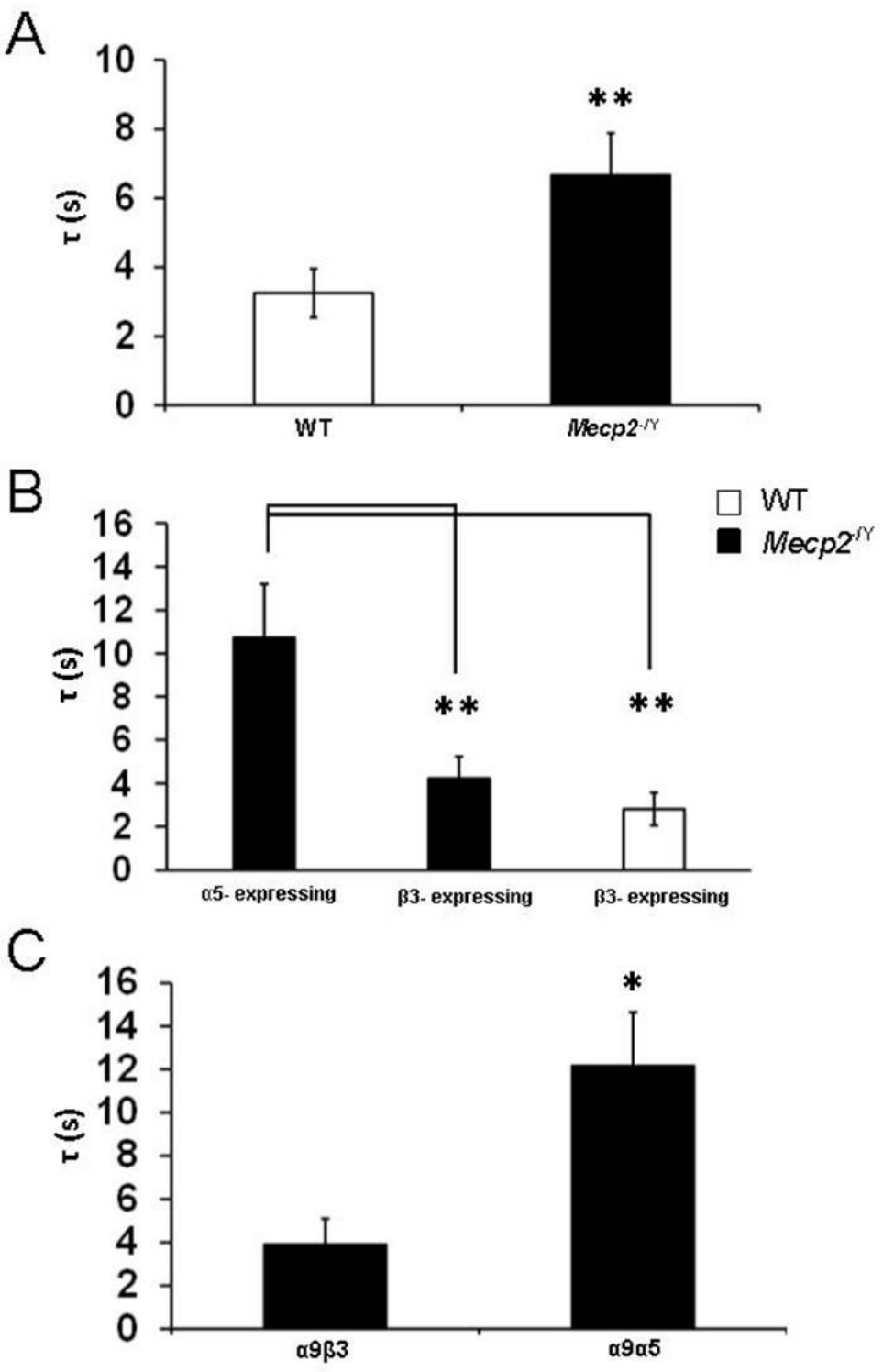

Figure 5.4 LC neurons from *Mecp2*$^{-/Y}$ mice expressing the α5 subunit had longer decay times than β3-expressing neurons.

White bars are data from WT mice and black bars are data from *Mecp2*$^{-/Y}$ mice. *A:* The nAChR current in LC neurons from *Mecp2*$^{-/Y}$ mice displayed longer decay times than WT mice; n = 19 and n = 18 (Mann-Whitney). *B:* α5-expressing LC neurons from *Mecp2*$^{-/Y}$ mice had a long decay time. β3- expressing LC neurons from WT and *Mecp2*$^{-/Y}$ mice had short decay times (n = 6 *Mecp2*$^{-/Y}$ with α5; n = 14 WT with β3, n = 6 *Mecp2*$^{-/Y}$ with β3 (one–way Anova) *C:* LC neurons from *Mecp2*$^{-/Y}$ mice that expressed α9α5 receptors had longer decay times than neurons that expressed α9β3 receptors (n = 5 α9α5 and n = 5 α9β3; Mann-Whitney). Bar graphs are means ± SE; (P < 0.05 *, P < 0.01 **)

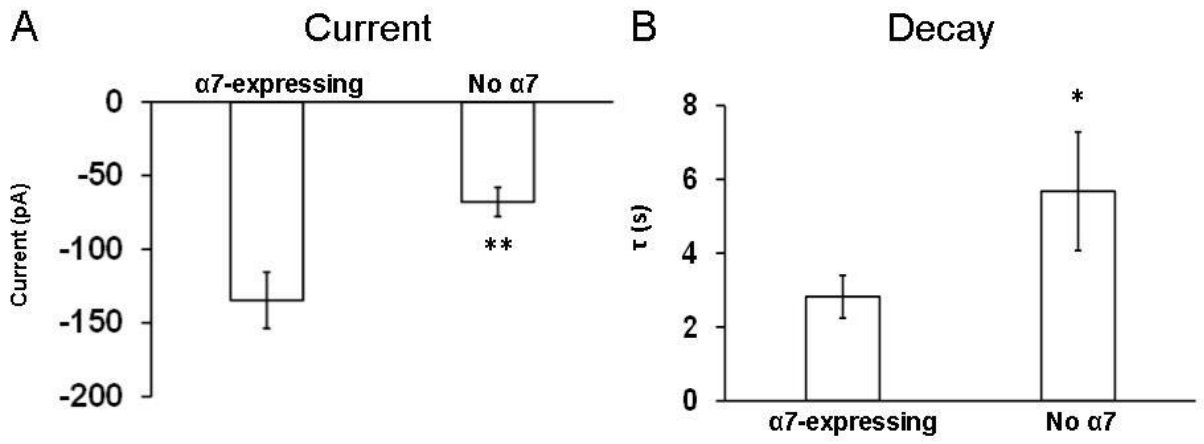

Figure 5.5 Presence of the α7 subunit affects the current amplitude and decay time constant in LC neurons from WT mice.

A. Cells expressing the α7 subunit have a larger whole cell nAChR current amplitude in WT mice than cells not expressing α7. *B.* Cells expressing the α7 subunit have a shorter whole cell nAChR current decay time constant in WT mice than cells not expressing α7. n= 14 α7 and n=5 No α7; student's t-test; P<0.05 *, P<0.01 **.

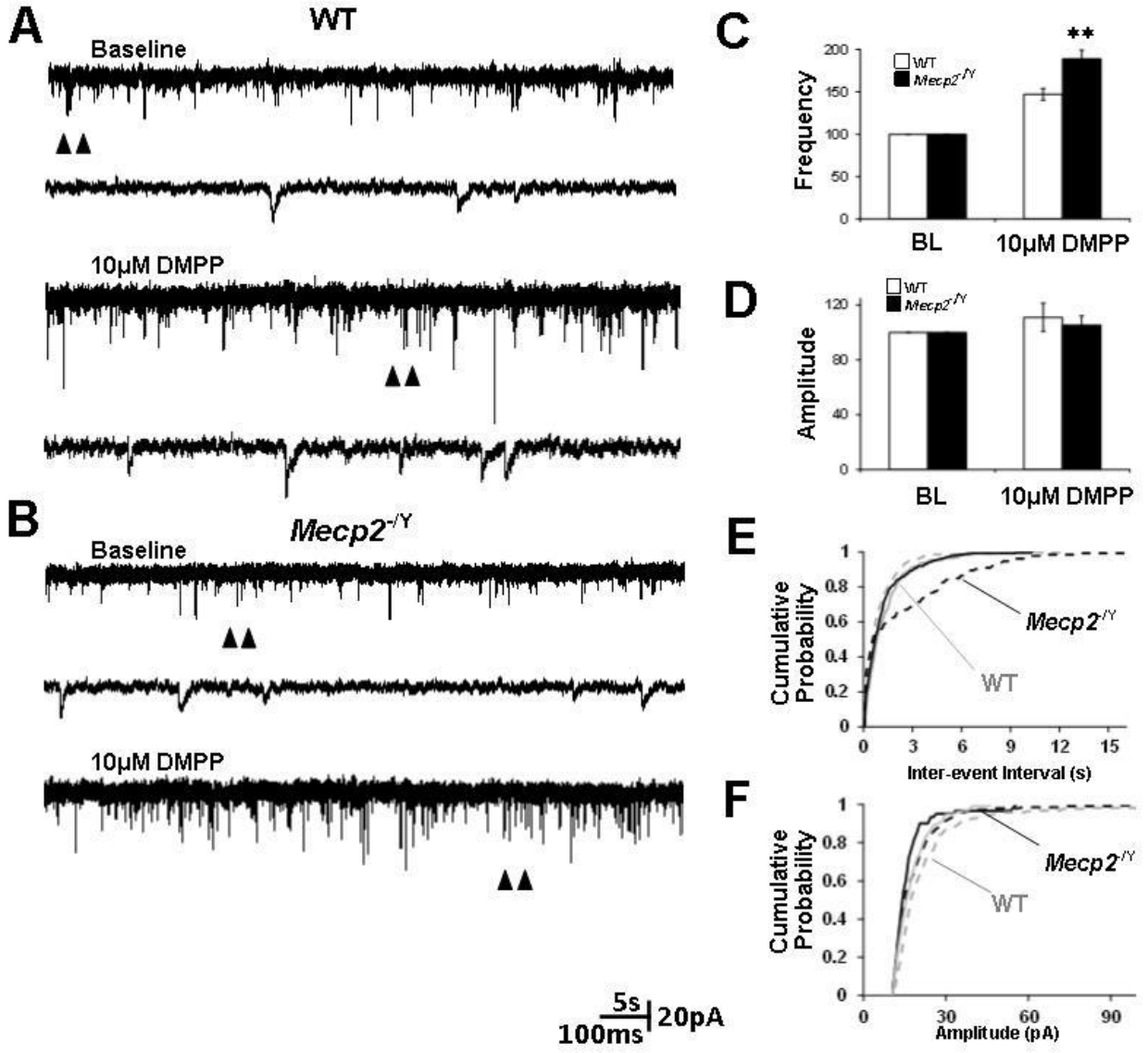

Figure 5.6 Cholinergic modulation of GABA-ergic input to LC neurons with nAChR agonist in *Mecp2*$^{-/Y}$ mice is enhanced compared to WT mice.

A: LC neurons of WT mice were patch clamped and GABA-ergic sIPSCs during the 5 min baseline and during a 5min, 10μM DMPP treatment were recorded. *B:* LC neurons of *Mecp2*$^{-/Y}$ mice were patch clamp and recordings during the 5 min baseline recording of GABA-ergic sIPSCs and during a 5min, 10μM DMPP treatment were taken.

C: The frequency increase seen in the WT mice was enhanced in *Mecp2*$^{-/Y}$ mice. *D:* The amplitude did not show a significant difference during DMPP treatment. There was no difference between WT and *Mecp2*$^{-/Y}$ mice as well. *E:* Cumulative fraction of Inter-event interval before and during 10μM DMPP treatment. Dashed lines are from baseline and the solid lines are from the 10μM DMPP treatment. Gray lines are from WT LC neurons and black lines are from *Mecp2*$^{-/Y}$ LC neurons. Shift to the left during DMPP treatment in *Mecp2*$^{-/Y}$ mice was greater than in WT mice. *F:* Cumulative fraction of amplitude before and during 10μM DMPP treatment. Dashed lines are from baseline and the solid lines are from the 10μM DMPP treatment. Gray lines are from WT LC neurons and black lines are from *Mecp2*$^{-/Y}$ LC neurons. *Mecp2*$^{-/Y}$ mice shifted due to the DMPP treatment. (n = 8 WT and n = 8 *Mecp2*$^{-/Y}$; Mann-Whitney; $P < 0.01$ **)

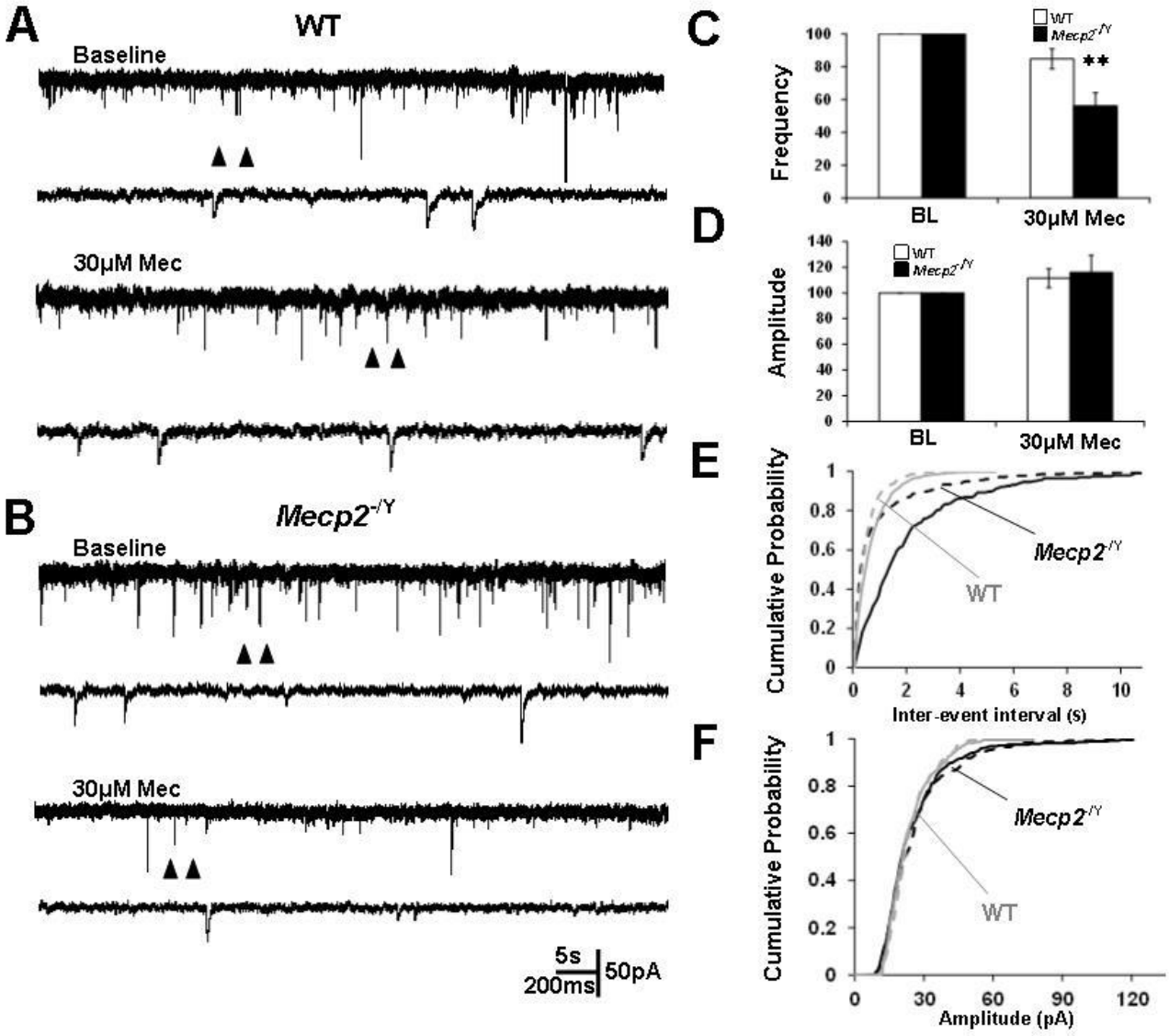

Figure 5.7 Cholinergic modulation of GABA inputs to the LC neurons with a nAChR antagonist is enhanced in *Mecp2*$^{-/Y}$ mice.

A: LC neurons of WT mice were patch clamped and GABA-ergic sIPSCs during the 5 min baseline and during a 5min, 30μM mecamylamine treatment were recorded. *B:* LC neurons of *Mecp2*$^{-/Y}$ mice were patch clamp and recordings during the 5 min baseline recording of GABA-ergic sIPSCs and during a 5min exposure to 30μM mecamylamine were taken. *C:* The frequency decrease seen in the WT mice was enhanced in *Mecp2*$^{-/Y}$ mice. *D:* The amplitude showed no significant difference during DMPP treatment. There was no difference between WT and *Mecp2*$^{-/Y}$ mice. *E:* Cumulative fraction of Inter-event

interval before and during 30μM mecamylamine treatment. Dashed lines are from baseline and the solid lines are from the 30μM mecamylamine treatment. Gray lines are from recordings of WT LC neurons and black lines are from *Mecp2*$^{-/Y}$ LC neurons. The shift to the right during mecamylamine treatment in *Mecp2*$^{-/Y}$ mice was greater than in WT mice. *F:* Cumulative fraction of amplitude before and during 30μM mecamylamine treatment. Dashed lines are from baseline and the solid lines indicate the 30μM mecamylamine treatment. Gray lines are from WT LC neurons and black lines are from *Mecp2*$^{-/Y}$ LC neurons. There is no shift between the baseline and drug treatment for both groups. Bar graphs are means ± SE; n = 9 WT and n = 17 *Mecp2*$^{-/Y}$ (Mann-Whitney; $P < 0.01$ **).

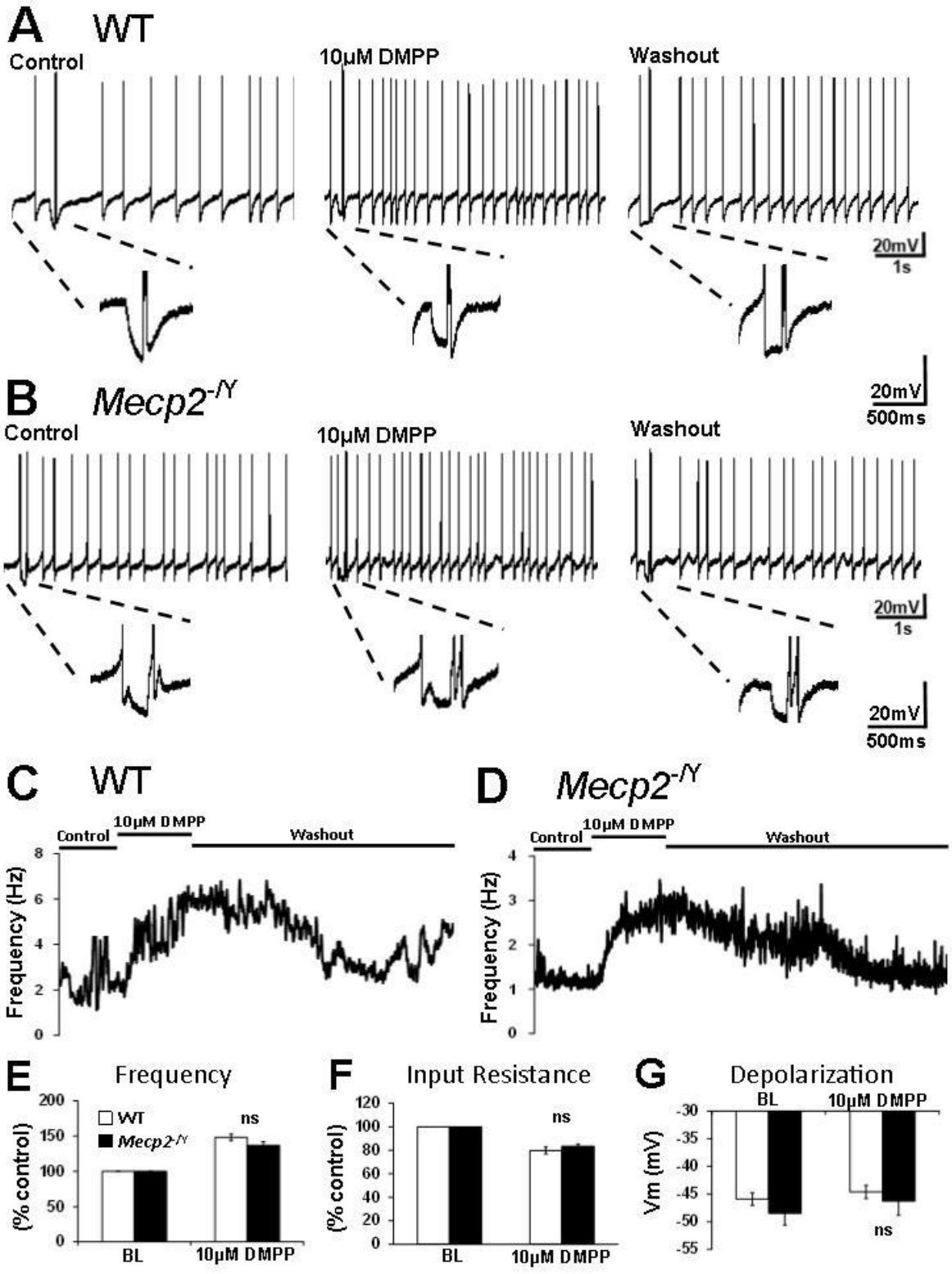

Figure 5.8 There is a small but insignificant difference in nicotinic modulation of LC neurons from WT and *Mecp2*$^{-/Y}$ mice.

A: Patch clamp recordings of LC neuronal firing activity in WT mice before, during and after 10μM DMPP treatment. Each inset is for the hyperpolarizing current indicating the input resistance. *B:* Patch clamp recordings of LC neuronal firing activity in *Mecp2*$^{-/Y}$ mice before, during and after 10μM DMPP treatment. Each inset is for the hyperpolarizing current indicating the input resistance. *C:* Frequency was analyzed from the recording made in (A). This shows that 10μM DMPP increases the frequency in WT mice. *D:* Frequency was analyzed from the recording in (B), and 10μM DMPP increased frequency in *Mecp2*$^{-/Y}$ mice. *E:* There was no significant difference in the increase in firing frequency between WT and *Mecp2*$^{-/Y}$ mice. *F:* The difference in input resistance modulation by 10μM DMPP between WT and *Mecp2*$^{-/Y}$ mice was insignificant. *G:* 10μM DMPP depolarized the LC neuron in WT and *Mecp2*$^{-/Y}$ mice. There was no significant difference between groups. Bar graphs are means ± SE; n = 11 WT and n = 13 *Mecp2*$^{-/Y}$ (Mann-Whitney; ns = Not Significant).

Table 4.1 Nicotinic Receptor PCR Primers

Target Gene		Primer Sequence	Accession No.
α2	Fw :	CTTTGGAGGCTACAATCGCTG	NM_144803
α2	Rv :	TTCCATTCCTGCTTTAGCCAG	
α3	Fw :	GACCTCCCAAACAGCATTGC	NM_145129
α3	Rv :	TCTGACAACCGAGGCACACA	
α4	Fw :	ACATGGAACAGGACCGCTG	NM_015730
α4	Rv :	ACAAAAGGCCGGCTGAGTG	
α5	Fw :	GCGCTCGATTGCATTCG	NM_176844
α5	Rv :	CCCTAGCGTCCCAATGATTG	
α6	Fw :	CCCCTGCCTCTTCATTTCC	NM_021369
α6	Rv :	ACCACAATGGACAGCGTG	
α7	Fw :	GCTGCAAAGAGCCATACCC	NM_007390
α7	Rv :	GATCTCAGCCACAAGCAGC	
α9	Fw :	CCAGCCATCACCAAAAGCTC	NM_001081104
α9	Rv :	ATGCCCTGAACCTCCCATTC	
α10	Fw :	ACTGGCTCACAAGCTGTTTCG	NM_001081424
α10	Rv :	CACCTCCAGGGTCACATTTAGAG	
β2	Fw :	CATTGCGGACCATATGCG	NM_009602
β2	Rv :	TCACGGGATGAGTAGCTGC	
β3	Fw :	CCAAGGCCATTGTGAAATCC	NM_009602
β3	Rv :	TCCGGTCAACGTTTCATTG	
β4	Fw :	TGGCTTGCACTGATCGCTC	NM_148944
β4	Rv :	AAATGAAAGACGGCCAGGG	
GAPDH	Fw :	CCAGCCTCGTCCCGTAGA	NM_008084
GAPDH	Rv :	TGCCGTGAGTGGAGTCATACTG	

6 HOMEOSTATIC REORGANIZATION OF HCN AND VOLTAGE-GATED NA^+ CHANNELS IN MESENCEPHALIC TRIGEMINAL PROPRIOSENSORY NEURONS OF A RETT SYNDROME MOUSE MODEL AND ITS IMPACT ON MEMBRANE EXCITABILITY

Submitted as Oginsky MF, Cui N, Zhong W, Johnson CM and Jiang C. Homeostatic reorganization of HCN and voltage-gated Na^+ channels in mesencephalic trigeminal propriosensory neurons of a Rett Syndrome mouse model and its impact on membrane excitability

6.1 Acknowledgements

This work was supported by the National Institute of Health (NS073875) to Chun Jiang. Also, this work was supported by the Brains and Behavior fellowship to Max F. Oginsky.

6.2 Abstract

RTT victims have motor defects seen in *Mecp2*-null mice as well. Motor neurons have been studied for possible roles in the movement abnormalities. However, propriosensory neurons, whose excitability can affect the feedback to motor neurons necessary for coordinated movement, have not. To address this issue, we studied the mesencephalic trigeminal (Me5) neurons. In whole-cell current clamp, the sag potential and PIR were reduced in *Mecp2*-null mice by ~35% and ~20%, respectively, suggesting a reduction in the hyperpolarization-activated current (I_H), a regulator of membrane excitability. In voltage-clamp, the I_H density was deficient by ~33%, and the steady-state

half-activation had a depolarizing shift of ~10mV in the *Mecp2*-null mice. Quantitative PCR analysis indicated that HCN2 was decreased by ~30%, and the HCN1 was upregulated by ~35% with no change in HCN4 in *Mecp2*$^{-/Y}$ mice compared to WT. Despite the major deficiency in I_H, the Me5 neurons were more excitable in *Mecp2*-null mice due to a decrease in the firing threshold. Consistently, the steady-state half-activation of voltage-gated Na^+ currents (I_{Na}) displayed a hyperpolarizing shift in the *Mecp2*-null mice with no change in the I_{Na} density. This seems to be due to NaV1.1, SCN1B and SCN4B overexpression and NaV1.2 and SCN3B under-expression. These data suggest that instead of disruption, the *Mecp2* knockout leads to reorganization of membrane ion channels, thereby reducing the impact of their defects on the membrane excitability of Me5 neurons.

6.3 Introduction

Rett syndrome (RTT) is an autism-spectrum disorder caused by mutations in the Methyl-CpG- binding protein 2 (*MECP2*) gene. People with RTT have motor defects that are also found in *Mecp2*$^{-/Y}$ mice. It is known that voluntary motor function relies on the pyramidal, extrapyramidal and propriosensory systems. Although defects in the motor systems have been described in humans (Chahrour and Zoghbi 2007; Hagberg et al. 1983; Rett 1966) and in mice (Blue et al. 1999; Jin et al. 2013c; Kao et al. 2013), there is still a lack of information of the propriosensory system with respect to changes in neuronal intrinsic membrane properties and cellular excitability. The propriosensory neurons act as a part of servo feedback control by providing motor neurons with essential information regarding muscle tension, joint angle, movement speed and spatial position of body parts (Cattaneo and Pavesi 2014; Winter et al. 2005).

Consequently, defects in proprioception play an important role in motor dysfunctions and diseases (Dietz and Duysens 2000; Patel et al. 2014).

The mesencephalic trigeminal nucleus (Me5) contains a group of neurons responsible for the proprioception of jaw and facial muscles (Hidaka et al. 1999; Kolta et al. 1990; Zakir et al. 2010). Defects in chewing and swallowing are seen in people with RTT (Isaacs et al. 2003; Motil et al. 2012) suggesting Me5 neurons may be affected. With clear anatomical location and morphological characteristics, these Me5 neurons are ideal for studying the effects of the *Mecp2* knockout on propriosensory neurons. Therefore, we performed these studies while paying special attention to ionic mechanisms underlying membrane excitability because changes in cellular excitability would affect proprioception and, ultimately, motor function.

Neuronal hyperexcitability has deleterious effects on various behaviors including movement (Vucic and Kiernan 2006; Zanette et al. 2002), anxiety (Davis et al. 1994; Zhou et al. 2010) and pain (Ke et al. 2012; Laedermann et al. 2013). Much work has been done on Me5 neurons concerning the ionic currents that underlie their excitability and activity (Del Negro and Chandler 1997; Enomoto et al. 2007; Enomoto et al. 2006; Hsiao et al. 2009; Khakh and Henderson 1998; Tanaka et al. 2003; Wu et al. 2005; Wu et al. 2001). In addition, blocking the various membrane currents in these neurons alters firing activity and neuronal excitability. Therefore, if the Mecp2 disruption affects ion channel expression, it will likely alter the excitability and proprioception function of the Me5 neurons.

In this study, we found that Me5 neurons in the *Mecp2*$^{-/Y}$ mice had major defects in the hyperpolarization-activated currents (I_H) and voltage-gated Na^+ currents (I_{Na}),

likely to result from abnormalities in the transcript expression levels of the subunits mediating the currents. These defects occur in a way that seems to reduce the impact of their changes on the membrane excitability. The seemingly normal homeostatic response to the defect in one current by changing another seems to prevent a drastic change in neuronal excitability and, presumably, the resultant devastating consequences of motor dysfunction.

6.4 Results

Several intrinsic membrane properties regulate cellular excitability, including the resting membrane potential, post-inhibitory rebound (PIR), firing threshold and repetitive firing, all of which were studied in Me5 neurons from both the WT and *Mecp2*$^{-/Y}$ mice. The average resting membrane potential was -56.3 ± 1.1mV WT (n= 33 neurons) vs. -56.3 ± 0.8mV *Mecp2*$^{-/Y}$ mice (n=30 neurons), which were not significantly different from each other (*p*=0.96).

6.4.1 Post-inhibitory rebound and sag in WT mice

With a series of hyperpolarizing currents, WT neurons displayed a large PIR (Fig 1A$_1$) and sag (Fig. 1A$_2$). The sag is the difference between the trough and the steady-state potentials (Fig. A$_3$), whereas the PIR is defined as the peak depolarization above the resting membrane potential immediately before firing (Fig. 1A$_4$). Measured at the sub-threshold firing level, the PIR and the sag averaged 14.9 ± 0.6mV (n=33 neurons, mean ± s.e.) and 63.8 ± 3.8mV (n=33 neurons), respectively (Fig. 1B). We compared the sag to its activation time constant using a Spearman's rank correlation and found that the larger the sag, the faster the time constant (r=0.66, Fig. 1C). A similar correlation was found between the PIR and sag (r=0.70, Fig. 1D). We calculated the

input resistance by dividing the peak potential by the injected current. We found that the resistance was 154.5 ± 12.4MΩ (n=33 neurons).

I_H is known to be the major player in both the sag and PIR. Thus, we blocked the I_H with ZD7288 (10μM). The ZD7288 treatment caused the sag and PIR to be greatly reduced (Fig. 1E_1-E_3). Such effects could mostly be washed out. The baseline PIR was reduced from 11.2 ± 0.8mV to 3.5 ± 0.5mV (n=6 neurons; P<0.001, Student's *t*-test; Fig. 1F) and the sag was reduced from 50.7 ± 7.8mV to 21.6 ± 5.0mV (n=6 neurons; P=0.010, Student's *t*-test; Fig. 1F). The resting membrane potential was hyperpolarized by the ZD7288 treatment from -52.9 ± 1.9mV to -59.1 ± 1.4mV (n=6 neurons; P<0.05, Student's *t*-test).

6.4.2 Decreases of PIR and sag in Mecp2$^{-/Y}$ mice

In comparison to WT Me5 neurons, the sag (immediately before firing) was reduced in the *Mecp2*$^{-/Y}$ mice (63.8 ± 3.8mV WT vs. 42.2 ± 3.3mV *Mecp2*$^{-/Y}$, n=33 and n=30 neurons, respectively; P<0.001, Student's *t*-test; Fig. 2A and C). The PIR (immediately before firing) was reduced as well (14.9 ± 0.6 mV WT vs. 10.8 ± 0.6mV *Mecp2*$^{-/Y}$, n=33 and n=30 neurons, respectively; P<0.001, Student's *t*-test; Fig. 2B and D). In order to determine the relationship between the sag amplitude and PIR amplitude, we compared them in a conventional scatter plot (Fig. 2E). Me5 neurons from *Mecp2*$^{-/Y}$ mice and WT mice overlapped to some degree. However, many of the WT Me5 neurons displayed relationships with large PIR and sag amplitudes whereas the *Mecp2*-null neurons displayed relationships with small PIR and sag amplitudes. These data indicate that the relationship between the sag and PIR indeed holds true in the *Mecp2*$^{-/Y}$ mice, just at smaller amplitudes compared to WT. The time constant for the sag was

significantly different between these neurons as well (18.1 ± 2.1ms in WT vs 27.0 ± 3.3ms in *Mecp2*$^{-/Y}$, n=33 and n=30 neurons, respectively; P<0.05, Student's *t*-test; Fig. 2F). Lastly, we found that the input resistance was increased from 154.5 ± 12.4MΩ WT (n=33 neurons) to 218.2 ± 26.7MΩ *Mecp2*$^{-/Y}$ (n=30 neurons) which was significantly different (P<0.05, Student's *t*-test).

6.4.3 Reduction in I_H in Mecp2$^{-/Y}$ mice

Based on the current clamp data and the ZD7288 effects, it is likely that I_H is involved the sag and PIR. Thus, we measured I_H in voltage clamp before and after ZD7288 treatment (Fig. 3A and $3A_2$). When we took the difference between them, we found that most of the inward currents elicited by our voltage protocol were the I_H (Fig. $3A_3$). Then, we examined the steady-state activation of the I_H by measuring the tail currents (Fig. $3A_1$) resulting from the return to -70mV after step command voltages. For the cell in Fig. $3A_1$, the maximum amplitude of I_H was -743.5pA. The voltage for half-activation ($V_{½}$) determined by fitting the data with the Boltzmann equation was -83.0mV with the slope Boltzmann constant, *k*, 15.0mV (Fig. 3B). In the I/V plot, the neuron in Fig. $3A_3$ had a reversal potential ~-30mV (Fig 3C) indicating a combination of Na^+ and K^+ for the currents, which is a characteristic of I_H. We were able to confirm that it was I_H by blocking the currents with 1mM Cs^+, a concentration known to block I_H mostly rather than K^+ currents (-1,937 ± 178pA at baseline vs. -568 ± 97pA with Cs^+, n=10 neurons, P<0.001; Student's *t*-test; Fig. 3D). Consistently, the specific I_H blocker ZD7288 suppressed the currents (-960 ± 180pA at baseline vs. -221.6 ± 7.7pA with ZD7288, n=8 neurons, P<0.001; Student's *t*-test; Fig. 3E).

To analyze the difference of I_H between the WT and *Mecp2*$^{-/Y}$ mice, we applied the same voltage-clamp protocol to *Mecp2*-null neurons. The I_H from *Mecp2*$^{-/Y}$ mice was much smaller than that from the WT (Fig. 4A & B). The current density in Me5 neurons from *Mecp2*$^{-/Y}$ mice was lower as well. When the cell was voltage-clamped at -130mV, the current density was 16.0 ± 0.8 pA/pF in WT vs. 10.1 ± 1.7 pA/pF in *Mecp2*$^{-/Y}$ (n=26 WT neurons and n=13 *Mecp2*$^{-/Y}$ neurons; P<0.001, Student's *t*-test; Fig. 4D). When the steady-state activation was compared between WT and *Mecp2*$^{-/Y}$ mice, we found that the $V_{½}$ was shifted toward more depolarizing potentials (-82.6 ± 1.5mV vs. -72.5 ± 2.7mV in 10 WT and 9 *Mecp2*$^{-/Y}$ neurons, respectively; P<0.01; Student's *t*-test; Fig. 4E & F). Furthermore, the activation time constant was longer in the *Mecp2*$^{-/Y}$ mice than in the WT (48.5 ± 3.2ms vs. 72.4 ± 8.9ms in 18 WT and in 17 *Mecp2*$^{-/Y}$ neurons, respectively*;* P<0.05; Student's *t*-test; Fig. 4C and G).

6.4.4 Impact on firing and repetitive firing activity

The reduction in I_H and the PIR should affect firing activity in Me5 neurons of *Mecp2*$^{-/Y}$ mice. Since these cells did not fire action potentials spontaneously, we studied the firing activity by giving a series of depolarizing currents. We found that in 13 of 18 WT neurons, only single action potentials were elicited (Fig. 5A and C), whereas the other 5 cells fired multiple action potentials during the depolarizing pulses. In contrast, 18 of 23 *Mecp2*-null neurons fired multiple action potentials in response to the same depolarizing current protocol, whereas only 5 cells fired single action potentials (Fig. 5B and C). The difference in their ratios was statistically significant (P<0.001, χ^2 test).

When we compared the frequency of action potentials during the depolarizing current injection between these mice, the overall firing rate was significantly higher in

Mecp2$^{-/Y}$ mice than in the WT (Fig. 5D). For example, when the Me5 neuron was injected with 290pA, the *Mecp2*$^{-/Y}$ firing frequency was 166.3 ± 30.7Hz (n=10 neurons) whereas the WT was 30.3 ± 14.1Hz (n=10 neurons; P<0.001, Student's *t*-test; Fig. 5D). There was little difference in spike frequency adaptation in Me5 neurons from WT and *Mecp2*$^{-/Y}$ mice (data not shown). These results suggest that the cellular excitability is increased in *Mecp2*–null neurons.

The increased cellular excitability in *Mecp2*-null neurons was quite surprising, with the decrease in the I_H we expected these neurons to be less excitable. Although reduction in the I_H was partially compensated by the shift in the $V_{½}$ to more depolarizing potentials, the average PIR remained small in *Mecp2*-null neurons (as mentioned above). It is likely that mechanisms other than the I_H may play a role. Thus, we analyzed the firing threshold using the maximum second derivative method (Sekerli et al. 2004). We found that the threshold was -34.7 ± 1.0mV in WT vs. 41.3± 1.1mV in the *Mecp2*$^{-/Y}$ (n=26 and n=25 neurons, respectively; P<0.001 Student's *t*-test; Fig. 5E and F). The latency to first spike was not significantly different (2.83 ± 0.26ms WT vs. 2.78 ± 0.22ms *Mecp2*$^{-/Y}$, n=21 and n=23 neurons, respectively; P>0.05; Student's *t*-test; Fig. 5G). These results indicate that despite the decreases in I_H and PIR, the firing threshold is reduced in *Mecp2*-null neurons making the cells more excitable in response to depolarization input.

6.4.5 Alteration of voltage-gated Na^+ currents in Mecp2$^{-/Y}$ mice

It is possible that the decreased firing threshold is attributable to the voltage-gated Na^+ currents (I_{Na}). Thus, we analyzed I_{Na} in voltage clamp. To minimize the space-clamp error, we reduced the extracellular Na^+ to 56mM instead of 145mM in

regular ACSF. The I_{Na} amplitude was about the same between the WT and *Mecp2*$^{-/Y}$ mice (-6.8 ± 0.7nA WT vs. -6.8 ± 0.6nA *Mecp2*$^{-/Y}$, n=8 neurons for both; Student's *t*-test, P>0.05, Fig. 6A & B). The current density was not significantly different either (-145.5 ± 15.4pA/pF in WT vs. -151.4 ± 15.4pA/pF in *Mecp2*$^{-/Y}$, n=8 neurons for both; P>0.05, Student's *t*-test; Fig. 6C). When the steady-state activation and inactivation of I_{Na} were compared between these neurons, we found that the activation curve was shifted to more hyperpolarizing potentials in *Mecp2*$^{-/Y}$ mice (Fig. 6D). The $V_{½}$ was -19.6 ± 2.6mV (n=8 neurons) for the WT and -25.9 ± 3.1mV (n=8 neurons) for the *Mecp2*$^{-/Y}$ mice, consistent with the decrease in firing threshold in the *Mecp2*-null neurons. In contrast, the I_{Na} inactivation was not significantly different between WT and *Mecp2*$^{-/Y}$ mice, which was fit with the same Boltzmann equation (Fig. 6D).

6.4.6 Evidence for altered expression of HCN and Na$^+$ channels in Mecp2$^{-/Y}$ mice

The changes in I_H may be related to alterations in the expression of the major pore-forming subunits that mediate the I_H. Thus, we performed qPCR analysis to determine the hyperpolarization-activated and cyclic nucleotide-gated (HCN) transcript levels in WT and *Mecp2*$^{-/Y}$ mice. Using the $2^{-\Delta CT}$ method in comparison to glyceraldehyde 3-phosphate dehydrogenase (GAPDH) (Livak and Schmittgen 2001), we found that in micropunches from WT mice the HCN2 transcripts were expressed the most (n=9 experiments) compared to GAPDH, the HCN1 and HCN4 transcripts were next (n=9 and n=8 experiments, respectively; Fig. 7A). The difference in the HCN2 expression was significantly different from HCN1 and HCN4 (one-way ANOVA, Fig. 7A). No significant difference was found between HCN1 and HCN4. When the relative quantity of HCN expression was compared to that of the WT using the $2^{-\Delta\Delta CT}$ method,

we found that HCN2 in the *Mecp2*$^{-/Y}$ mice was reduced (P<0.001; Student's *t*-test; n=9 experiments, Fig. 7B). In contrast, the HCN1 transcript expression was increased to (P<0.001; Student's *t*-test; n=9 experiments; Fig. 7B), and the HCN4 expression remained unchanged (P>0.05; Student's *t*-test; n=8 experiments, Fig. 7B).

Since functional Na^+ channels consist of one α and two auxiliary β subunits which can affect the current kinetics, we performed qPCR on the four CNS-expressing α subunits (NaV1.1, 1.2, 1.3 and 1.6) and four β subunits (SCN(1-4)B). We compared the expression levels of each subunit to GAPDH using the $2^{-\Delta CT}$ method. The NaV1.2 and SCN1B were the most abundant subunits in the WT group (n=9 experiments for both; Fig. 8A), followed by SCN2B (n=8 experiments), NaV1.6 (n=9 experiments), NaV1.1 (n=9 experiments), SCN3B (n=9 experiments) and SCN4B (n=9 experiments). The NaV1.3 was expressed in a very low level (n=9 experiments).

When the relative expression of these Na^+ channel subunits was compared between the WT and *Mecp2*$^{-/Y}$ mouse, we found that the most abundant subunit, NaV1.2 was decreased (n=9 experiments; P<0.001, Student's *t*-test; Fig. 8B) and another abundant subunit, SCN1B, was increased (n=9 experiments; P<0.05, Student's *t*-test; Fig. 8B). The lesser expressed subunits, NaV1.1 and SCN4B were increased (n=9 experiments for both; P<0.001NaV1.1 and P<0.001SNC4B, Student's *t*-test; Fig. 8B) and SCN3B was decreased (n=9 experiments; P<0.01, Student's *t*-test; Fig. 8B). NaV1.3, NaV1.6 and SCN2 expression levels were altered very little in the *Mecp2*$^{-/Y}$ mice compared to WT (n=6 experiments; n=8 experiments; n=8 experiments, respectively; Fig.8B).

6.5 Discussion

In the present study, we provide first evidence for dysfunction in propriosensory neurons of *Mecp2*$^{-/Y}$ mice. We find that the sag potential and the PIR are greatly reduced in Me5 neurons from *Mecp2*$^{-/Y}$ mice, due to a decrease in I_H. However, the *Mecp2*-null Me5 neurons do not show a decrease in excitability, but are hyperexcitable instead. Our results suggest that the hyperexcitability of the Me5 neurons results from a reduction in the firing threshold, attributable to a hyperpolarizing shift in the I_{Na} $V_{½}$ of activation. The molecular basis for the changes in I_H and I_{Na} properties seems to be related to changes in the channel expression levels.

6.5.1 I_H alterations in Mecp2$^{-/Y}$ mice

The I_H is produced by HCN channels and plays a role in many different functions such as PIR, setting of the resting membrane potential, regulation of membrane excitability, pacemaking, integrating synaptic input and bursting of action potentials (Chan et al. 2011; Li et al. 2012; Lupica et al. 2001; Nolan et al. 2007; Ying et al. 2011). All four HCN transcripts have been reported in the rodent brain (Santoro et al. 2000). In Me5 neurons of the *Mecp2*$^{-/Y}$ mice, the I_H density is decreased by ~30%, consistent with reductions in the sag and PIR. Its $V_{½}$ of activation displays a depolarizing shift of ~10mV. We find that in WT mice the HCN2 is expressed the most, with HCN1 an order of magnitude less and HCN4 two orders less. The HCN3 transcript is not detected in the Me5 area. In the *Mecp2*$^{-/Y}$ mice, the HCN2 expression is reduced by ~30% and the HCN1 was increased by ~35% with no change in HCN4. Therefore, the HCN2 deficiency in *Mecp2*-null neurons appears to underlie the decrease in the I_H density.

The alterations in the HCN transcript expression may explain the changes in the I_H properties as well. Concerning the activation $V_{½}$ in WT animals, the $V_{½}$ is ~ −70mV for HCN1, ~ −100mV for HCN4, and −75mV to −95mV for HCN2 and HCN3, respectively (Altomare et al. 2003; Baruscotti et al. 2005; Stieber et al. 2005; Wahl-Schott and Biel 2009). The *Mecp2*-null Me5 neurons show an increase in HCN1 expression and a decrease in HCN2 expression. The expression level of HCN2 is 10-fold higher than HCN1 in Me5 neurons of WT mice. Thus, a 30% reduction in the HCN2 expression appears to be the main reason for the shift in the activation $V_{½}$ of I_H.

A decrease in the I_H density would result in a decrease in membrane excitability. (Deng et al. 2014; Funahashi et al. 2003; Kim and Holt 2013). The unexpected increase in the excitability in *Mecp2*-null neurons, despite the decrease in the I_H density, may be attributed to the depolarizing shift in the $V_{½}$ of activation. Although the combination of the reduction in HCN2 and increase in HCN1 may explain the decrease in the I_H current density and the activation $V_{½}$ shift to a depolarizing potential, it cannot explain the decrease in firing threshold. Therefore, we studied the voltage-gated Na^+ currents.

6.5.2 I_{Na} alterations in Mecp2$^{-/Y}$ mice

Functional Na^+ channels consist of one large α subunit (NaV 1.1 to 1.9) and two smaller auxiliary β (β1-β4) subunits. The α subunits are responsible for voltage-dependent gating properties, whereas the β subunits modify the gating, Na^+ channel expression and cell adhesion (Patino et al. 2011). Our voltage clamp experiments showed a hyperpolarizing shift of the $V_{½}$ of activation by ~5mV in the *Mecp2*$^{-/Y}$ mice. We have found alterations in the expression of NaV1.1, NaV1.2 and SCN1B, SCN3B

and SCN4B indicating a cause for the hyperpolarizing shift in the V½ of activation and firing threshold.

Previous studies indicate that the level of NaV1.2 is reduced in LC neurons from *Mecp2*$^{-/Y}$ mice (Zhang et al. 2010a). We find similar results in Me5 neurons including that the NaV1.2 is the most expressed α subunit in the WT mice. The SCN1B and SCN4B expressions are increased in *Mecp2*$^{-/Y}$ mice compared to WT. These two subunits modulate the V½ of activation in Na^+ currents by causing a hyperpolarizing shift (Aman et al. 2009; Barela et al. 2006). Currents involving the NaV1.2 show more positive activation V½ values than currents composed of the other α subunits (OuYang and Hemmings 2007; Rush et al. 2005; Xu et al. 2007), whereas the NaV1.1 mediated currents tend to have more negative V½ values than other subunits. Taken together, these data indicate that the hyperpolarizing shift in the V½ of activation is due to alterations in the transcript expression of the NaV1.1, NaV1.2, SCN1B and SCN4B Na^+ channel subunits. Based on other studies (Dai et al. 2002; Power et al. 2012), it is likely that the shift in the V½ underlies the decreased threshold found in the Me5 neurons.

6.5.3 Homeostatic reorganization of HCN and voltage-gated Na^+ channels in Mecp2$^{-/Y}$ mice

Me5 neurons are propriosensory cells that monitor, and respond to, muscle stretch through muscle spindles and Golgi tendon organs. Neuroanatomical studies indicate that not only do Me5 neurons innervate trigeminal motor neurons, but also premotor interneurons in the supratrigeminal nucleus, spinal trigeminal subnucleus and parvocellular reticular formation (Luo et al. 2001). Many of these interneurons are inhibitory which also play a role in coordinated movements (Turman and Chandler

1994). Through these interneurons, motor neurons for mastication and facial expression are regulated by Me5 neuronal activity, thereby affecting the coordinated and rhythmic mastication as well as meaningful facial expression.

In *Mecp2*$^{-/Y}$ mice, the Me5 neurons show defects in both I_H and I_{Na}, likely because of the defective expression of several subunits of these channels. The defects in these ion channels seem to counterbalance each other, as the I_H defects tend to reduce membrane excitability, and the I_{Na} defects tend to increase it, thereby reducing any possible negative consequences. A straightforward explanation for this phenomenon is that there may be a physiological homeostatic compensatory mechanism in these neurons, although which current initiates the homeostatic reorganization of the other is still unclear. Regardless of the cause vs. the compensator, the impact of the homeostatic reorganization is very clear. Without the homeostatic reorganization, the Me5 neurons would either be severely hypoexcitable or extremely hyperexcitable, which would make the voluntary movement of jaw and certain facial muscles very difficult or maybe even impossible. Despite the homeostatic reorganization, the Me5 neurons are somewhat hyperexcitable due to the decrease in firing threshold. However imperfect this may be, it seems to be more beneficial than if the homeostatic reorganization of these ion channels did not occur at all.

6.5.4 Other possible contributors to the intrinsic hyperexcitability

There has been much work that shows neuronal excitability is regulated by K^+ currents (Barros et al. 1994; Gryshchenko et al. 1999; Perez et al. 2006) and the persistent Na^+ currents (I_{NaP}) (Astman et al. 1998; Vervaeke et al. 2006). The inwardly rectifying K^+ currents (I_{Kir}) that are present in Me5 neurons (Del Negro and Chandler

1997; Tanaka et al. 2003) are altered in LC neurons of *Mecp2*$^{-/Y}$ mice (Zhang et al. 2011). Although the I_{Kir} regulates cell excitability, we did not see any difference in Me5 neurons when we blocked I_{Kir} with Ba^{2+} (data not shown). There is an increased I_{NaP} in cardiomyocytes from *Mecp2*$^{-/Y}$ mice (McCauley et al. 2011) but no studies have been performed on neurons. I_{NaP} does play a role in regulating the excitability and bursting in Me5 neurons (Enomoto et al. 2006; Wu et al. 2005) and the knockout of NaV1.6 decreases the I_{NaP} and excitability in Me5 neurons (Enomoto et al. 2007). Since we see no change in NaV1.6 expression here, NaV1.6 is unlikely to affect the excitability in *Mecp2*-null Me5 neurons. It is possible that the increase in the expression of the other voltage-gated Na^+ channels increases the I_{NaP} in *Mecp2*$^{-/Y}$ mice, but as of now, it remains unclear.

In conclusion, we have found major defects in HCN channels with respect to their electrophysiological properties and subunit expression in *Mecp2*–null Me5 neurons. The ~30% decrease in I_H does not cause a decrease in membrane excitability. Instead, the membrane excitability is slightly increased in the *Mecp2*–null neurons, likely to result from the hyperpolarizing shift in the I_{Na} $V_{½}$ of activation. This seemingly paradoxical phenomenon can reduce the impact of the defects in these two major groups of ion channels and allows Me5 neurons to maintain decent proprioception in mastication and facial expression in the presence of the *Mecp2* disruption. These findings may have an impact on the understanding of propriosensory neurons regarding their function in motor control and the development of motor impairment in people with RTT. Also, these findings may provide insight into ion channel reorganization and its role in alleviating symptoms caused by genetic defects in cellular functions.

6.6 Figures

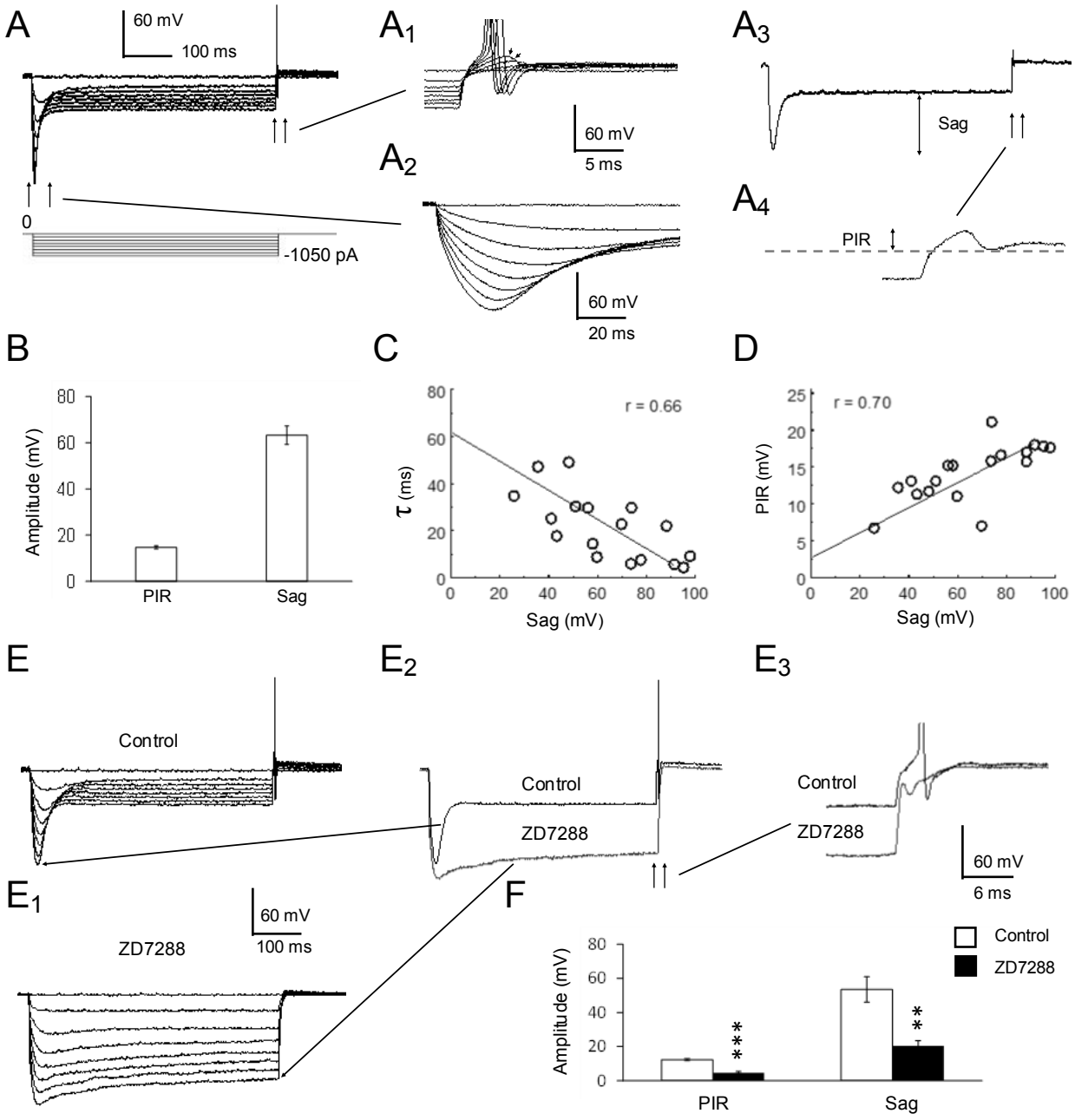

Figure 6.1 ZD7288 blocks the strong sag and PIR in Me5 trigeminal neurons.

A: The Me5 neuron responded to the hyperpolarizing current with a strong PIR and sag, A_1 and A_2. The sag was described as the difference between the peak voltage and the steady-state voltage during the current injection, A_3. The PIR was the difference between the baseline voltage and the peak rebound voltage after the termination of the current injection, A_4. *B:* The PIR and sag in the Me5 neurons from WT mice. *C:* Correlation between the sag time constant and sag voltage. *D:* The correlation between the PIR and sag. *E:* The I_H antagonist ZD7288 blocks the sag and PIR. *E_1:* The recordings after ZD7288 application to same neuron as in E. *E_2:* Overlay of the maximum sweep from traces in E and E_1. *E_3:* Overlay of the maximum sweep from E_2 focusing on the PIR. *F:* The PIR and sag are less after the ZD7288 treatment. Bar graphs are means ± SE; n=6 neurons (Student's *t*-test; $P < 0.01$ **, $P < 0.001$ ***)

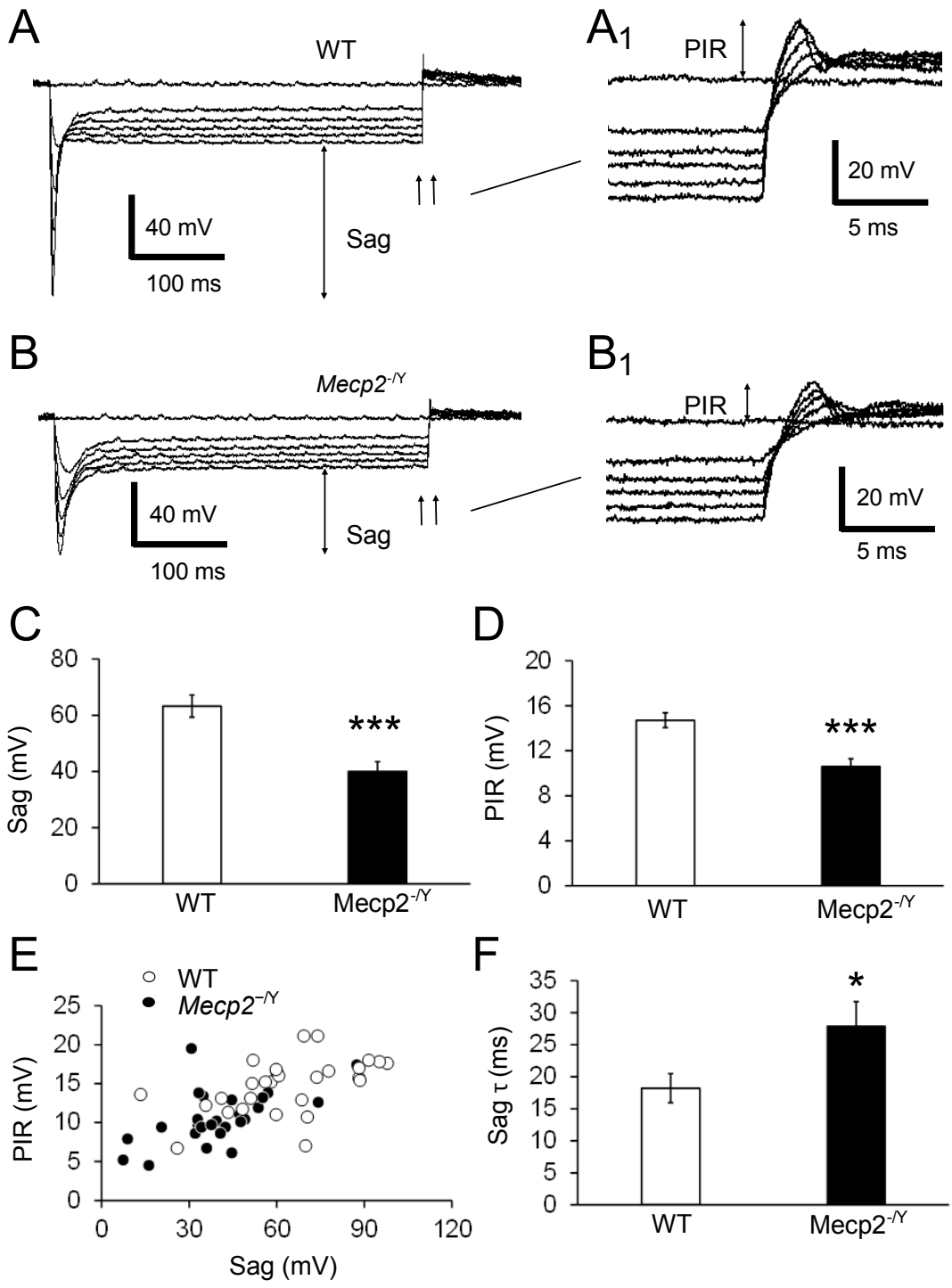

Figure 6.2 . PIR and sag are less in Me5 trigeminal neurons from *Mecp2*$^{-/Y}$ mice.

A: The sag from a Me5 neuron from WT mouse. A_1*:* The PIR from a Me5 neuron from a WT mouse. The sag was defined as the difference between the peak voltage induced by the hyperpolarizing current injection and the steady-state voltage. The PIR was defined as the difference between the resting membrane potential and the peak depolarization. Only recordings without action potentials shown. *B:* The sag in a Me5 neuron from a *Mecp2*$^{-/Y}$ mouse. B_1*:* The PIR in a Me5 neuron from a *Mecp2*$^{-/Y}$ mouse. *C:* The sag is smaller in *Mecp2*$^{-/Y}$ mice than in WT. *D:* The PIR is smaller in *Mecp2*$^{-/Y}$ mice than in WT. *E:* The WT population of cells (open circles) have larger PIR and sag values than the *Mecp2*$^{-/Y}$ mice (filled circles). *F:* The sag time constant is longer in *Mecp2*$^{-/Y}$ mice than in WT. Bar graphs are means ± SE; n = 33 WT neurons and n=30 *Mecp2*$^{-/Y}$ neurons (Student's *t*-test; $P < 0.05$ *, $P < 0.001$ ***)

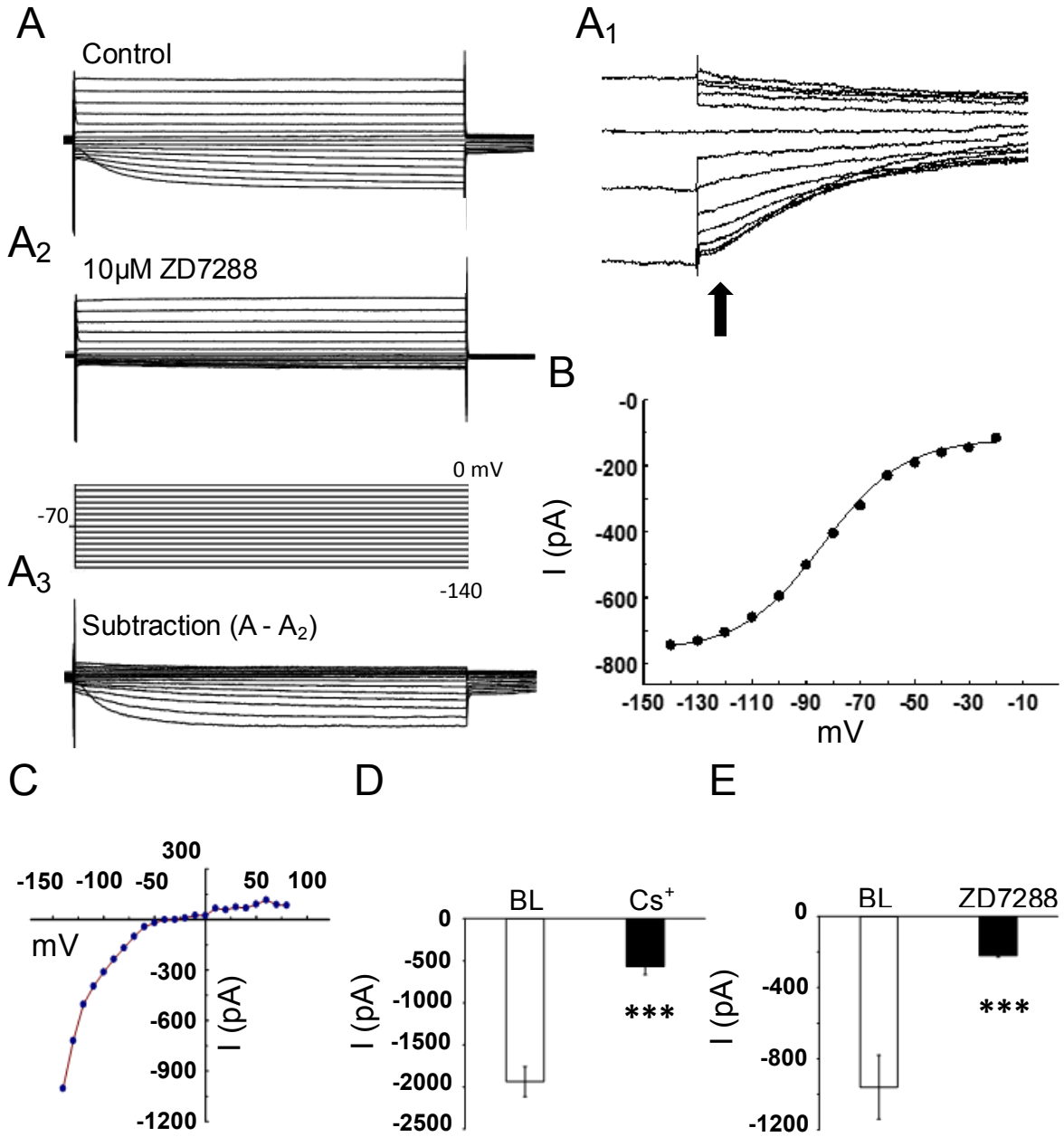

Figure 6.3 The hyperpolarization-activated current in Me5 trigeminal propriosensory neurons.

A: The hyperpolarization-activated current in Me5 neurons. The cell was held at -70mV and a voltage step protocol was administered from -140mV to 0mV. *A_1:* The tail current after the cell returned to -70mV. The arrow indicates where the current values used for the steady-state activation curve were taken. *A_2:* ZD7288 blocks the hyperpolarization-activated current in Me5 neurons. *A_3:* The trace from A_2 was subtracted from trace in A.

B: The steady-state activation was determined from the tail current in A_1. *C:* Current/voltage plot made from subtracted trace in A_3. *D:* Cesium strongly reduced the hyperpolarization-activated current *E:* ZD7288 reduced the hyperpolarization-activated current. Bar graphs are means ± SE; n = 10 Cs^+ neurons and n=8 ZD7288 neurons (Student's *t*-test; $p < 0.001$ ***)

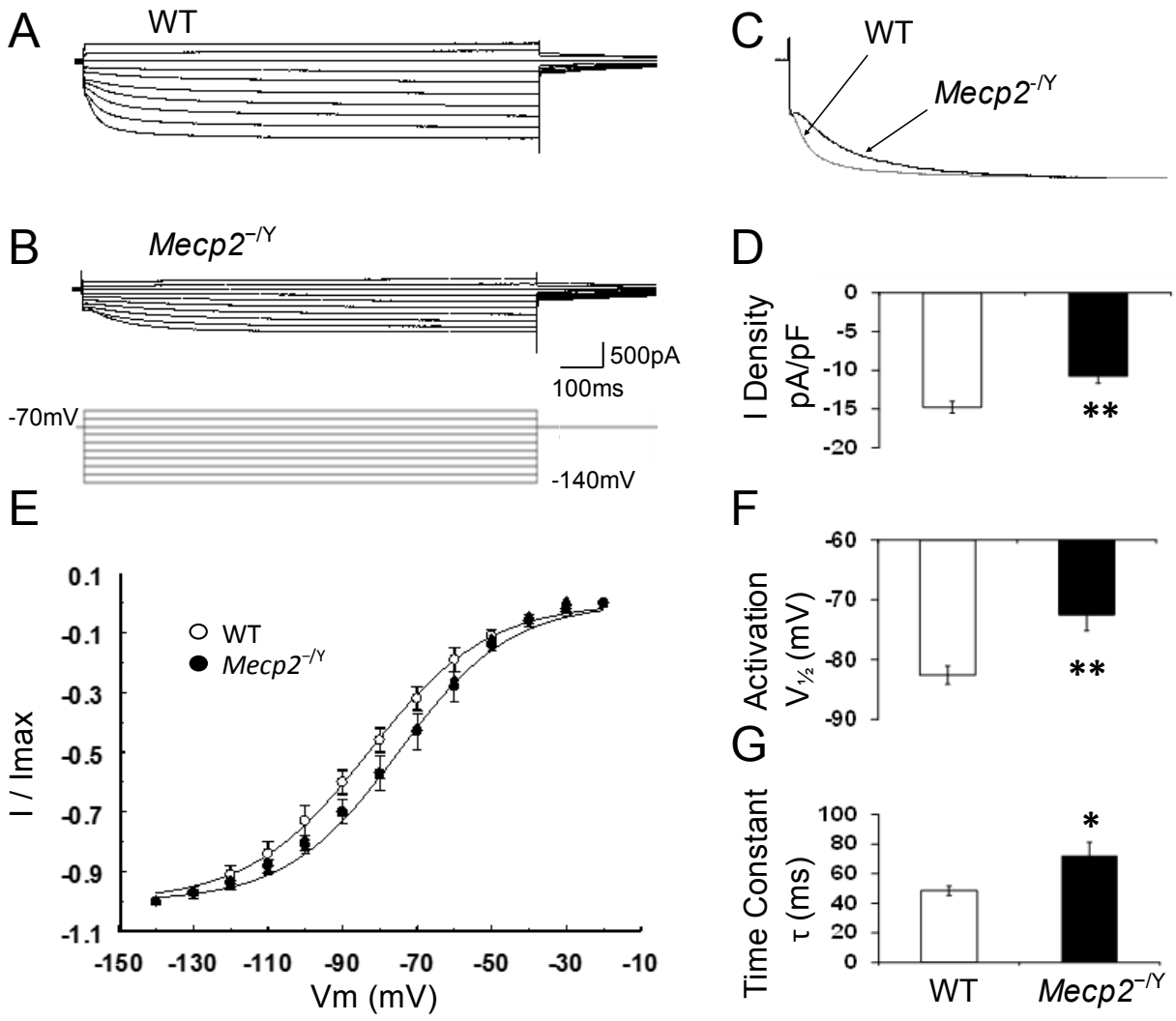

Figure 6.4 The hyperpolarization-activated current was altered in Me5 trigeminal neurons from *Mecp2*$^{-/Y}$ mice.

A: Me5 neuron voltage-clamp recording from WT mouse. *B:* Me5 neuron voltage-clamp recording from *Mecp2*$^{-/Y}$ mouse. *C:* Comparison between the activation of the current in WT and *Mecp2*$^{-/Y}$ mice. *D:* The steady state activation curves of the hyperpolarization-activated current in *Mecp2*$^{-/Y}$ (closed circle) mice compared to the WT (open circle). *E:* The current density was smaller *Mecp2*$^{-/Y}$ mice than in WT (n = 26 WT and n=10 *Mecp2*$^{-/Y}$). *F:* The half-activation was depolarized in *Mecp2*$^{-/Y}$ mice compared to WT (n

= 10 WT neurons and n=9 *Mecp2*$^{-/Y}$ neurons). *G:* The activation time constant was longer in *Mecp2*$^{-/Y}$ mice than in WT (n = 18 WT neurons and n=17 *Mecp2*$^{-/Y}$ neurons). Bar graphs are means ± SE, (Student's *t*-test; $p < 0.05$ *, $p < 0.01$ **)

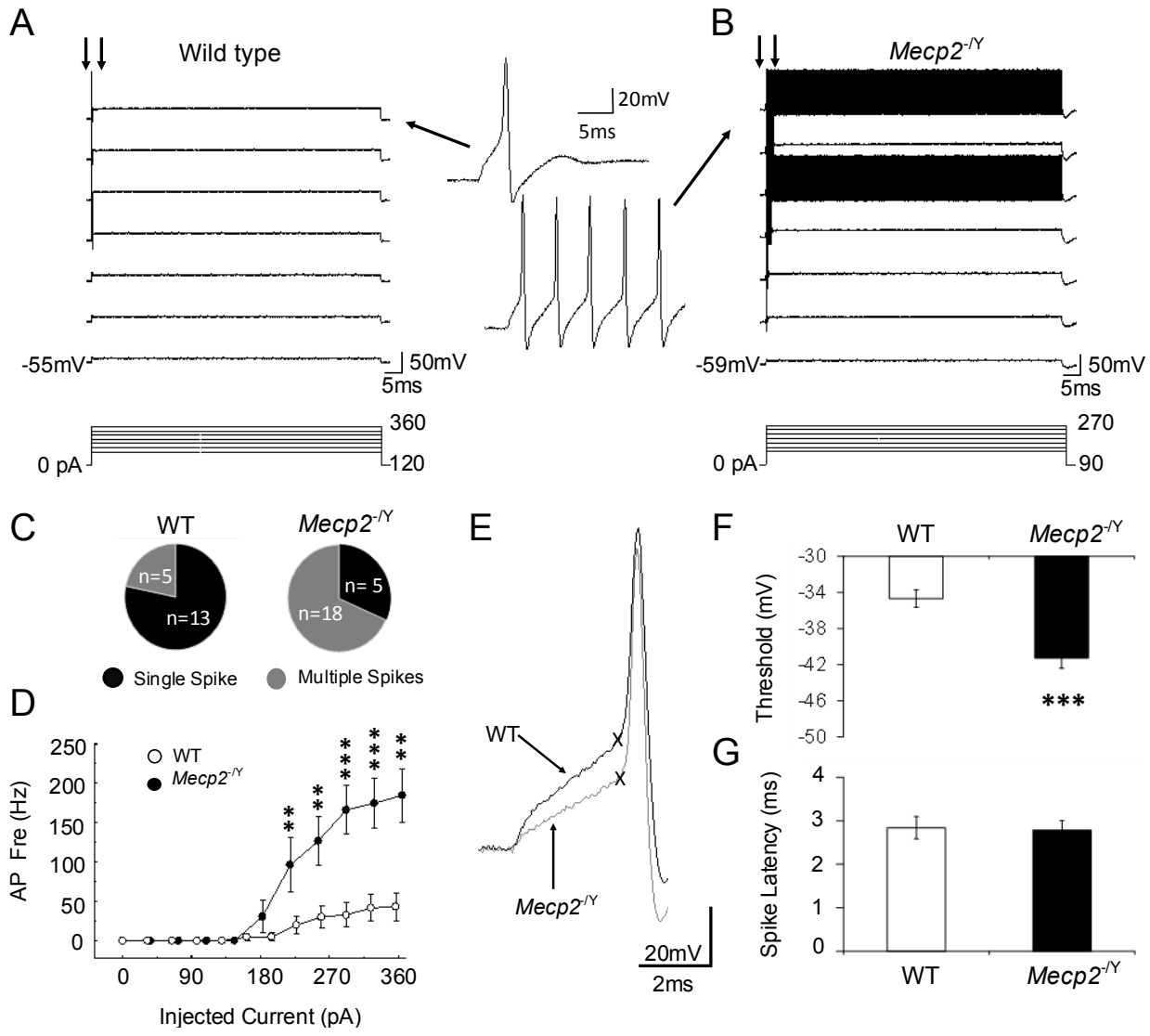

Figure 6.5 Excitability was increased in Me5 neurons of *Mecp2*$^{-/Y}$ mice.

A: A series of depolarizing currents elicited single action potentials in most WT cells. *B:* A series of depolarizing currents elicited multiple action potentials in most *Mecp2*-null neurons. The middle between A and B show typical action potentials during injected currents. *C:* Pie charts depicting average of neurons that responded with single action potentials or multiple action potentials in WT and *Mecp2*$^{-/Y}$ mice. *D:* The spontaneous frequency of action potentials due to depolarizing injected current compared between WT (open circles) and *Mecp2*$^{-/Y}$ (dark circles) mice; n=10 WT neurons and n=10

Mecp2$^{-/Y}$ neurons. *E:* Action potential threshold comparison between WT and *Mecp2*$^{-/Y}$ mice. The threshold (X) was determined using the maximum second derivative *F:* The threshold was decreased in *Mecp2*$^{-/Y}$ mice compared to WT; n=28 WT neurons and n=26 *Mecp2*$^{-/Y}$ neurons. *G:* The spike latency was unchanged between WT and *Mecp2*$^{-/Y}$ mice; n=28 WT neurons and n=26 *Mecp2*$^{-/Y}$ neurons. Graphs are means ± SE; (Student's *t*-test; P < 0.01 **, P < 0.001 ***)

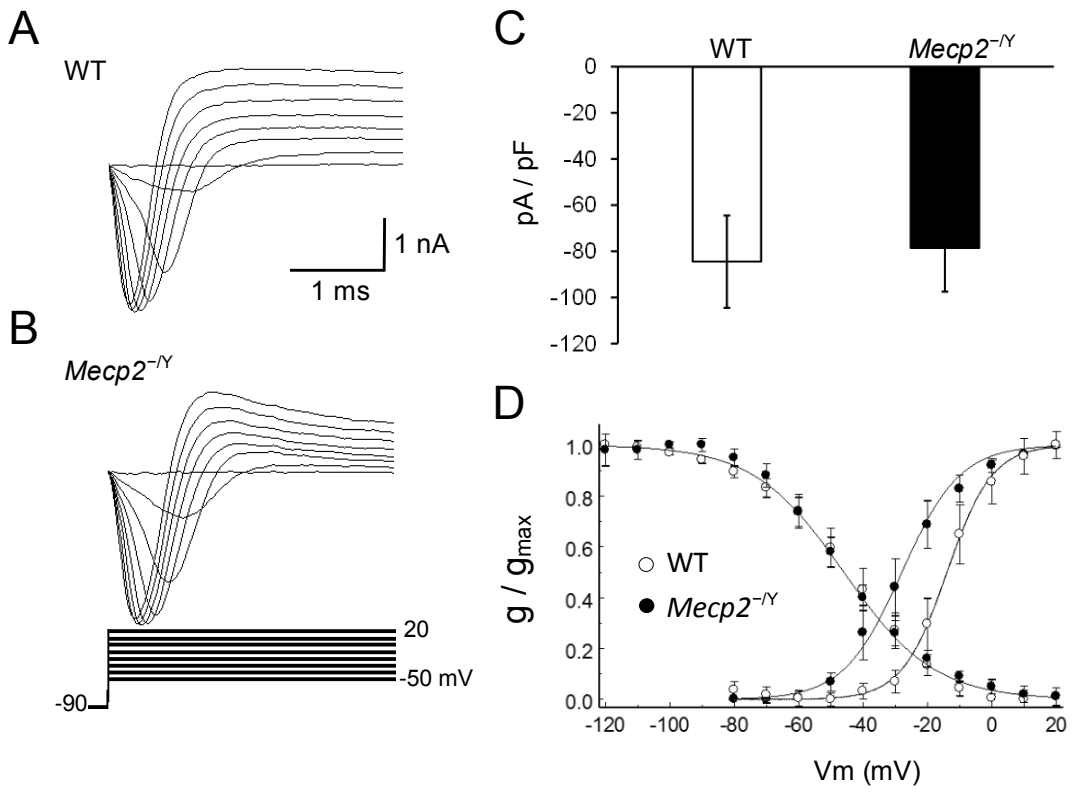

Figure 6.6 The steady state half-activation of voltage-gated sodium current was shifted in the hyperpolarized direction in *Mecp2*$^{-/Y}$ mice.

A: The voltage-gated sodium current recordings from WT and *Mecp2*$^{-/Y}$ mice when the cell was held at -90mV and a step protocol from -80mV to +60mV. *B*: The voltage-gated sodium current recordings from *Mecp2*$^{-/Y}$ mice. Note: only the recordings from steps -50mV to +20mV are shown. *C:* The current density was similar between WT and *Mecp2*$^{-/Y}$ mice. *D*: The steady-state half-inactivation was different between the WT (open circle) and *Mecp2*$^{-/Y}$ mice (closed circle) by ~15mV. The steady state half-activation was shifted in the hyperpolarized direction in *Mecp2*$^{-/Y}$ mice compared to WT. Bar graphs are means ± SE; n=8 WT neurons and n=8 *Mecp2*$^{-/Y}$ neurons (Student's *t*-test, P > 0.05)

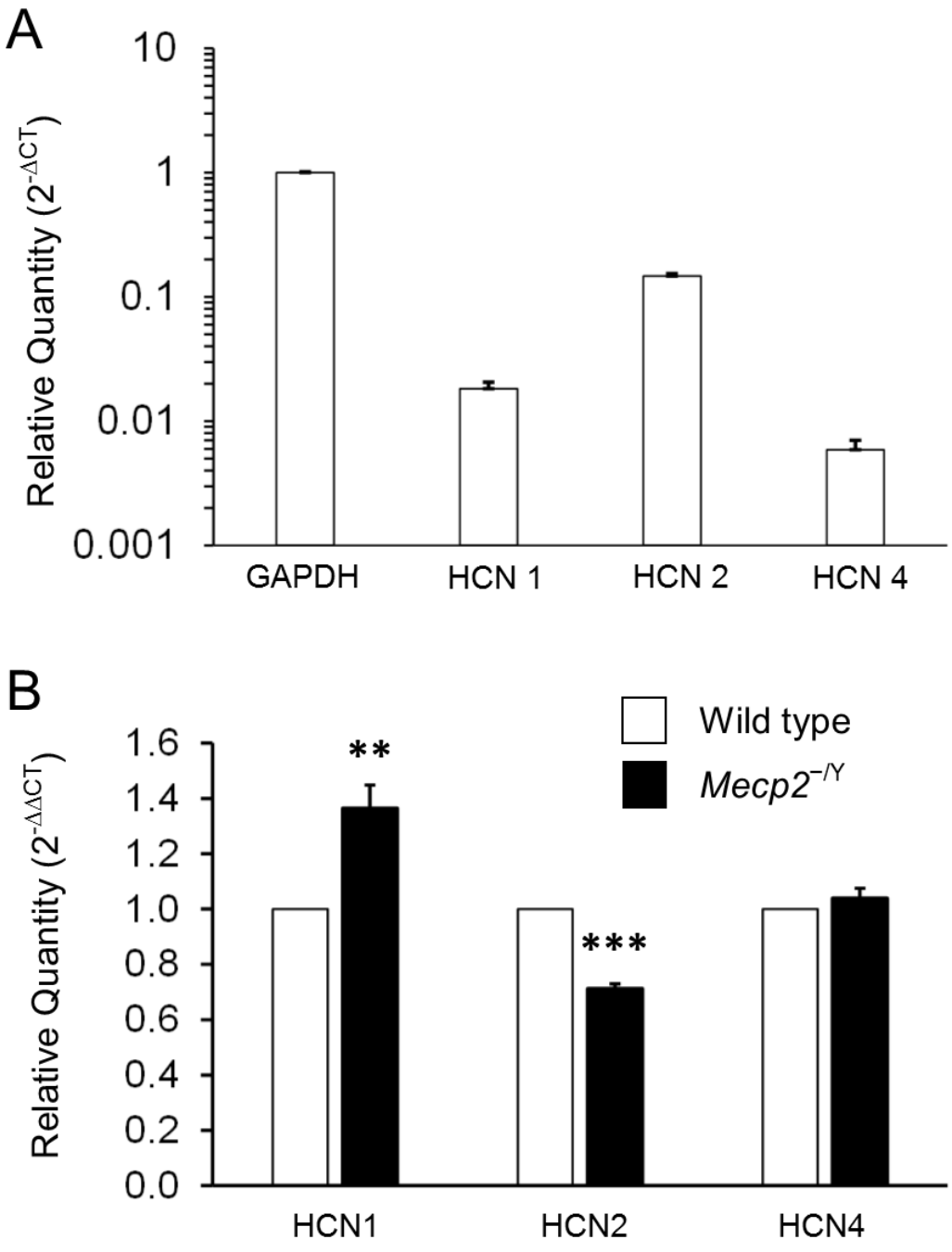

Figure 6.7 Alterations in HCN subunit expression in Me5 neurons.

A: The relative quantity of the HCN subunits compared to GAPDH. *B:* The relative quantity of the HCN subunits of *Mecp2*$^{-/Y}$ mice compared to WT. Bar graphs are means

± SE; n=9 experiments HCN1 and HCN2, n=8 experiments HCN4, (one-way ANOVA and Student's *t*-test; $p < 0.01$ **, $p < 0.001$ ***)

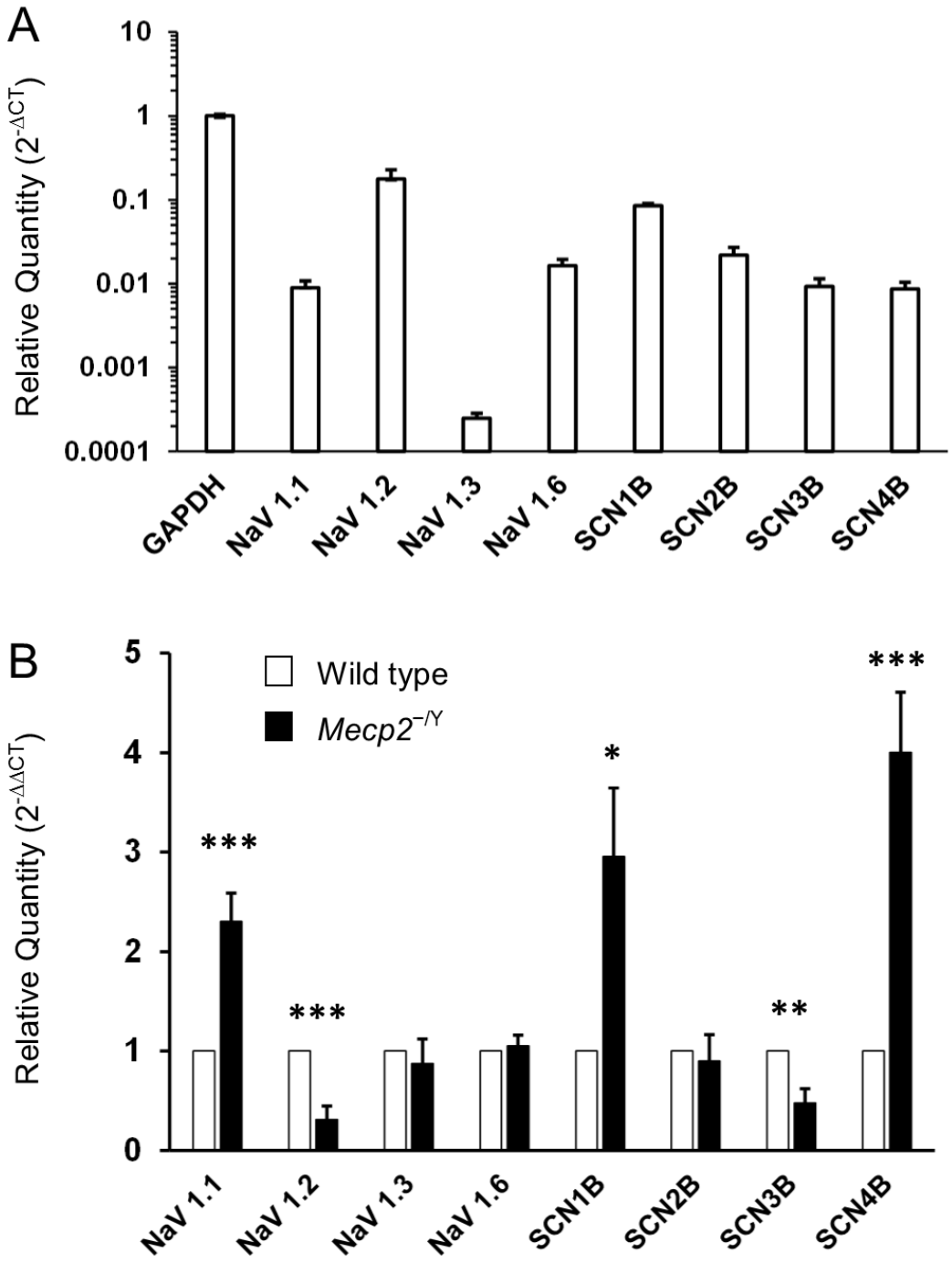

Figure 6.8 Alterations in NaV and SCN subunit expression in Me5 neurons.

A: The relative quantity of the NaV and SCN subunits compared to GAPDH. *B:* The relative quantity of the NaV and SCN subunits of *Mecp2*$^{-/Y}$ mice compared to WT. Bar

graphs are means ± SE; n=9 experiments NaV1.1, NaV1.2, NaV1.6, SCN1B, SCN3B, SCN4B, n=8 experiments SCN2B, n=6 experiments NaV1.3 (one-way ANOVA and Student's *t*-test; $p < 0.01$ **, $p < 0.001$ ***)

Table 5.1 Na+ Channel PCR Primers

Target Gene	Primer Sequence	Accession No.
GAPDH FW	CCAGCCTCGTCCCGTAGA	NM_008084
GAPDH RW	TGCCGTGAGTGGAGTCATACTG	
$Na_V1.1$ Fw	TCATCATCTTCGGGTCCTTC	NM_018733.2
$Na_V1.1$ RV	GGTCGAGGGATAGGCTTTTG	
$Na_V1.2$ Fw	GCTAAAGTGGGTTGCATATG	NM_001099298.2
$Na_V1.2$ RV	CCTCAGTGCTCTTAATGTTC	
$Na_V1.3$ Fw	CGCTTGACGCTGTCTTCTG	NM_018732.3
$Na_V1.3$ RV	GACTTCAGTGGGATAGGAGGG	
$Na_V1.6$ Fw	AGTCAGACCCCGAAGGCAG	U26707.1
$Na_V1.6$ RV	TGTTGACCTGGCAGCACTTG	
SCN1B Fw	CGAGGCTGTGTATGGGATGAC	NM_011322.2
SCN1B Rv	CCCTCAAAGCGCTCATCTTC	
SCN2B Fw	GGTCTGGTGGCGATTTAAACTG	NM_001014761.2
SCN2B Rv	AACGACTCAGCCCTATCTTTCC	
SCN3B Fw	TGTAATGTGTCCAGGGAGTTTG	NM_001286614.1
SCN3B Rv	TTCGGCCTTAGAGACCTTTCTG	
SCN4B Fw	AGCCTCGCTTTCTGATGGTGATC	NM_001013390.2
SCN4B Rv	TCCCTTCCCTGTCTTCAATCTC	

7 GENERAL DISCUSSION

7.1 Homeostatic compensation in animal models

Homeostasis occurs in cells, tissues, organs and organisms. For proper neuronal function the balance among various membrane ion channels and synaptic currents must be maintained. Recent studies indicate that membrane conductance varies from neurons to neurons even though the neuronal output is quite robust and stereotypical (Prinz et al. 2004). The stability of neuronal activity seems to be related to the covariation of certain membrane conductance pairs (Zhao and Golowasch 2012). The alteration of one conductance in the pair may not alter the neuronal firing activity. This is because the other membrane conductance is also altered (Khorkova and Golowasch 2007; MacLean et al. 2003). These conductance alterations are related to the ion channel expression level, turnover rate, phosphorylation, membrane trafficking, etc. (Schulz et al. 2006; Tobin et al. 2009), which are consistent with the compensatory neuroadaptation theory. It is likely that similar neuroadaptations that occur in WT animals happen in diseased mouse models of RTT.

7.1.1 Gene knockout mouse models

There are many examples where the knockout of a gene from an organism initiates compensatory mechanisms. Alterations in the gene expression levels in response to the knockout of another gene indicate that cells have the ability to adapt to the genetic variations. For example, when the α1 subunit gene of the $GABA_A$ receptor is knocked out, other genes start acting in the functional deficiency caused by the gene ablation (Ogris et al. 2006). Due to the α1 $GABA_A$ receptor subunit knockout, there is an increase in expression of α6, α3 and α4 -containing channels. This is not necessarily

caused by upregulation of the genes. Instead, the gene products are not degraded as much and are incorporated into functional receptors. The global knockout of the β3 GABA receptor gene causes the downregulation of the α2 and α3 subunits (Ramadan et al. 2003). These changes are not limited to the GABA system. When the NE transporter is knocked out, there is an increase in α2 adrenoceptors, dopamine and serotonin transporters (Gilsbach et al. 2006; Solich et al. 2011). Several lines of knockout mice have been used to study the function of nAChRs because of their role in nicotine addiction (Drago et al. 2003). In α7 nAChR knockout mice, the α2, α9, α10, β4, muscarinic 1 and muscarinic 4 receptor subunits were upregulated in retinal neurons (Smith et al. 2014). Further, the α3 and α4 nAChR subunits are upregulated in the cortex and hippocampus of α7 nAChR knockout mice. These results suggest that neurons have the ability to alter the expression of one gene to compensate for a deficiency in the other.

7.1.2 Parkinson's disease mouse models

The loss of dopamine signaling has been shown to be the major cause of Parkinson's disease. Specifically, dopaminergic neurons from the substantia nigra pars compacta die due to dysfunction in the L-type Ca(v)1.3 Ca^{2+} channel (Chan et al. 2007). Despite the death of these neurons, the advent of the symptoms do not occur until the level of striatal dopamine is <5% of WT values (Golden et al. 2013). This cannot be explained without consideration of neuroadaptations compensating for the diminishment of dopamine signaling in the striatum. Indeed, neurons of the striatum are able to adapt to the reduction of dopamine. The decrease in cholinergic and GABAergic neurons of the striatum seems to occur to adjust to the decline in dopamine (Lloyd 1977). Further,

when 90% of the substantia pars compacta neurons are destroyed, there is an upregulation in TH expression and release of dopamine from the remaining neurons (Zigmond et al. 1984). The dopamine transporter activity is decreased when substantia nigra pars compacta neurons are lesioned. This seems to help maintain the dopamine levels despite the reduced number of dopaminergic neurons (Sossi et al. 2009). These examples offer reasons why the decrease in dopamine does not immediately result in obvious Parkinson's disease symptoms.

7.1.3 Rett Syndrome mouse models

There are many mouse models used to study the impact of mutations in the *Mecp2* gene. Depending on the question being asked, one model may be more appropriate than another. For instance, some mutations have more severe symptoms than others. For our purposes, we used the model where exons 3 and 4 were removed, and the model recapitulates all RTT-like symptoms. Using this model we have found evidence where neurons are adapting to changes in synaptic signaling and membrane ionic currents. RTT is characterized by deficits in inhibitory systems. It seems that other systems are able to act on minimizing the *Mecp2*-null effect. In the mice, GABA synaptic transmission is defective, whereas the NE modulation of glycinergic input to hypoglossal neurons is augmented (Jin et al. 2013c). The upregulation of the inhibitory glycinergic synaptic currents seems to reduce the hyperexcitability of hypoglossal neurons. The ACh modulation of GABA input to LC neurons is increased in *Mecp2*$^{-/Y}$ mice, which seems to increase the GABAergic input to the LC. The alteration of presynaptic neuron signaling is just one neuroadaptation occurring to maintain homeostasis. Other compensatory neuroadaptations occur in postsynaptic neurons as well. The expression

of nAChR receptor subunits in LC neurons is reorganized. The reduction in α3,α4, α7 and β3 seems to be offset by the increase in the α5 subunit. The nAChR current properties are altered due to the changes in the expression of the subunits that mediate it. The ability of the cholinergic neurons to modulate LC activity is maintained. This compensatory neuroadaptation allows the signaling between cholinergic and NEergic neurons to be preserved in spite of the problems caused by the knockout of the *Mecp2* gene.

Not only do ligand-gated ion channels or ionotropic receptors seem to be affected by the MeCP2 dysfunction, voltage-gated ion channels are altered as well. We have shown that the expression of HCN and voltage-gated Na^+ channels is altered in Me5 propriosensory neurons. These alterations in the channels suggest that the MeCP2 deficiency is affecting the expression of one group of ion channel. The alterations in the one group compensate for the changes in the other. It is difficult to say if HCN or voltage-gated Na^+ channel expression is affected by the *Mecp2*-null and which one compensates. It does seem clear that without the compensatory mechanisms, the neuron would be completely unable to function properly. For example, if the *Mecp2* knockout decreases I_H without any compensation by I_{Na}, it is likely that the neuron would not be able to fire action potentials as easily. Therefore, the reduction in the threshold becomes necessary for these neurons to communicate with other brain stem neurons as to the state of the muscles in the jaw. If the opposite is true, where the MeCP2 dysfunction affects I_{Na} without any compensation from I_H, these neurons would be extremely hyperexcitable. Even with the compensatory mechanisms described here,

there is still some hyperexcitability. However, if the reduction in I_H did not occur, then the impact of the alterations in I_{Na} would likely be much worse than seen here.

It must be considered whether the compensatory mechanisms described in this thesis may be occurring in other neurons. It is unclear how the mechanisms underlying the neuroadaptations are manifested. However, it seems that the changes in ion channel and receptor expression from *Mecp2*$^{-/Y}$ mice depend on the specific function of the neuron. For instance, LC neurons do not display a PIR or I_H but do have a decreased threshold. It is unclear why the altered threshold occurs in LC neurons. It is unlikely to be directly caused by the MeCP2 defect and may be due to some unknown reason. Alterations in ionic currents, other than the ones studied here, may be occurring to maintain the function of neurons depending on a specific need.

7.2 Evolutionary considerations

Evolution seems to have occurred in such a way that a given function may be produced by more than one protein that serves the same or similar purpose. This known evolutionary conservation is interesting because there is strong evidence suggesting that the ionic current density can vary greatly but without changing the neuron activity. For example, in central pattern generators the density of various membrane currents in neurons is not the same from cell to cell (Prinz et al. 2004). However, the rhythmic pattern generated in these neurons is quite consistent. It seems that the density of specific currents may not be kept at a fixed level within a neuron. Rather, there are many combinations of current densities that are available to the neuron to keep it functioning properly. The latter enables dynamic regulation as well as a better tolerance of unexpected variation in ion channel activity. As a result, the firing activity is

maintained, even though the many currents underlying the firing properties such as threshold, resting membrane potential, interspike interval, PIR, etc. may change within the neurons.

7.2.1 Degeneracy of ionic currents

In order for the many currents in a neuron to regulate the same firing property, the underlying channels must have some common features. Evolution has created a couple of different ways for this to be possible. The premise of degeneracy of ionic currents fulfills this role. Degeneracy refers to the fact that multiple currents underlie specific features of neuronal firing properties. One way is to simply have multiple channels from the same family. For instance, I_H is mediated by four different HCN (1-4) channels. As we show here, If HCN2 expression is altered, then HCN1 can be upregulated to replace it. In another way, pairs of currents are correlated with the magnitude of a firing feature. In dopaminergic neurons, I_H and I_A are covaried in such a way as to maintain the PIR (Amendola et al. 2012). The first current in the pair may be altered and homeostatic compensation by the change in the second current maintains proper firing. Homeostatic compensation has been well studied in the invertebrate pyloric network of the stomatogastric ganglion in decapods. The pyloric network features a stereotypical triphasic rhythm that is very robust despite the differences in ionic currents from animal to animal. Similar to the study in dopaminergic neurons, the interburst interval is regulated by I_H and I_A in the pyloric network. When I_A is increased, the expected increase in the interburst interval is not seen. This is because of a compensatory increase in I_H (MacLean et al. 2003). There are other pairs of ionic

currents that underlie other bursting feature in these neurons (Zhao and Golowasch 2012).

7.2.2 Ionic currents change depending on the presence of modulatory input

The presence of neuromodulatory input seems to regulate the magnitude of the ionic currents. When the modulatory input to pyloric neurons is blocked, the current magnitudes change and become deregulated (Khorkova and Golowasch 2007). The removal of the modulatory input causes the pyloric rhythm to be lost. However, the rhythm will return because of the upregulation of specific genes (Thoby-Brisson and Simmers 2000). This type of response indicates that the ionic currents are configured in one way when the modulatory input is present. The ionic currents can be reconfigured when the modulatory input is not present so the network starts bursting again. It is unclear how the ionic currents are reconfigured exactly. It does seem likely that this is able to occur because multiple currents can regulate many of the same firing features. Therefore, these data reinforce the premise that stable neuron activity is made possible by the degeneracy of ionic currents

7.2.3 Protein expression from cell to cell and animal to animal

The magnitude of membrane currents has been shown to be directly correlated with the mRNA levels in a neuron (Baro et al. 1997; MacLean et al. 2005). Further, the expression of the mRNA from different pairs of ion channels has been correlated with firing features that have been well characterized electrophysiologically (Schulz et al. 2006; Tobin et al. 2009). These studies indicate that the alteration of currents is because there are changes in protein expression levels. We see this in our studies as well. The alteration of the receptors and ion channel expression patterns underlie the

differences in the currents. The whole cell nAChR current in LC neurons from WT has a large peak amplitude and a short decay time whereas the opposite is true in *Mecp2*$^{-/Y}$ mice. In these mice, the peak amplitude is small and the decay time is long. Therefore the modulation of LC neurons is preserved. The alteration in the voltage-gated Na^+ channels changes the threshold by ~5mV. This seems to be done because the PIR is ~5mV less. Therefore, the changes in mRNA levels in *Mecp2*$^{-/Y}$ mice are done to preserve neuronal firing properties just as it is done in normal animals.

7.2.4 Similarities between WT animals and animal models of disease

To determine if homeostatic compensation is a general mechanism among neurons in *Mecp2*$^{-/Y}$ mice, we examined two different neurons and two different types of ion channels that underlie the breathing abnormalities and movement problems. Dysfunction in LC neurons from *Mecp2*$^{-/Y}$ mice seems to contribute to the breathing problems in RTT. We found that the synaptic modulation through nAChRs is maintained because of the reorganization of the receptor subunits. In the Me5 propriosensory neurons we have found that membrane ionic currents are altered in such a way that preserved normal function to some extent. These changes in the membrane ionic currents can be attributed to the reorganization of the voltage-gated channel subunits. Therefore, it does seem that the homeostatic compensation of ion channels is a general mechanism in place to limit abnormal neuron activity.

7.3 Conclusion

This dissertation attempts to address two specific aims that ask questions regarding how neurons are able to remain viable despite the dysfunction of a crucial protein. To answer these questions, we took advantage of a mouse model where exons 3 and 4 of the *Mecp2* gene were knocked out. In the first specific aim we elucidated the modulation of LC neurons by ACh in *Mecp2*$^{-/Y}$ mice. We found that the nAChR expression was altered to maintain normal cholinergic modulation of LC activity. Secondly, we found that the cholinergic modulation of GABA input to the LC was enhanced in *Mecp2*$^{-/Y}$ mice. In our second aim, we found that I_{Na} and I_H were changed in *Mecp2*$^{-/Y}$ mice. The alteration in the expression of the channels that mediate these currents seems to underlie the differences.

The importance of these findings is that compensatory mechanisms are in place in neurons from diseased animals. Specifically, the changes in expression levels of receptors and ion channels can be modified to maintain a functional neuron. In some cases this may be very precise, as seen in cholinergic modulation of LC neurons. In others, the alterations may have deleterious effects such as the hyperexcitability found in Me5 neurons from *Mecp2*$^{-/Y}$ mice. Furthermore, this dissertation provides a basis for those who may be interested in finding ways to enhance what the body is doing naturally to thwart the problems caused by the MeCP2 deficiency.

REFERENCES

Abdala AP, Dutschmann M, Bissonnette JM, and Paton JF. Correction of respiratory disorders in a mouse model of Rett syndrome. *Proc Natl Acad Sci U S A* 107: 18208-18213, 2010.

Albuquerque EX, Alkondon M, Pereira EF, Castro NG, Schrattenholz A, Barbosa CT, Bonfante-Cabarcas R, Aracava Y, Eisenberg HM, and Maelicke A. Properties of neuronal nicotinic acetylcholine receptors: pharmacological characterization and modulation of synaptic function. *J Pharmacol Exp Ther* 280: 1117-1136, 1997.
Alkondon M, and Albuquerque EX. Diversity of nicotinic acetylcholine receptors in rat hippocampal neurons. I. Pharmacological and functional evidence for distinct structural subtypes. *J Pharmacol Exp Ther* 265: 1455-1473, 1993.
Alkondon M, Pereira EF, Cortes WS, Maelicke A, and Albuquerque EX. Choline is a selective agonist of alpha7 nicotinic acetylcholine receptors in the rat brain neurons. *Eur J Neurosci* 9: 2734-2742, 1997.
Alkondon M, Pereira EF, Eisenberg HM, and Albuquerque EX. Choline and selective antagonists identify two subtypes of nicotinic acetylcholine receptors that modulate GABA release from CA1 interneurons in rat hippocampal slices. *J Neurosci* 19: 2693-2705, 1999.
Altomare C, Terragni B, Brioschi C, Milanesi R, Pagliuca C, Viscomi C, Moroni A, Baruscotti M, and DiFrancesco D. Heteromeric HCN1-HCN4 channels: a comparison with native pacemaker channels from the rabbit sinoatrial node. *J Physiol* 549: 347-359, 2003.
Aman TK, Grieco-Calub TM, Chen C, Rusconi R, Slat EA, Isom LL, and Raman IM. Regulation of persistent Na current by interactions between beta subunits of voltage-gated Na channels. *J Neurosci* 29: 2027-2042, 2009.
Amendola J, Woodhouse A, Martin-Eauclaire MF, and Goaillard JM. Ca(2)(+)/cAMP-sensitive covariation of I(A) and I(H) voltage dependences tunes rebound firing in dopaminergic neurons. *J Neurosci* 32: 2166-2181, 2012.
Amir RE, Van den Veyver IB, Wan M, Tran CQ, Francke U, and Zoghbi HY. Rett syndrome is caused by mutations in X-linked MECP2, encoding methyl-CpG-binding protein 2. *Nat Genet* 23: 185-188, 1999.
Andaku DK, Mercadante MT, and Schwartzman JS. Buspirone in Rett syndrome respiratory dysfunction. *Brain & development* 27: 437-438, 2005.
Aracri P, Consonni S, Morini R, Perrella M, Rodighiero S, Amadeo A, and Becchetti A. Tonic modulation of GABA release by nicotinic acetylcholine receptors in layer V of the murine prefrontal cortex. *Cereb Cortex* 20: 1539-1555, 2010.
Arendt KL, Sarti F, and Chen L. Chronic inactivation of a neural circuit enhances LTP by inducing silent synapse formation. *J Neurosci* 33: 2087-2096, 2013.
Arnsten AF, Cai JX, and Goldman-Rakic PS. The alpha-2 adrenergic agonist guanfacine improves memory in aged monkeys without sedative or hypotensive side effects: evidence for alpha-2 receptor subtypes. *J Neurosci* 8: 4287-4298, 1988.
Ascoli GA, Gasparini S, Medinilla V, and Migliore M. Local control of postinhibitory rebound spiking in CA1 pyramidal neuron dendrites. *J Neurosci* 30: 6434-6442, 2010.
Astman N, Gutnick MJ, and Fleidervish IA. Activation of protein kinase C increases neuronal excitability by regulating persistent Na+ current in mouse neocortical slices. *J Neurophysiol* 80: 1547-1551, 1998.
Aston-Jones G, Zhu Y, and Card JP. Numerous GABAergic afferents to locus ceruleus in the pericerulear dendritic zone: possible interneuronal pool. *J Neurosci* 24: 2313-2321, 2004.
Baba H, Goldstein PA, Okamoto M, Kohno T, Ataka T, Yoshimura M, and Shimoji K. Norepinephrine facilitates inhibitory transmission in substantia gelatinosa of adult rat spinal cord (part 2): effects on somatodendritic sites of GABAergic neurons. *Anesthesiology* 92: 485-492, 2000a.

Baba H, Shimoji K, and Yoshimura M. Norepinephrine facilitates inhibitory transmission in substantia gelatinosa of adult rat spinal cord (part 1): effects on axon terminals of GABAergic and glycinergic neurons. *Anesthesiology* 92: 473-484, 2000b.

Banerjee A, Gonzalez-Rueda A, Sampaio-Baptista C, Paulsen O, and Rodriguez-Moreno A. Distinct mechanisms of spike timing-dependent LTD at vertical and horizontal inputs onto L2/3 pyramidal neurons in mouse barrel cortex. *Physiological reports* 2: e00271, 2014.

Barela AJ, Waddy SP, Lickfett JG, Hunter J, Anido A, Helmers SL, Goldin AL, and Escayg A. An epilepsy mutation in the sodium channel SCN1A that decreases channel excitability. *J Neurosci* 26: 2714-2723, 2006.

Baro DJ, Levini RM, Kim MT, Willms AR, Lanning CC, Rodriguez HE, and Harris-Warrick RM. Quantitative single-cell-reverse transcription-PCR demonstrates that A-current magnitude varies as a linear function of shal gene expression in identified stomatogastric neurons. *J Neurosci* 17: 6597-6610, 1997.

Barros F, Villalobos C, Garcia-Sancho J, del Camino D, and de la Pena P. The role of the inwardly rectifying K+ current in resting potential and thyrotropin-releasing-hormone-induced changes in cell excitability of GH3 rat anterior pituitary cells. *Pflugers Archiv : European journal of physiology* 426: 221-230, 1994.

Baruscotti M, Bucchi A, and Difrancesco D. Physiology and pharmacology of the cardiac pacemaker ("funny") current. *Pharmacology & therapeutics* 107: 59-79, 2005.

Bassani S, Folci A, Zapata J, and Passafaro M. AMPAR trafficking in synapse maturation and plasticity. *Cell Mol Life Sci* 70: 4411-4430, 2013.

Belichenko PV, Wright EE, Belichenko NP, Masliah E, Li HH, Mobley WC, and Francke U. Widespread changes in dendritic and axonal morphology in Mecp2-mutant mouse models of Rett syndrome: evidence for disruption of neuronal networks. *J Comp Neurol* 514: 240-258, 2009.

Blackman MP, Djukic B, Nelson SB, and Turrigiano GG. A Critical and Cell-Autonomous Role for MeCP2 in Synaptic Scaling Up. *J Neurosci* 32: 13529-13536, 2012.

Blue ME, Naidu S, and Johnston MV. Altered development of glutamate and GABA receptors in the basal ganglia of girls with Rett syndrome. *Exp Neurol* 156: 345-352, 1999.

Boffi JC, Wedemeyer C, Lipovsek M, Katz E, Calvo DJ, and Elgoyhen AB. Positive modulation of the alpha9alpha10 nicotinic cholinergic receptor by ascorbic acid. *Br J Pharmacol* 168: 954-965, 2013.

Bongianni F, Mutolo D, Cinelli E, and Pantaleo T. Respiratory responses induced by blockades of GABA and glycine receptors within the Botzinger complex and the pre-Botzinger complex of the rabbit. *Brain Res* 1344: 134-147, 2010.

Bonin RP, Zurek AA, Yu J, Bayliss DA, and Orser BA. Hyperpolarization-activated current (In) is reduced in hippocampal neurons from Gabra5-/- mice. *PLoS One* 8: e58679, 2013.

Boorman JP, Beato M, Groot-Kormelink PJ, Broadbent SD, and Sivilotti LG. The effects of beta3 subunit incorporation on the pharmacology and single channel properties of oocyte-expressed human alpha3beta4 neuronal nicotinic receptors. *J Biol Chem* 278: 44033-44040, 2003.

Brightwell JJ, and Taylor BK. Noradrenergic neurons in the locus coeruleus contribute to neuropathic pain. *Neuroscience* 160: 174-185, 2009.

Butt AM, and Kalsi A. Inwardly rectifying potassium channels (Kir) in central nervous system glia: a special role for Kir4.1 in glial functions. *Journal of cellular and molecular medicine* 10: 33-44, 2006.

Carotenuto M, Esposito M, D'Aniello A, Rippa CD, Precenzano F, Pascotto A, Bravaccio C, and Elia M. Polysomnographic findings in Rett syndrome: a case-control study. *Sleep Breath* 17: 93-98, 2013.
Carter ME, Yizhar O, Chikahisa S, Nguyen H, Adamantidis A, Nishino S, Deisseroth K, and de Lecea L. Tuning arousal with optogenetic modulation of locus coeruleus neurons. *Nat Neurosci* 13: 1526-1533, 2010.
Castillo PE. Presynaptic LTP and LTD of excitatory and inhibitory synapses. *Cold Spring Harbor perspectives in biology* 4: 2012.
Cattaneo L, and Pavesi G. The facial motor system. *Neuroscience and biobehavioral reviews* 38: 135-159, 2014.
Chahrour M, and Zoghbi HY. The story of Rett syndrome: from clinic to neurobiology. *Neuron* 56: 422-437, 2007.
Chan CS, Glajch KE, Gertler TS, Guzman JN, Mercer JN, Lewis AS, Goldberg AB, Tkatch T, Shigemoto R, Fleming SM, Chetkovich DM, Osten P, Kita H, and Surmeier DJ. HCN channelopathy in external globus pallidus neurons in models of Parkinson's disease. *Nat Neurosci* 14: 85-92, 2011.
Chan CS, Guzman JN, Ilijic E, Mercer JN, Rick C, Tkatch T, Meredith GE, and Surmeier DJ. 'Rejuvenation' protects neurons in mouse models of Parkinson's disease. *Nature* 447: 1081-1086, 2007.
Chao HT, Chen H, Samaco RC, Xue M, Chahrour M, Yoo J, Neul JL, Gong S, Lu HC, Heintz N, Ekker M, Rubenstein JL, Noebels JL, Rosenmund C, and Zoghbi HY. Dysfunction in GABA signalling mediates autism-like stereotypies and Rett syndrome phenotypes. *Nature* 468: 263-269, 2010.
Chao HT, Zoghbi HY, and Rosenmund C. MeCP2 controls excitatory synaptic strength by regulating glutamatergic synapse number. *Neuron* 56: 58-65, 2007.
Chapleau CA, Calfa GD, Lane MC, Albertson AJ, Larimore JL, Kudo S, Armstrong DL, Percy AK, and Pozzo-Miller L. Dendritic spine pathologies in hippocampal pyramidal neurons from Rett syndrome brain and after expression of Rett-associated MECP2 mutations. *Neurobiol Dis* 35: 219-233, 2009.
Chen S, Benninger F, and Yaari Y. Role of small conductance Ca(2)(+)-activated K(+) channels in controlling CA1 pyramidal cell excitability. *J Neurosci* 34: 8219-8230, 2014.
Ciuraszkiewicz A, Schreibmayer W, Platzer D, Orr-Urtreger A, Scholze P, and Huck S. Single-channel properties of alpha3beta4, alpha3beta4alpha5 and alpha3beta4beta2 nicotinic acetylcholine receptors in mice lacking specific nicotinic acetylcholine receptor subunits. *J Physiol* 591: 3271-3288, 2013.
Cohen AS, Coussens CM, Raymond CR, and Abraham WC. Long-lasting increase in cellular excitability associated with the priming of LTP induction in rat hippocampus. *J Neurophysiol* 82: 3139-3148, 1999.
Cucchiaro G, Chaijale N, and Commons KG. The locus coeruleus nucleus as a site of action of the antinociceptive and behavioral effects of the nicotinic receptor agonist, epibatidine. *Neuropharmacology* 50: 769-776, 2006.
Cui N, Zhang X, Tadepalli JS, Yu L, Gai H, Petit J, Pamulapati RT, Jin X, and Jiang C. Involvement of TRP channels in the CO(2) chemosensitivity of locus coeruleus neurons. *J Neurophysiol* 105: 2791-2801, 2011.

Dai Y, Jones KE, Fedirchuk B, McCrea DA, and Jordan LM. A modelling study of locomotion-induced hyperpolarization of voltage threshold in cat lumbar motoneurones. *J Physiol* 544: 521-536, 2002.
Dash B, Chang Y, and Lukas RJ. Reporter mutation studies show that nicotinic acetylcholine receptor (nAChR) alpha5 Subunits and/or variants modulate function of alpha6*-nAChR. *J Biol Chem* 286: 37905-37918, 2011.
Davis M, Rainnie D, and Cassell M. Neurotransmission in the rat amygdala related to fear and anxiety. *Trends Neurosci* 17: 208-214, 1994.
Dean JB, Czyzyk-Krzeska M, and Millhorn DE. Experimentally induced postinhibitory rebound in rat nucleus ambiguus is dependent on hyperpolarization parameters and membrane potential. *Neurosci Res* 6: 487-493, 1989.
Del Negro CA, and Chandler SH. Physiological and theoretical analysis of K+ currents controlling discharge in neonatal rat mesencephalic trigeminal neurons. *J Neurophysiol* 77: 537-553, 1997.
Deng WS, Jiang YX, Han XH, Xue Y, Wang H, Sun P, and Chen L. HCN Channels Modulate the Activity of the Subthalamic Nucleus In Vivo. *J Mol Neurosci* 2014.
Dietz V, and Duysens J. Significance of load receptor input during locomotion: a review. *Gait & posture* 11: 102-110, 2000.
Dimitrov EL, Yanagawa Y, and Usdin TB. Forebrain GABAergic projections to locus coeruleus in mouse. *J Comp Neurol* 521: 2373-2397, 2013.
Doi A, and Ramirez JM. Neuromodulation and the orchestration of the respiratory rhythm. *Respir Physiol Neurobiol* 164: 96-104, 2008.
Drago J, McColl CD, Horne MK, Finkelstein DI, and Ross SA. Neuronal nicotinic receptors: insights gained from gene knockout and knockin mutant mice. *Cell Mol Life Sci* 60: 1267-1280, 2003.
Dugger BN, Murray ME, Boeve BF, Parisi JE, Benarroch EE, Ferman TJ, and Dickson DW. Neuropathological analysis of brainstem cholinergic and catecholaminergic nuclei in relation to rapid eye movement (REM) sleep behaviour disorder. *Neuropathol Appl Neurobiol* 38: 142-152, 2012.
Ennis M, and Shipley MT. Tonic activation of locus coeruleus neurons by systemic or intracoerulear microinjection of an irreversible acetylcholinesterase inhibitor: increased discharge rate and induction of C-fos. *Exp Neurol* 118: 164-177, 1992.
Enomoto A, Han JM, Hsiao CF, and Chandler SH. Sodium currents in mesencephalic trigeminal neurons from Nav1.6 null mice. *J Neurophysiol* 98: 710-719, 2007.
Enomoto A, Han JM, Hsiao CF, Wu N, and Chandler SH. Participation of sodium currents in burst generation and control of membrane excitability in mesencephalic trigeminal neurons. *J Neurosci* 26: 3412-3422, 2006.
Flood P, Ramirez-Latorre J, and Role L. Alpha 4 beta 2 neuronal nicotinic acetylcholine receptors in the central nervous system are inhibited by isoflurane and propofol, but alpha 7-type nicotinic acetylcholine receptors are unaffected. *Anesthesiology* 86: 859-865, 1997.
Franowicz JS, and Arnsten AF. Treatment with the noradrenergic alpha-2 agonist clonidine, but not diazepam, improves spatial working memory in normal young rhesus monkeys. *Neuropsychopharmacology* 21: 611-621, 1999.
Funahashi M, Mitoh Y, Kohjitani A, and Matsuo R. Role of the hyperpolarization-activated cation current (Ih) in pacemaker activity in area postrema neurons of rat brain slices. *J Physiol* 552: 135-148, 2003.

Funahashi M, Mitoh Y, and Matsuo R. Nicotinic modulation of area postrema neuronal excitability in rat brain slices. *Brain Res* 1017: 227-233, 2004.
Ganesh A, Gonzalez-Sulser A, Chaijale N, and Cucchiaro G. Electrophysiologic effects of systemic and locally infused epibatidine on locus coeruleus neurons. *Eur J Pharmacol* 584: 93-99, 2008.
Gao C, Sun X, and Wolf ME. Activation of D1 dopamine receptors increases surface expression of AMPA receptors and facilitates their synaptic incorporation in cultured hippocampal neurons. *J Neurochem* 98: 1664-1677, 2006.
Garcia-Ramirez DL, Calvo JR, Hochman S, and Quevedo JN. Serotonin, dopamine and noradrenaline adjust actions of myelinated afferents via modulation of presynaptic inhibition in the mouse spinal cord. *PLoS One* 9: e89999, 2014.
Garduno J, Galindo-Charles L, Jimenez-Rodriguez J, Galarraga E, Tapia D, Mihailescu S, and Hernandez-Lopez S. Presynaptic alpha4beta2 nicotinic acetylcholine receptors increase glutamate release and serotonin neuron excitability in the dorsal raphe nucleus. *J Neurosci* 32: 15148-15157, 2012.
Gilsbach R, Faron-Gorecka A, Rogoz Z, Bruss M, Caron MG, Dziedzicka-Wasylewska M, and Bonisch H. Norepinephrine transporter knockout-induced up-regulation of brain alpha2A/C-adrenergic receptors. *J Neurochem* 96: 1111-1120, 2006.
Gokben S, Ardic UA, and Serdaroglu G. Use of buspirone and fluoxetine for breathing problems in Rett syndrome. *Pediatric neurology* 46: 192-194, 2012.
Golden JP, Demaro JA, 3rd, Knoten A, Hoshi M, Pehek E, Johnson EM, Jr., Gereau RWt, and Jain S. Dopamine-dependent compensation maintains motor behavior in mice with developmental ablation of dopaminergic neurons. *J Neurosci* 33: 17095-17107, 2013.
Gotti C, Moretti M, Zanardi A, Gaimarri A, Champtiaux N, Changeux JP, Whiteaker P, Marks MJ, Clementi F, and Zoli M. Heterogeneity and selective targeting of neuronal nicotinic acetylcholine receptor (nAChR) subtypes expressed on retinal afferents of the superior colliculus and lateral geniculate nucleus: identification of a new native nAChR subtype alpha3beta2(alpha5 or beta3) enriched in retinocollicular afferents. *Mol Pharmacol* 68: 1162-1171, 2005.
Groen MR, Paulsen O, Perez-Garci E, Nevian T, Wortel J, Dekker MP, Mansvelder HD, van Ooyen A, and Meredith RM. Development of dendritic tonic GABAergic inhibition regulates excitability and plasticity in CA1 pyramidal neurons. *J Neurophysiol* 112: 287-299, 2014.
Gryshchenko O, Fischer IR, Dittrich M, Viatchenko-Karpinski S, Soest J, Bohm-Pinger MM, Igelmund P, Fleischmann BK, and Hescheler J. Role of ATP-dependent K(+) channels in the electrical excitability of early embryonic stem cell-derived cardiomyocytes. *Journal of cell science* 112 (Pt 17): 2903-2912, 1999.
Gueorguiev VD, Zeman RJ, Meyer EM, and Sabban EL. Involvement of alpha7 nicotinic acetylcholine receptors in activation of tyrosine hydroxylase and dopamine beta-hydroxylase gene expression in PC12 cells. *J Neurochem* 75: 1997-2005, 2000.
Guy J, Cheval H, Selfridge J, and Bird A. The role of MeCP2 in the brain. *Annu Rev Cell Dev Biol* 27: 631-652, 2011.
Guy J, Hendrich B, Holmes M, Martin JE, and Bird A. A mouse Mecp2-null mutation causes neurological symptoms that mimic Rett syndrome. *Nat Genet* 27: 322-326, 2001.

Hagberg B, Aicardi J, Dias K, and Ramos O. A progressive syndrome of autism, dementia, ataxia, and loss of purposeful hand use in girls: Rett's syndrome: report of 35 cases. *Ann Neurol* 14: 471-479, 1983.
Han G, An L, Yang B, Si L, and Zhang T. Nicotine-induced impairments of spatial cognition and long-term potentiation in adolescent male rats. *Human & experimental toxicology* 33: 203-213, 2014.
Harnett MT, Xu NL, Magee JC, and Williams SR. Potassium channels control the interaction between active dendritic integration compartments in layer 5 cortical pyramidal neurons. *Neuron* 79: 516-529, 2013.
Harris-Warrick RM, Coniglio LM, Levini RM, Gueron S, and Guckenheimer J. Dopamine modulation of two subthreshold currents produces phase shifts in activity of an identified motoneuron. *J Neurophysiol* 74: 1404-1420, 1995.
He C, Chen F, Li B, and Hu Z. Neurophysiology of HCN channels: from cellular functions to multiple regulations. *Progress in neurobiology* 112: 1-23, 2014.
Hidaka O, Morimoto T, Kato T, Masuda Y, Inoue T, and Takada K. Behavior of jaw muscle spindle afferents during cortically induced rhythmic jaw movements in the anesthetized rabbit. *J Neurophysiol* 82: 2633-2640, 1999.
Hogg RC, Raggenbass M, and Bertrand D. Nicotinic acetylcholine receptors: from structure to brain function. *Rev Physiol Biochem Pharmacol* 147: 1-46, 2003.
Hsiao CF, Kaur G, Vong A, Bawa H, and Chandler SH. Participation of Kv1 channels in control of membrane excitability and burst generation in mesencephalic V neurons. *J Neurophysiol* 101: 1407-1418, 2009.
Ide S, Itoh M, and Goto Y. Defect in normal developmental increase of the brain biogenic amine concentrations in the mecp2-null mouse. *Neurosci Lett* 386: 14-17, 2005.
Isaacs JS, Murdock M, Lane J, and Percy AK. Eating difficulties in girls with Rett syndrome compared with other developmental disabilities. *Journal of the American Dietetic Association* 103: 224-230, 2003.
Ji D, and Dani JA. Inhibition and disinhibition of pyramidal neurons by activation of nicotinic receptors on hippocampal interneurons. *J Neurophysiol* 83: 2682-2690, 2000.
Jin X, Cui N, Zhong W, Jin XT, and Jiang C. GABAergic synaptic inputs of locus coeruleus neurons in wild-type and Mecp2-null mice. *Am J Physiol Cell Physiol* 304: C844-857, 2013a.
Jin X, Zhong W, and Jiang C. Time-dependent modulation of GABA(A)-ergic synaptic transmission by allopregnanolone in locus coeruleus neurons of Mecp2-null mice. *Am J Physiol Cell Physiol* 305: C1151-1160, 2013b.
Jin XT, Cui N, Zhong W, Jin X, Wu Z, and Jiang C. Pre- and postsynaptic modulations of hypoglossal motoneurons by alpha-adrenoceptor activation in wild-type and Mecp2(-/Y) mice. *Am J Physiol Cell Physiol* 305: C1080-1090, 2013c.
John J, and Manchanda R. Modulation of synaptic potentials and cell excitability by dendritic KIR and KAs channels in nucleus accumbens medium spiny neurons: a computational study. *Journal of biosciences* 36: 309-328, 2011.
Johnston D, Hoffman DA, Magee JC, Poolos NP, Watanabe S, Colbert CM, and Migliore M. Dendritic potassium channels in hippocampal pyramidal neurons. *J Physiol* 525 Pt 1: 75-81, 2000.
Kao FC, Su SH, Carlson GC, and Liao W. MeCP2-mediated alterations of striatal features accompany psychomotor deficits in a mouse model of Rett syndrome. *Brain structure & function* 2013.

Kawahara Y, Kawahara H, and Westerink BH. Tonic regulation of the activity of noradrenergic neurons in the locus coeruleus of the conscious rat studied by dual-probe microdialysis. *Brain Res* 823: 42-48, 1999.
Ke CB, He WS, Li CJ, Shi D, Gao F, and Tian YK. Enhanced SCN7A/Nax expression contributes to bone cancer pain by increasing excitability of neurons in dorsal root ganglion. *Neuroscience* 227: 80-89, 2012.
Kerr AM, Armstrong DD, Prescott RJ, Doyle D, and Kearney DL. Rett syndrome: analysis of deaths in the British survey. *European child & adolescent psychiatry* 6 Suppl 1: 71-74, 1997.
Khakh BS, and Henderson G. Hyperpolarization-activated cationic currents (Ih) in neurones of the trigeminal mesencephalic nucleus of the rat. *J Physiol* 510 (Pt 3): 695-704, 1998.
Khorkova O, and Golowasch J. Neuromodulators, not activity, control coordinated expression of ionic currents. *J Neurosci* 27: 8709-8718, 2007.
Kile BM, Guillot TS, Venton BJ, Wetsel WC, Augustine GJ, and Wightman RM. Synapsins differentially control dopamine and serotonin release. *J Neurosci* 30: 9762-9770, 2010.
Kim E, and Hoffman DA. Dynamic regulation of synaptic maturation state by voltage-gated A-type K+ channels in CA1 hippocampal pyramidal neurons. *J Neurosci* 32: 14427-14432, 2012.
Kim YH, and Holt JR. Functional contributions of HCN channels in the primary auditory neurons of the mouse inner ear. *J Gen Physiol* 142: 207-223, 2013.
Kodangattil JN, Dacher M, Authement ME, and Nugent FS. Spike timing-dependent plasticity at GABAergic synapses in the ventral tegmental area. *J Physiol* 591: 4699-4710, 2013.
Kolta A, Lund JP, and Rossignol S. Modulation of activity of spindle afferents recorded in trigeminal mesencephalic nucleus of rabbit during fictive mastication. *J Neurophysiol* 64: 1067-1076, 1990.
Laedermann CJ, Cachemaille M, Kirschmann G, Pertin M, Gosselin RD, Chang I, Albesa M, Towne C, Schneider BL, Kellenberger S, Abriel H, and Decosterd I. Dysregulation of voltage-gated sodium channels by ubiquitin ligase NEDD4-2 in neuropathic pain. *J Clin Invest* 123: 3002-3013, 2013.
Lena C, de Kerchove D'Exaerde A, Cordero-Erausquin M, Le Novere N, del Mar Arroyo-Jimenez M, and Changeux JP. Diversity and distribution of nicotinic acetylcholine receptors in the locus ceruleus neurons. *Proc Natl Acad Sci U S A* 96: 12126-12131, 1999.
Li B, Luo C, Tang W, Chen Z, Li Q, Hu B, Lin J, Zhu G, Zhang JH, and Feng H. Role of HCN channels in neuronal hyperexcitability after subarachnoid hemorrhage in rats. *J Neurosci* 32: 3164-3175, 2012.
Liu L, Orozco IJ, Planel E, Wen Y, Bretteville A, Krishnamurthy P, Wang L, Herman M, Figueroa H, Yu WH, Arancio O, and Duff K. A transgenic rat that develops Alzheimer's disease-like amyloid pathology, deficits in synaptic plasticity and cognitive impairment. *Neurobiol Dis* 31: 46-57, 2008.
Liu QS, and Berg DK. Extracellular calcium regulates responses of both alpha3- and alpha7-containing nicotinic receptors on chick ciliary ganglion neurons. *J Neurophysiol* 82: 1124-1132, 1999.
Livak KJ, and Schmittgen TD. Analysis of relative gene expression data using real-time quantitative PCR and the 2(-Delta Delta C(T)) Method. *Methods* 25: 402-408, 2001.
Lloyd KG. CNS compensation to dopamine neuron loss in Parkinson's disease. *Adv Exp Med Biol* 90: 255-266, 1977.

Lozada AF, Wang X, Gounko NV, Massey KA, Duan J, Liu Z, and Berg DK. Glutamatergic synapse formation is promoted by alpha7-containing nicotinic acetylcholine receptors. *J Neurosci* 32: 7651-7661, 2012a.
Lozada AF, Wang X, Gounko NV, Massey KA, Duan J, Liu Z, and Berg DK. Induction of dendritic spines by beta2-containing nicotinic receptors. *J Neurosci* 32: 8391-8400, 2012b.
Luo P, Moritani M, and Dessem D. Jaw-muscle spindle afferent pathways to the trigeminal motor nucleus in the rat. *J Comp Neurol* 435: 341-353, 2001.
Lupica CR, Bell JA, Hoffman AF, and Watson PL. Contribution of the hyperpolarization-activated current (I(h)) to membrane potential and GABA release in hippocampal interneurons. *J Neurophysiol* 86: 261-268, 2001.
MacLean JN, Zhang Y, Goeritz ML, Casey R, Oliva R, Guckenheimer J, and Harris-Warrick RM. Activity-independent coregulation of IA and Ih in rhythmically active neurons. *J Neurophysiol* 94: 3601-3617, 2005.
MacLean JN, Zhang Y, Johnson BR, and Harris-Warrick RM. Activity-independent homeostasis in rhythmically active neurons. *Neuron* 37: 109-120, 2003.
Maloku E, Kadriu B, Zhubi A, Dong E, Pibiri F, Satta R, and Guidotti A. Selective alpha4beta2 nicotinic acetylcholine receptor agonists target epigenetic mechanisms in cortical GABAergic neurons. *Neuropsychopharmacology* 36: 1366-1374, 2011.
Martin SJ, Shires KL, and Spooner PA. The relationship between tetanus intensity and the magnitude of hippocampal long-term potentiation in vivo. *Neuroscience* 231: 363-372, 2013.
McCallum SE, Parameswaran N, Perez XA, Bao S, McIntosh JM, Grady SR, and Quik M. Compensation in pre-synaptic dopaminergic function following nigrostriatal damage in primates. *J Neurochem* 96: 960-972, 2006.
McCauley MD, Wang T, Mike E, Herrera J, Beavers DL, Huang TW, Ward CS, Skinner S, Percy AK, Glaze DG, Wehrens XH, and Neul JL. Pathogenesis of lethal cardiac arrhythmias in Mecp2 mutant mice: implication for therapy in Rett syndrome. *Science translational medicine* 3: 113ra125, 2011.
McCoy JG, and Strecker RE. The cognitive cost of sleep lost. *Neurobiol Learn Mem* 96: 564-582, 2011.
McDermott CM, and Schrader LA. Activation of kappa opioid receptors increases intrinsic excitability of dentate gyrus granule cells. *J Physiol* 589: 3517-3532, 2011.
Medrihan L, Tantalaki E, Aramuni G, Sargsyan V, Dudanova I, Missler M, and Zhang W. Early defects of GABAergic synapses in the brain stem of a MeCP2 mouse model of Rett syndrome. *J Neurophysiol* 99: 112-121, 2008.
Mitchell SN. Role of the locus coeruleus in the noradrenergic response to a systemic administration of nicotine. *Neuropharmacology* 32: 937-949, 1993.
Mizuno T, Kanazawa I, and Sakurai M. Differential induction of LTP and LTD is not determined solely by instantaneous calcium concentration: an essential involvement of a temporal factor. *Eur J Neurosci* 14: 701-708, 2001.
Mori F, Nistico R, Mandolesi G, Piccinin S, Mango D, Kusayanagi H, Berretta N, Bergami A, Gentile A, Musella A, Nicoletti CG, Nicoletti F, Buttari F, Mercuri NB, Martino G, Furlan R, and Centonze D. Interleukin-1beta promotes long-term potentiation in patients with multiple sclerosis. *Neuromolecular Med* 16: 38-51, 2014.
Motil KJ, Caeg E, Barrish JO, Geerts S, Lane JB, Percy AK, Annese F, McNair L, Skinner SA, Lee HS, Neul JL, and Glaze DG. Gastrointestinal and nutritional problems occur

frequently throughout life in girls and women with Rett syndrome. *Journal of pediatric gastroenterology and nutrition* 55: 292-298, 2012.
Muere C, Neumueller S, Miller J, Olesiak S, Hodges MR, Pan L, and Forster HV. Atropine microdialysis within or near the pre-Botzinger Complex increases breathing frequency more during wakefulness than during NREM sleep. *Journal of applied physiology* 114: 694-704, 2013.
Murchison CF, Schutsky K, Jin SH, and Thomas SA. Norepinephrine and ss(1)-adrenergic signaling facilitate activation of hippocampal CA1 pyramidal neurons during contextual memory retrieval. *Neuroscience* 181: 109-116, 2011.
Na ES, Nelson ED, Adachi M, Autry AE, Mahgoub MA, Kavalali ET, and Monteggia LM. A mouse model for MeCP2 duplication syndrome: MeCP2 overexpression impairs learning and memory and synaptic transmission. *J Neurosci* 32: 3109-3117, 2012.
Nag N, and Berger-Sweeney JE. Postnatal dietary choline supplementation alters behavior in a mouse model of Rett syndrome. *Neurobiol Dis* 26: 473-480, 2007.
Nakamura M, and Jang IS. Presynaptic nicotinic acetylcholine receptors enhance GABAergic synaptic transmission in rat periaqueductal gray neurons. *Eur J Pharmacol* 640: 178-184, 2010.
Nguyen MV, Du F, Felice CA, Shan X, Nigam A, Mandel G, Robinson JK, and Ballas N. MeCP2 is critical for maintaining mature neuronal networks and global brain anatomy during late stages of postnatal brain development and in the mature adult brain. *J Neurosci* 32: 10021-10034, 2012.
Nolan MF, Dudman JT, Dodson PD, and Santoro B. HCN1 channels control resting and active integrative properties of stellate cells from layer II of the entorhinal cortex. *J Neurosci* 27: 12440-12451, 2007.
Nordman JC, Phillips WS, Kodama N, Clark SG, Del Negro CA, and Kabbani N. Axon targeting of the alpha 7 nicotinic receptor in developing hippocampal neurons by Gprin1 regulates growth. *J Neurochem* 129: 649-662, 2014.
Nugent FS, and Kauer JA. LTP of GABAergic synapses in the ventral tegmental area and beyond. *J Physiol* 586: 1487-1493, 2008.
O'Donnell J, Zeppenfeld D, McConnell E, Pena S, and Nedergaard M. Norepinephrine: a neuromodulator that boosts the function of multiple cell types to optimize CNS performance. *Neurochem Res* 37: 2496-2512, 2012.
Ogris W, Lehner R, Fuchs K, Furtmuller B, Hoger H, Homanics GE, and Sieghart W. Investigation of the abundance and subunit composition of GABAA receptor subtypes in the cerebellum of alpha1-subunit-deficient mice. *J Neurochem* 96: 136-147, 2006.
Ortinski PI, Turner JR, Barberis A, Motamedi G, Yasuda RP, Wolfe BB, Kellar KJ, and Vicini S. Deletion of the GABA(A) receptor alpha1 subunit increases tonic GABA(A) receptor current: a role for GABA uptake transporters. *J Neurosci* 26: 9323-9331, 2006.
Osterhout CA, Sterling CR, Chikaraishi DM, and Tank AW. Induction of tyrosine hydroxylase in the locus coeruleus of transgenic mice in response to stress or nicotine treatment: lack of activation of tyrosine hydroxylase promoter activity. *J Neurochem* 94: 731-741, 2005.
OuYang W, and Hemmings HC, Jr. Isoform-selective effects of isoflurane on voltage-gated Na+ channels. *Anesthesiology* 107: 91-98, 2007.
Pal D, and Mallick BN. Neural mechanism of rapid eye movement sleep generation with reference to REM-OFF neurons in locus coeruleus. *Indian J Med Res* 125: 721-739, 2007.
Panayotis N, Ghata A, Villard L, and Roux JC. Biogenic amines and their metabolites are differentially affected in the Mecp2-deficient mouse brain. *BMC Neurosci* 12: 47, 2011.

Patel N, Jankovic J, and Hallett M. Sensory aspects of movement disorders. *The Lancet Neurology* 13: 100-112, 2014.
Patino GA, Brackenbury WJ, Bao Y, Lopez-Santiago LF, O'Malley HA, Chen C, Calhoun JD, Lafreniere RG, Cossette P, Rouleau GA, and Isom LL. Voltage-gated Na+ channel beta1B: a secreted cell adhesion molecule involved in human epilepsy. *J Neurosci* 31: 14577-14591, 2011.
Perez MF, White FJ, and Hu XT. Dopamine D(2) receptor modulation of K(+) channel activity regulates excitability of nucleus accumbens neurons at different membrane potentials. *J Neurophysiol* 96: 2217-2228, 2006.
Perry TL, Dunn HG, Ho HH, and Crichton JU. Cerebrospinal fluid values for monoamine metabolites, gamma-aminobutyric acid, and other amino compounds in Rett syndrome. *The Journal of pediatrics* 112: 234-238, 1988.
Podda MV, Riccardi E, D'Ascenzo M, Azzena GB, and Grassi C. Dopamine D1-like receptor activation depolarizes medium spiny neurons of the mouse nucleus accumbens by inhibiting inwardly rectifying K+ currents through a cAMP-dependent protein kinase A-independent mechanism. *Neuroscience* 167: 678-690, 2010.
Power KE, Carlin KP, and Fedirchuk B. Modulation of voltage-gated sodium channels hyperpolarizes the voltage threshold for activation in spinal motoneurones. *Experimental brain research* 217: 311-322, 2012.
Prinz AA, Bucher D, and Marder E. Similar network activity from disparate circuit parameters. *Nat Neurosci* 7: 1345-1352, 2004.
Ramadan E, Fu Z, Losi G, Homanics GE, Neale JH, and Vicini S. GABA(A) receptor beta3 subunit deletion decreases alpha2/3 subunits and IPSC duration. *J Neurophysiol* 89: 128-134, 2003.
Ramakers GM, and Storm JF. A postsynaptic transient K(+) current modulated by arachidonic acid regulates synaptic integration and threshold for LTP induction in hippocampal pyramidal cells. *Proc Natl Acad Sci U S A* 99: 10144-10149, 2002.
Raman IM, and Bean BP. Resurgent sodium current and action potential formation in dissociated cerebellar Purkinje neurons. *J Neurosci* 17: 4517-4526, 1997.
Rett A. [On a unusual brain atrophy syndrome in hyperammonemia in childhood]. *Wiener medizinische Wochenschrift* 116: 723-726, 1966.
Romanelli MN, Gratteri P, Guandalini L, Martini E, Bonaccini C, and Gualtieri F. Central nicotinic receptors: structure, function, ligands, and therapeutic potential. *ChemMedChem* 2: 746-767, 2007.
Rothlin CV, Katz E, Verbitsky M, Vetter DE, Heinemann SF, and Elgoyhen AB. Block of the alpha9 nicotinic receptor by ototoxic aminoglycosides. *Neuropharmacology* 39: 2525-2532, 2000.
Roux JC, Dura E, Moncla A, Mancini J, and Villard L. Treatment with desipramine improves breathing and survival in a mouse model for Rett syndrome. *Eur J Neurosci* 25: 1915-1922, 2007.
Rush AM, Dib-Hajj SD, and Waxman SG. Electrophysiological properties of two axonal sodium channels, Nav1.2 and Nav1.6, expressed in mouse spinal sensory neurones. *J Physiol* 564: 803-815, 2005.
Rusznak Z, Pal B, Koszeghy A, Fu Y, Szucs G, and Paxinos G. The hyperpolarization-activated non-specific cation current (In) adjusts the membrane properties, excitability, and

activity pattern of the giant cells in the rat dorsal cochlear nucleus. *Eur J Neurosci* 37: 876-890, 2013.
Santoro B, Chen S, Luthi A, Pavlidis P, Shumyatsky GP, Tibbs GR, and Siegelbaum SA. Molecular and functional heterogeneity of hyperpolarization-activated pacemaker channels in the mouse CNS. *J Neurosci* 20: 5264-5275, 2000.
Santos M, Summavielle T, Teixeira-Castro A, Silva-Fernandes A, Duarte-Silva S, Marques F, Martins L, Dierssen M, Oliveira P, Sousa N, and Maciel P. Monoamine deficits in the brain of methyl-CpG binding protein 2 null mice suggest the involvement of the cerebral cortex in early stages of Rett syndrome. *Neuroscience* 170: 453-467, 2010.
Schaevitz LR, Nicolai R, Lopez CM, D'Iddio S, Iannoni E, and Berger-Sweeney JE. Acetyl-L-carnitine improves behavior and dendritic morphology in a mouse model of Rett syndrome. *PLoS One* 7: e51586, 2012.
Schulz DJ, Goaillard JM, and Marder E. Variable channel expression in identified single and electrically coupled neurons in different animals. *Nat Neurosci* 9: 356-362, 2006.
Sekerli M, Del Negro CA, Lee RH, and Butera RJ. Estimating action potential thresholds from neuronal time-series: new metrics and evaluation of methodologies. *IEEE transactions on bio-medical engineering* 51: 1665-1672, 2004.
Shao XM, and Feldman JL. Respiratory rhythm generation and synaptic inhibition of expiratory neurons in pre-Botzinger complex: differential roles of glycinergic and GABAergic neural transmission. *J Neurophysiol* 77: 1853-1860, 1997.
Shepherd GM, and Katz DM. Synaptic microcircuit dysfunction in genetic models of neurodevelopmental disorders: focus on Mecp2 and Met. *Curr Opin Neurobiol* 21: 827-833, 2011.
Smith ML, Souza FG, Bruce KS, Strang CE, Morley BJ, and Keyser KT. Acetylcholine receptors in the retinas of the alpha7 nicotinic acetylcholine receptor knockout mouse. *Molecular vision* 20: 1328-1356, 2014.
Solich J, Faron-Gorecka A, Kusmider M, Palach P, Gaska M, and Dziedzicka-Wasylewska M. Norepinephrine transporter (NET) knock-out upregulates dopamine and serotonin transporters in the mouse brain. *Neurochem Int* 59: 185-191, 2011.
Sossi V, Dinelle K, Topping GJ, Holden JE, Doudet D, Schulzer M, Ruth TJ, Stoessl AJ, and de la Fuente-Fernandez R. Dopamine transporter relation to levodopa-derived synaptic dopamine in a rat model of Parkinson's: an in vivo imaging study. *J Neurochem* 109: 85-92, 2009.
Stieber J, Stockl G, Herrmann S, Hassfurth B, and Hofmann F. Functional expression of the human HCN3 channel. *J Biol Chem* 280: 34635-34643, 2005.
Sudhof TC. Calcium control of neurotransmitter release. *Cold Spring Harbor perspectives in biology* 4: a011353, 2012.
Takahashi K, Kayama Y, Lin JS, and Sakai K. Locus coeruleus neuronal activity during the sleep-waking cycle in mice. *Neuroscience* 169: 1115-1126, 2010.
Tanaka S, Wu N, Hsaio CF, Turman J, Jr., and Chandler SH. Development of inward rectification and control of membrane excitability in mesencephalic v neurons. *J Neurophysiol* 89: 1288-1298, 2003.
Taneja P, Ogier M, Brooks-Harris G, Schmid DA, Katz DM, and Nelson SB. Pathophysiology of locus ceruleus neurons in a mouse model of Rett syndrome. *J Neurosci* 29: 12187-12195, 2009.

Taylor MM, and Doshi S. Insights into the cellular and molecular contributions of MeCP2 overexpression to disease pathophysiology. *J Neurosci* 32: 9451-9453, 2012.
Thoby-Brisson M, and Simmers J. Transition to endogenous bursting after long-term decentralization requires De novo transcription in a critical time window. *J Neurophysiol* 84: 596-599, 2000.
Tobin AE, Cruz-Bermudez ND, Marder E, and Schulz DJ. Correlations in ion channel mRNA in rhythmically active neurons. *PLoS One* 4: e6742, 2009.
Tryba AK, Pena F, Lieske SP, Viemari JC, Thoby-Brisson M, and Ramirez JM. Differential modulation of neural network and pacemaker activity underlying eupnea and sigh-breathing activities. *J Neurophysiol* 99: 2114-2125, 2008.
Turman J, Jr., and Chandler SH. Immunohistochemical evidence for GABA and glycine-containing trigeminal premotoneurons in the guinea pig. *Synapse* 18: 7-20, 1994.
Vandael DH, Zuccotti A, Striessnig J, and Carbone E. Ca(V)1.3-driven SK channel activation regulates pacemaking and spike frequency adaptation in mouse chromaffin cells. *J Neurosci* 32: 16345-16359, 2012.
Vergara C, Latorre R, Marrion NV, and Adelman JP. Calcium-activated potassium channels. *Curr Opin Neurobiol* 8: 321-329, 1998.
Vervaeke K, Hu H, Graham LJ, and Storm JF. Contrasting effects of the persistent Na+ current on neuronal excitability and spike timing. *Neuron* 49: 257-270, 2006.
Veyrac A, Nguyen V, Marien M, Didier A, and Jourdan F. Noradrenergic control of odor recognition in a nonassociative olfactory learning task in the mouse. *Learn Mem* 14: 847-854, 2007.
Viemari JC, Bevengut M, Burnet H, Coulon P, Pequignot JM, Tiveron MC, and Hilaire G. Phox2a gene, A6 neurons, and noradrenaline are essential for development of normal respiratory rhythm in mice. *J Neurosci* 24: 928-937, 2004.
Viemari JC, Garcia AJ, 3rd, Doi A, Elsen G, and Ramirez JM. beta-Noradrenergic receptor activation specifically modulates the generation of sighs in vivo and in vitro. *Frontiers in neural circuits* 7: 179, 2013.
Viemari JC, Garcia AJ, 3rd, Doi A, and Ramirez JM. Activation of alpha-2 noradrenergic receptors is critical for the generation of fictive eupnea and fictive gasping inspiratory activities in mammals in vitro. *Eur J Neurosci* 33: 2228-2237, 2011.
Viemari JC, and Ramirez JM. Norepinephrine differentially modulates different types of respiratory pacemaker and nonpacemaker neurons. *J Neurophysiol* 95: 2070-2082, 2006.
Viemari JC, Roux JC, Tryba AK, Saywell V, Burnet H, Pena F, Zanella S, Bevengut M, Barthelemy-Requin M, Herzing LB, Moncla A, Mancini J, Ramirez JM, Villard L, and Hilaire G. Mecp2 deficiency disrupts norepinephrine and respiratory systems in mice. *J Neurosci* 25: 11521-11530, 2005.
Vincler MA, and Eisenach JC. Immunocytochemical localization of the alpha3, alpha4, alpha5, alpha7, beta2, beta3 and beta4 nicotinic acetylcholine receptor subunits in the locus coeruleus of the rat. *Brain Res* 974: 25-36, 2003.
Vucic S, and Kiernan MC. Novel threshold tracking techniques suggest that cortical hyperexcitability is an early feature of motor neuron disease. *Brain* 129: 2436-2446, 2006.
Wahl-Schott C, and Biel M. HCN channels: structure, cellular regulation and physiological function. *Cell Mol Life Sci* 66: 470-494, 2009.
Weng SM, Bailey ME, and Cobb SR. Rett syndrome: from bed to bench. *Pediatr Neonatol* 52: 309-316, 2011.

Wenk GL, and Hauss-Wegrzyniak B. Altered cholinergic function in the basal forebrain of girls with Rett syndrome. *Neuropediatrics* 30: 125-129, 1999.
Wenk GL, and Mobley SL. Choline acetyltransferase activity and vesamicol binding in Rett syndrome and in rats with nucleus basalis lesions. *Neuroscience* 73: 79-84, 1996.
Winter JA, Allen TJ, and Proske U. Muscle spindle signals combine with the sense of effort to indicate limb position. *J Physiol* 568: 1035-1046, 2005.
Wu N, Enomoto A, Tanaka S, Hsiao CF, Nykamp DQ, Izhikevich E, and Chandler SH. Persistent sodium currents in mesencephalic v neurons participate in burst generation and control of membrane excitability. *J Neurophysiol* 93: 2710-2722, 2005.
Wu N, Hsiao CF, and Chandler SH. Membrane resonance and subthreshold membrane oscillations in mesencephalic V neurons: participants in burst generation. *J Neurosci* 21: 3729-3739, 2001.
Xu R, Thomas EA, Gazina EV, Richards KL, Quick M, Wallace RH, Harkin LA, Heron SE, Berkovic SF, Scheffer IE, Mulley JC, and Petrou S. Generalized epilepsy with febrile seizures plus-associated sodium channel beta1 subunit mutations severely reduce beta subunit-mediated modulation of sodium channel function. *Neuroscience* 148: 164-174, 2007.
Yang K, Buhlman L, Khan GM, Nichols RA, Jin G, McIntosh JM, Whiteaker P, Lukas RJ, and Wu J. Functional nicotinic acetylcholine receptors containing alpha6 subunits are on GABAergic neuronal boutons adherent to ventral tegmental area dopamine neurons. *J Neurosci* 31: 2537-2548, 2011.
Yang YR, Chang KC, Chen CL, and Chiu TH. Arecoline excites rat locus coeruleus neurons by activating the M2-muscarinic receptor. *The Chinese journal of physiology* 43: 23-28, 2000.
Ye Z, McGee TP, Houston CM, and Brickley SG. The contribution of delta subunit-containing GABAA receptors to phasic and tonic conductance changes in cerebellum, thalamus and neocortex. *Frontiers in neural circuits* 7: 203, 2013.
Ying SW, Tibbs GR, Picollo A, Abbas SY, Sanford RL, Accardi A, Hofmann F, Ludwig A, and Goldstein PA. PIP2-mediated HCN3 channel gating is crucial for rhythmic burst firing in thalamic intergeniculate leaflet neurons. *J Neurosci* 31: 10412-10423, 2011.
Yoshizumi M, Parker RA, Eisenach JC, and Hayashida K. Gabapentin inhibits gamma-amino butyric acid release in the locus coeruleus but not in the spinal dorsal horn after peripheral nerve injury in rats. *Anesthesiology* 116: 1347-1353, 2012.
Zakir HM, Kitagawa J, Yamada Y, Kurose M, Mostafeezur RM, and Yamamura K. Modulation of spindle discharge from jaw-closing muscles during chewing foods of different hardness in awake rabbits. *Brain Res Bull* 83: 380-386, 2010.
Zanella S, Mebarek S, Lajard AM, Picard N, Dutschmann M, and Hilaire G. Oral treatment with desipramine improves breathing and life span in Rett syndrome mouse model. *Respir Physiol Neurobiol* 160: 116-121, 2008.
Zanette G, Tamburin S, Manganotti P, Refatti N, Forgione A, and Rizzuto N. Different mechanisms contribute to motor cortex hyperexcitability in amyotrophic lateral sclerosis. *Clinical neurophysiology : official journal of the International Federation of Clinical Neurophysiology* 113: 1688-1697, 2002.
Zappettini S, Grilli M, Lagomarsino F, Cavallero A, Fedele E, and Marchi M. Presynaptic nicotinic alpha7 and non-alpha7 receptors stimulate endogenous GABA release from rat hippocampal synaptosomes through two mechanisms of action. *PLoS One* 6: e16911, 2011.

Zhang X, Cui N, Wu Z, Su J, Tadepalli JS, Sekizar S, and Jiang C. Intrinsic membrane properties of locus coeruleus neurons in Mecp2-null mice. *Am J Physiol Cell Physiol* 298: C635-646, 2010a.

Zhang X, Su J, Cui N, Gai H, Wu Z, and Jiang C. The disruption of central CO2 chemosensitivity in a mouse model of Rett syndrome. *Am J Physiol Cell Physiol* 301: C729-738, 2011.

Zhang X, Su J, Rojas A, and Jiang C. Pontine norepinephrine defects in Mecp2-null mice involve deficient expression of dopamine beta-hydroxylase but not a loss of catecholaminergic neurons. *Biochem Biophys Res Commun* 394: 285-290, 2010b.

Zhao L, Kuo YP, George AA, Peng JH, Purandare MS, Schroeder KM, Lukas RJ, and Wu J. Functional properties of homomeric, human alpha 7-nicotinic acetylcholine receptors heterologously expressed in the SH-EP1 human epithelial cell line. *J Pharmacol Exp Ther* 305: 1132-1141, 2003.

Zhao S, and Golowasch J. Ionic current correlations underlie the global tuning of large numbers of neuronal activity attributes. *J Neurosci* 32: 13380-13388, 2012.

Zhong LR, Estes S, Artinian L, and Rehder V. Acetylcholine elongates neuronal growth cone filopodia via activation of nicotinic acetylcholine receptors. *Developmental neurobiology* 73: 487-501, 2013.

Zhou R, Wang S, and Zhu X. Prenatal ethanol exposure attenuates GABAergic inhibition in basolateral amygdala leading to neuronal hyperexcitability and anxiety-like behavior of adult rat offspring. *Neuroscience* 170: 749-757, 2010.

Zigmond MJ, Acheson AL, Stachowiak MK, and Stricker EM. Neurochemical compensation after nigrostriatal bundle injury in an animal model of preclinical parkinsonism. *Arch Neurol* 41: 856-861, 1984.

Zoghbi HY, Milstien S, Butler IJ, Smith EO, Kaufman S, Glaze DG, and Percy AK. Cerebrospinal fluid biogenic amines and biopterin in Rett syndrome. *Ann Neurol* 25: 56-60, 1989.

Zoghbi HY, Percy AK, Glaze DG, Butler IJ, and Riccardi VM. Reduction of biogenic amine levels in the Rett syndrome. *N Engl J Med* 313: 921-924, 1985.

Zou S, Li L, Pei L, Vukusic B, Van Tol HH, Lee FJ, Wan Q, and Liu F. Protein-protein coupling/uncoupling enables dopamine D2 receptor regulation of AMPA receptor-mediated excitotoxicity. *J Neurosci* 25: 4385-4395, 2005.

Zwart R, and Vijverberg HP. Potentiation and inhibition of neuronal nicotinic receptors by atropine: competitive and noncompetitive effects. *Mol Pharmacol* 52: 886-895, 1997.

APPENDIX

Curriculum Vitae

Research Interests
1) Homeostatic mechanisms of the reward system in addiction models
2) Homeostatic mechanisms regulating membrane currents and neuronal activity
3) Neuronal network control of behavior

Methods of Independent Expertise

Rodent brain slice patch clamp electrophysiology of excitatory and inhibitory postsynaptic currents including analysis with pClamp and Mini Analysis, electrophysiology of intrinsic membrane properties of neurons, Optogenetics in brain slice preparations, Brain slice vibratome sectioning, Local drug application to patched neurons, Single cell PCR, Quantitative PCR, Transgenic mouse breeding, Western blotting, Stomatogastric ganglion (STG) dissection and isolation from lobster, Immunohistochemistry of STG whole mount preparation, confocal imaging, Matlab and CONTENT programming to study computational models of mammalian systems

Education

Doctorate of Philosophy: Biology **Advisor: Chun Jiang**	Georgia State University	(2008 - *2014*)
BAChelor of Science: Biology **Advisor: Daniel Wujek**	Central Michigan University	(1997- 2001)

Primary Publications

Oginsky M.F., Cui N., Zhong W., Johnson C.M., Jiang C. Alterations in the cholinergic system of brainstem neurons in a mouse model of Rett Syndrome. *American Journal of Physiology. Cell Physiology*. 307(6):C508-20. (2014)

Oginsky M.F., Rodgers E.W., Clark M.C., Simmons R., Krenz W.D., Baro D.J. D(2) receptors receive paracrine neurotransmission and are consistently targeted to a subset of synaptic structures in an identified neuron of the crustacean stomatogastric nervous system. *Journal of Comparative Neurology*. 518(3):255-76. (2010)

Oginsky M.F., Cui N., Zhong W., Jiang C. Homeostatic reorganization of HCN and voltage-gated Na^+ channels in mesencephalic trigeminal propriosensory neurons of a Rett syndrome mouse model and its impact on membrane excitability. *Experimental Neurology*. (In Review)

Jin X., Li S., Bondy B., Zhong W., **Oginsky.M.F.,** Wu Y., Jiang C. Optogenetic identification of local GABAergic signaling in the locus coeruleus (*In preparation*)

Johnson C.J., Zhong W.,Cui N., **Oginsky M.F.**, Jiang C., Breathing disorders in female mice of a Rett syndrome model. *Journal of Experimental Biology* (*In review*)

Zhong W., Jin X., **Oginsky M.F.,** Bondy B., Jiang C. (2014) Upregulation of extrasynaptic GABAA receptors in Mecp2$^{-/Y}$ mice. *(In preparation)*

Posters and Presentations

Oginsky M.F., Cui N., Zhong W., Jiang C. (2014) Alterations of h-currents and voltage-gated Na^+ currents in mesencephalic trigeminal propriosensory neurons increase excitability in a mouse model for Rett Syndrome. Society for Neuroscience Meeting, Washington D.C.

Zhong W., Jin X., **Oginsky M.F.,** Bondy B., Jiang C. (2014) Upregulation of extrasynaptic GABAA receptors in Mecp2$^{-/Y}$ mice. Society for Neuroscience Meeting, Washington D.C.

Oginsky M.F., Zhong, W., Johnson, C.M., Cui, N., Jiang, C. (2013) MeCP2-null mice displayed possible endogenous mechanisms in defective neurotransmitter systems. Society for Neuroscience Meeting, San Diego, CA

Oginsky M.F., Cui, N., Johnson, C.M., Jiang C., (2012) Pre-and Postsynaptic cholinergic modulation Locus Coeruleus neurons in wild type and Mecp2-null mice. Society for Neuroscience Meeting, New Orleans, LA

Oginsky M.F., Cymablyuk G.S., (2012) Homeostatic regulation in a single neuron model from the Pre-Bötzinger Complex. Computational Neuroscience Meeting, Atlanta, GA

Jin X., Cui N., Zhong W., **Oginsky M.F.**, Jiang C., (2012), Modulation of $GABA_A$-synaptic currents by $GABA_B$-ergic presynaptic inputs in locus coeruleus neurons. FASEB Meeting, San Diego, CA

Rodgers E., **Oginsky M.F.,** Krenz W.D., Baro D.J., (2010) Stable dopamine (DA) induced changes in ion current densities are mediated by new protein synthesis. Society for Neuroscience Meeting, San Diego, CA

Oginsky M.F., Clark, M.C., Baro D.J., (2008) The Pyloric Dilator neuron receives dopamine through paracrine neurotransmission. Society for Neuroscience Meeting, Washington D.C.

Zhang H., Krenz W.D., **Oginsky M.F.**, Baro D.J., (2008)., Spatial and Temporal modulation of neurons by DA. Society for Neuroscience Meeting, Washington D.C.

Invited Addresses

Homeostatic reorganization of HCN and voltage-gated Na^+ channels in mesencephalic trigeminal propriosensory neurons of a Rett syndrome mouse model and its impact on membrane excitability *Undergraduate Biology Seminar Series (2014)*

Mecp2$^{-/Y}$ mice displayed possible endogenous mechanisms in defective neurotransmitter systems *Brains and Behavior retreat* (2014)

Homeostatic regulation in a single neuron model from the Pre-Bötzinger Complex *Neuroscience Institute Breakfast and Lecture Series* (2014)

Mecp2$^{-/Y}$ mice displayed possible endogenous mechanisms in defective neurotransmitter systems *Undergraduate Biology Seminar Series* (2013)

Awards

Brains and Behavior Fellowship 2009-present
Outstanding TeAChing Assistant 2012 and 2014

TeAChing

Biol 1103: Introductory Biology Lab. *Georgia State University*. 2008-present